U.S. DEPARTMENT OF ENERGY

PNNL-19189

Prepared for the U.S. Department of Energy
under Contract DE-AC05-76RL01830

Wind Energy Management System EMS Integration Project

Incorporating Wind Generation and Load Forecast Uncertainties into Power Grid Operations

YV Makarov
Z Huang
PV Etingov
J Ma
RT Guttromson
K Subbarao
BB Chakrabarti

January 2010

Pacific Northwest
NATIONAL LABORATORY

Proudly Operated by Battelle Since 1965

PACIFIC NORTHWEST NATIONAL LABORATORY
operated by
BATTELLE
for the
UNITED STATES DEPARTMENT OF ENERGY
under Contract DE-AC05-76RL01830

Printed in the United States of America

Available to DOE and DOE contractors from the
Office of Scientific and Technical Information,
P.O. Box 62, Oak Ridge, TN 37831-0062;
ph: (865) 576-8401
fax: (865) 576-5728
email: reports@adonis.osti.gov

Available to the public from the National Technical Information Service,
U.S. Department of Commerce, 5285 Port Royal Rd., Springfield, VA 22161
ph: (800) 553-6847
fax: (703) 605-6900
email: orders@ntis.fedworld.gov
online ordering: http://www.ntis.gov/ordering.htm

This document was printed on recycled paper.
(9/2003)

PNNL-19189

Wind Energy Management System (EMS) Integration Project

Incorporating Wind Generation and Load Forecast Uncertainties into Power Grid Operations

YV Makarov[1]
Z Huang[2]
PV Etingov[3]
J Ma[4]
RT Guttromson[5]
K Subbarao[6]
BB Chakrabarti[7]

Subcontractors:
AREVA T&D Corporation, Redmond, Washington
University of Washington, Seattle, Washington

January 2010

Prepared for
the U.S. Department of Energy
under Contract DE-AC05-76RL01830

Pacific Northwest National Laboratory
Richland, Washington 99352

---

[1] Principal Investigator, Chief Scientist – Power Systems
[2] Project Manager, Senior Research Engineer
[3] Project Lead, Senior Research Engineer
[4] Research Engineer
[5] Program Manager, Renewables Integration
[6] Senior Research Engineer
[7] Visiting Scientist, Transpower, New Zealand

Abstract

The power system balancing process, which includes the scheduling, real time dispatch (load following) and regulation processes, is traditionally based on deterministic models. Since the conventional generation needs time to be committed and dispatched to a desired megawatt level, the scheduling and load following processes use load and wind and solar power production forecasts to achieve future balance between the conventional generation and energy storage on the one side, and system load, intermittent resources (such as wind and solar generation), and scheduled interchange on the other side. Although in real life the forecasting procedures imply some uncertainty around the load and wind/solar forecasts (caused by forecast errors), only their mean values are actually used in the generation dispatch and commitment procedures. Since the actual load and intermittent generation can deviate from their forecasts, it becomes increasingly unclear (especially, with the increasing penetration of renewable resources) whether the system would be actually able to meet the conventional generation requirements within the look-ahead horizon, what the additional balancing efforts would be needed as we get closer to the real time, and what additional costs would be incurred by those needs.

To improve the system control performance characteristics, maintain system reliability, and minimize expenses related to the system balancing functions, it becomes necessary to incorporate the predicted uncertainty ranges into the scheduling, load following, and, in some extent, into the regulation processes. It is also important to address the uncertainty problem comprehensively by including all sources of uncertainty (load, intermittent generation, generators' forced outages, etc.) into consideration. All aspects of uncertainty such as the imbalance size (which is the same as capacity needed to mitigate the imbalance) and generation ramping requirement must be taken into account. The latter unique features make this work a significant step forward toward the objective of incorporating of wind, solar, load, and other uncertainties into power system operations.

Currently, uncertainties associated with wind and load forecasts, as well as uncertainties associated with random generator outages and unexpected disconnection of supply lines, are not taken into account in power grid operation. Thus, operators have little means to weigh the likelihood and magnitude of upcoming events of power imbalance. In this project, funded by the U.S. Department of Energy (DOE), a framework has been developed for incorporating uncertainties associated with wind and load forecast errors, unpredicted ramps, and forced generation disconnections into the energy management system (EMS) as well as generation dispatch and commitment applications.

A new approach to evaluate the uncertainty ranges for the required generation performance envelope including balancing capacity, ramping capability, and ramp duration has been proposed. The approach includes three stages: forecast and actual data acquisition, statistical analysis of retrospective information, and prediction of future grid balancing requirements for specified time horizons and confidence levels. Assessment of the capacity and ramping requirements is performed using a specially developed probabilistic algorithm based on a histogram analysis, incorporating all sources of uncertainties of both continuous (wind and load forecast errors) and discrete (forced generator outages and start-up failures) nature. A new method called the "flying brick" technique has been developed to evaluate the look-ahead required generation performance envelope for the worst case scenario within a user-specified confidence level. A self-validation algorithm has been developed to validate the accuracy of the confidence intervals.

To demonstrate the validity of the developed uncertainty assessment methods and its impact on grid operation, a framework for integrating the proposed methods with EMS systems has been developed through collaboration with AREVA's specialists. AREVA has been subcontracted with Pacific Northwest National Laboratory (PNNL) to facilitate the actual integration onto their software platform. Collaboration with software vendors such as AREVA will make PNNL's tools and methodologies developed under this DOE-funded project accessible to a large number of power industry customers. Demonstration through integration with an actual EMS system will prove the applicability of the developed tools and methodologies for actual grid operation and pave the road for integration with EMS systems from other vendors.

The California Energy Commission (CEC) sponsors a parallel project where these ideas and tools have been leveraged so that they will be integrated into the California Independent System Operator (CAISO) market and EMS systems. These efforts aim to bring the wind and load uncertainty information into CAISO's grid operation environment.

Executive Summary

The work reported herein was performed by the Pacific Northwest National Laboratory (PNNL) and funded by the U.S. Department of Energy Office of the Energy Efficiency and Renewable Energy (DOE EERE).

Because conventional generators need time to be committed and dispatched to a desired megawatt level, scheduling and load following processes use load and wind power production forecasts to achieve future balance between conventional generation and energy storage on the one side and system load, intermittent resources (such as wind and solar generation), and scheduled interchange on the other side. The power system balancing process, which includes scheduling, real-time dispatch (load following), and regulation processes is traditionally based on deterministic models.

Uncertainties in forecasting the output of intermittent resources such as wind and solar generation, as well as system loads, are not reflected in existing energy management systems (EMS) and tools for generation commitment, dispatch, and market operation. With the growing penetration of intermittent resources, these uncertainties could result in significant unexpected load following and dispatch problems, and pose serious risks to control and operation performance characteristics as well as reliability of a power grid. Without knowing the risks posed by the uncertainties, system operators have limited means to weigh the likelihood of occurrence and the magnitude of problems to mitigate adverse impacts caused by them. Some important questions need to be addressed in counteracting the impact of uncertainties. For instance, when and if should one start more units to balance against possible fast ramps in the future over a given time horizon?

Furthermore, these uncertainties could require procuring additional costly balancing services. Major unexpected variations in wind power, unfavorably combined with load forecast errors and forced generator outages, could cause significant power mismatches, which could be essentially unmanageable without knowing these variations in advance.

Because the actual load and intermittent generation can deviate from forecasts, it becomes increasingly unclear (especially with the increasing penetration of renewable resources) whether the system would be actually able to meet the conventional generation requirements within the look-ahead horizon, what the additional balancing efforts would be needed as we get closer to the real time, and what additional costs would be incurred by those needs.

In order to improve the system control performance characteristics, maintain system reliability, and minimize expenses related to the system balancing functions, it becomes necessary to incorporate the projected uncertainty ranges into the scheduling, load following, and, in some extent, into the regulation processes. This need has been realized already, and some wind forecast service providers offer the uncertainty information for their forecasts. Works are in place to develop methodologies and tools to incorporate these uncertainties into power system operations. Unfortunately, in many cases, these efforts are limited to wind generation uncertainties only and ignore the fact that there are additional sources of uncertainty such as system loads and forced generation outages. Most of these works are considering only the uncertainty ranges for the megawatt imbalances and do not address additional essential characteristics such as ramps and ramp duration uncertainties.

It is very important to address the uncertainty problem comprehensively by including all sources of uncertainty (load, intermittent generation, generators' forced outages, etc.) into consideration. All aspect of uncertainty such as the imbalance size (which is the same as capacity needed to mitigate the imbalance) and generation ramping requirement must be taken into account. The latter unique features make this work a significant step forward toward the objective of incorporating of wind, solar, load, and other uncertainties into power system operations.

Some of the existing works are also targeting similar objectives. At the same time, these works primarily concentrate on the wind generation uncertainties, whereas the other important sources of uncertainty are not addressed. This limited consideration could be misleading to power system operators responsible for system reliability and control performance characteristics.

In this project, all uncertainties associated with wind power generation forecasting, load demand forecasting, and generation supply interruptions caused by forced outages are taken into account in the evaluation of uncertainty ranges for the required generation performance envelope including balancing capacity, ramping capability, and ramp duration. A probabilistic algorithm, based on the proposed histogram analysis to assess the capacity and ramping requirements, is presented. Preliminary simulation was performed using California Independent System Operator (ISO)'s system model and data. This report presents these simulation results confirming the validity and efficiency of the proposed solutions.

The work pursues the following objectives:

- Develop a probabilistic model to evaluate uncertainties of wind and load forecast errors and to provide rapid (every 5 minutes) look-ahead (up to 5-8 hours ahead) assessments of their uncertainty ranges.
- Elaborate similar models to evaluate uncertainties caused by generator random forced outages, failures to start up, and contingency reserve activation processes.
- Create an integrated tool that consolidates the above-mentioned continuous and discrete random factors, contributing to the overall uncertainty, to evaluate look-ahead, worst-case balancing generation requirements (performance envelopes) in terms of the required capacity, ramping capability, and ramp duration.
- Build a methodology and procedures for self-validation of the predicted performance envelope for each look-ahead interval.
- Develop visualization displays to communicate information about the expected ramps and their uncertainty ranges.
- Implement a prototype unit commitment program incorporating future uncertainties.
- Integrate the developed tools with the AREVA EMS system
- Use actual California ISO data to perform simulation.

The following results have been achieved in this work:

- Innovative methodology and prototype tools that are capable of evaluating future generation requirements, including the required capacity, ramping capability, and ramp duration capability (performance envelope) in view of uncertainties caused by wind generation and load forecast errors as well as unexpected generation outages, have been developed. The approach includes three stages: (1) statistical and actual data acquisition, (2) statistical analysis of retrospective information, and (3) prediction of future grid balancing requirements for specified time horizons and confidence intervals. Assessment of the capacity and ramping requirements is performed using a specially developed probabilistic algorithm based on a histogram analysis incorporating all sources of uncertainty and parameters of a continuous and discrete nature.

- A “flying brick” method has been developed to assess the look ahead worst case performance envelope requirement to be able to ensure the system capability to balance against the uncertainties with certain specified degree of confidence. The “flying brick” approach idea is to include simultaneously the ramp rate, ramp duration, and capacity requirements directly into the balancing process.
- A self-validation approach has been proposed. The purpose of the self-validation algorithm is to verify that the uncertainty ranges predicted based on retrospective information are valid for the future dispatch intervals.
- A MATLAB prototype of the new probabilistic tool has been developed and tested.
- Simulations using real life data from California ISO have been carried out. The data was provided by the California ISO engineering support team created for this project. Simulation results have shown that the proposed methodology is quite accurate and efficient.
- The concept of probabilistic tool integration into EMS has been developed. The concept includes three levels of integration: a passive level, an active level, and a proactive level. The passive integration level implies integration of wind forecast information and its visualization without introducing any changes to the EMS algorithms. On the active level, the unit commitment (UC) and economic dispatch (ED) procedures are repeated several times for every dispatch intervals to determine whether the system can meet extreme generation requirements caused by uncertainties for certain confidence level. The system “break points” are communicated to the user. The proactive level requires some modifications of the UC and ED algorithms in order to directly incorporate uncertainties into these procedures. In this case, the generation units will be committed and dispatched, so that these uncertainties would not create “breaking points.”
- A framework of probabilistic tool integration with AREVA’s EMS has been developed.
- An industrial software prototype and specification.

The following recommendations for next phase have been made:

- Integrate PNNL’s tool with an existing power grid operation software platform such as AREVA’s EMS or California ISO EMS.
- Conduct real-time simulation using the integrated system package with test systems.
- Continue development of the proactive integration approach.

Acknowledgements

The Pacific Northwest National Laboratory project team would like to thank the following people and organizations for their support on the project.

U.S. Department of Energy, Office of Energy Efficiency and Renewable Energy (EERE)
Megan McCluer, Program Manager, Wind and Hydropower Technologies Program
Stan Calvert, Manager, Technology Application

California Institute of Energy Environment (CIEE)
Dr. Merwin Brown, Director of Transmission Research
Larry Miller, Senior Research Advisor
Jim Cole, Senior Advisor

California Energy Commission (CEC)
Jamie Patterson, Contract Manager

California Independent System Operator (California CAISO)
Clyde Loutan, Senior Advisor, Planning and Infrastructure Development
Grant Rosenblum, Manager, Renewables Integration
Tim VanBlaricom, Manager, Floor Operations
William Bonnell, Program Manager, Renewable Energy

AREVA T&D Corporation
Brad Nelson, Principal Power Systems Engineer
David Thomas, Principal Power Systems Engineer

University of Washington
Dr. Richard D. Christie
Scott D. James Macpherson

Pacific Northwest National Laboratory
Dr. Kevin Schneider, Senior Research Engineer
John C. Bower, Senior Research Engineer
Christopher A. Bonebrake, Scientist
Kristy Huston, Technician
Matthew L. Hauer, Research Engineer
Dr. Tony B. Nguyen, Senior Research Engineer
Susan J. Arey, Project Specialist
Sheena L. Kanyid, Contracting Officer
Evan O. Jones, Product Line Manager
Carl H. Imhoff, Market Sector Manager, Energy Infrastructure
Mark P. Morgan, Manager, Energy Technology Development
Kim A. Chamberlin, Administrator

Glossary

Abbreviation	Term	Meaning
AS	Ancillary Services	Services that are necessary to support the transmission of capacity and energy from resources to loads while maintaining reliable operation of the power system in accordance with Good Utility Practice. Ancillary services include scheduling, system control and dispatch, reactive supply and voltage control from generation sources, regulation and frequency response, energy imbalance, operating reserve – spinning, and operating reserve – supplemental.
AGC	Automatic Generation Control	Generation equipment that automatically responds to signals from the EMS control in real time to control the power output of electric generators within a prescribed area in response to a change in system frequency, tie line loading, or the relation of these to each other, so as to maintain the target system frequency and/or the established interchange with other areas within the predetermined limits.
BPA	Bonneville Power Administration	A U.S. government electric utility in the Pacific Northwest.
CAISO	California Independent System Operator Corp.	Independent system operator controlling most of the California electric power system.
CEC	California Energy Commission	California's primary energy policy and planning agency.
CDF	Cumulative Distribution Function	Describes the probability distribution of a real-valued random variable.
COPT	Capacity Outage Probability Table	A table that contains all the capacity states in an ascending order of outages magnitude. Each outage (capacity state) is multiplied by its probability. If the system contains identical units, binomial distribution can be used. If the units are not identical, then an appropriate procedure is used.
CV	Columbia Vista	Columbia Vista Corporation
DAM	Day Ahead Market	The market for energy for the following day, or more specifically, the market for energy 24 hours in advance of a given time in any day.
DOE	Department of Energy	U.S. Department of Energy
EERE	Energy Efficiency and Renewable Energy	Office of Energy Efficiency and Renewable Energy within the U.S. Department of Energy
EFORd	Equivalent Forced Outage	A measure of the probability that a generating unit will not be available due to forced outages or forced deratings when there

	Rate demand	is a demand on the unit to generate. Used in the calculation of unforced capacity rating of wholesale electrical generating plants.
EMS	Energy Management System	A computer control system used by electric utility dispatchers to monitor the real-time performance of the various elements of an electric system and to control generation and transmission facilities.
FOP	Full Outage Probability	The probability of full outage.
FOR	Forced outage rate	This expresses the probability of outage of generating units (not operating).
FORd	Forced Outage Rate demand	The forced outage rate equals the historical percentage of the generator's maximum output lost to forced outages when such output is demanded.
GADS	Generating Availability Data System	A database produced by the North American Electricity Reliability Council. GADS is the main source of power station outage data in North America. It comprises the generating unit availability for over 90% of the total installed generating capacity of the continent, and tracks a large number of variables, providing detailed descriptions of unit operations and outage conditions. One example of such detail is that in its data pertaining to forced outages and unplanned unit failures, it makes the fine distinction between immediate, delayed, and postponed outages.
HAS	Hour Ahead Scheduling	A process for trading hourly energy and ancillary services based on bids submitted up to 75 minutes ahead of a trading hour.
HE	Hour Ending	This is used to define the trading interval.
IEEE	Institute of Electrical and Electronics Engineers	An international non-profit, professional organization for the advancement of technology related to electricity. IEEE is the world's largest professional association advancing innovation and technological excellence for the benefit of humanity.
ISO	Independent System Operator	Independent system operators operate the power system under their jurisdiction.
MATLAB	MATLAB Software	A numerical computing environment and programming language.
MRTU	Market Redesign and Technology Upgrade	New market design at the California ISO.
MTTF	Mean Time To Failure	An estimate of the average, or mean time, until a design's or component's first failure,
MTTR	Mean Time To Repair	Basic measure of the maintainability of repairable items, it represents the average (mean) time required to repair a failed component or device.
NERC	North America Electric Reliability Corporation	NERC's mission is to improve the reliability and security of the bulk power system in North America. To achieve that, NERC develops and enforces reliability standards; monitors the bulk power system; assesses future adequacy; audits

		owners, operators, and users for preparedness; and educates and trains industry personnel. NERC is a self-regulatory organization that relies on the diverse and collective expertise of industry participants. As the Electric Reliability Organization, NERC is subject to audit by the U.S. Federal Energy Regulatory Commission and governmental authorities in Canada.
NRTO	Near Real Time Optimizer	An optimizer running near real time.
PDF	Probability Density Function	A real-valued function whose integral over any set gives the probability that a random variable has values in this set. Also known as density function; frequency function.
PNNL	Pacific Northwest National Laboratory	A U.S. Department of Energy national laboratory located in the Pacific Northwest. The Laboratory is operated by Battelle Memorial Institute.
RTED	Real Time Economic Dispatch	A market for trading imbalance energy and dispatching ancillary services at regular intervals.
RTM	Real Time Market	Real time market (RTM) at California ISO is a market for trading energy and ancillary services in real time.
RTO	Regional Transmission Organization	A Regional Transmission Organization (RTO) in the United States is an organization that is responsible for moving electricity over large interstate areas. Like a transmission system operator (TSO), an RTO coordinates, controls, and monitors an electricity transmission grid that is larger with much higher voltages than the typical power company's distribution grid. TSOs in Europe cross state and provincial borders like RTOs.
RTUC	Real Time Unit Commitment	RTUC looks out between four and seven 15-minute intervals to ensure there is sufficient capacity to meet the demand. RTUC commits and de-commits short start units and procures additional AS.
RUC	Residual Unit Commitment	The RUC process provides a reliability backstop for the California ISO to commit additional units in order to meet its reliability requirements. The California ISO performs RUC during its DAM and RTM mainly to commit additional resources.
STUC	Short Term Unit Commitment	A reliability function for committing short and medium start units to meet the California ISO forecast of California ISO demand. The STUC function is performed hourly, in conjunction with RTUC, and looks ahead up to three to five hours beyond the trading hour.
UC	Unit Commitment	A program used to commit an appropriate number of generating units for each hour for an elongated period (e.g., 24 hours) so that demand and ancillary services can be met at minimum cost, taking into account resource and operating constraints.
UR	Uncertainty Range	Defines an interval within which a numerical result is expected to lie within a specified level of confidence.

VSTLP	Very Short-Term Load Predictor	Load forecast in a very short term.
WECC	Western Electricity Coordinating Council	WECC is responsible for coordinating and promoting electric system reliability in the Western Interconnection. WECC supports efficient competitive power markets, ensures open and non-discriminatory transmission access among members, provides a forum for resolving transmission access disputes, and provides an environment for coordinating the operating and planning activities of its members as set forth in the WECC Bylaws.

Contents

Figures

Tables

1.0 Introduction

The work described in this report was performed by the Pacific Northwest National Laboratory (PNNL) and funded by the Office Energy Efficiency and Renewable Energy, U.S. Department of Energy (DOE-EERE).

Because conventional generators need time to be committed and dispatched to a desired megawatt (MW) level, the scheduling and load following processes use load and wind power production forecasts to achieve future balance between the conventional generation and energy storage on the one side, and system load, intermittent resources (such as wind and solar generation) and scheduled interchange on the other side. The power system balancing process, which includes the scheduling, real time dispatch (load following) and regulation processes, is traditionally based on deterministic models.

Uncertainties in forecasting the output of intermittent resources such as wind and solar generation, as well as system loads are not reflected in existing energy management systems (EMS) and tools for generation commitment, dispatch and market operation. With the growing penetration of intermittent resources, these uncertainties could result in significant unexpected load following and dispatch problems, and pose serious risks to control and operation performance characteristics as well as the reliability of a power grid. Without knowing the risks posed by the uncertainties, the system operators have limited means to weigh the likelihood of occurrence and the magnitude of problems to mitigate adverse impacts caused by them. Some important questions need to be addressed in counteracting the impact of uncertainties. For instance, when and if should one start more units to balance against possible fast ramps in the future over a given time horizon?

Furthermore, these uncertainties could require procuring additional costly balancing services. Major unexpected variations in wind power, unfavorably combined with load forecast errors and forced generator outages could cause significant power mismatches, which could be essentially unmanageable without knowing these variations in advance.

Because the actual load and intermittent generation can deviate from the forecasts, it becomes increasingly unclear (especially, with the increasing penetration of renewable resources) whether the system would be actually able to meet the conventional generation requirements within the look-ahead horizon, what the additional balancing efforts would be needed as we get closer to the real time, and what additional costs would be incurred by those needs.

In order to improve the system control performance characteristics, maintain system reliability, and minimize expenses related to the system balancing functions, it becomes necessary to incorporate the projected uncertainty ranges into the scheduling, load following, and, in some extent, into the regulation processes. This need has been realized already, and some wind forecast service providers offer the uncertainty information for their forecasts. Works are in place to develop methodologies and tools to incorporate these uncertainties into power system operations. Unfortunately, in many cases, these efforts are limited to wind generation uncertainties only, and ignore the fact that there are additional sources of uncertainty such as system loads and forced generation outages. Most of the works are considering only the uncertainty ranges for the MW imbalances, and do not address additional essential characteristics such as ramps and ramp duration uncertainties.

It is very important to address the uncertainty problem comprehensively, by including all sources of uncertainty (load, intermittent generation, generators' forced outages, etc.) into consideration. All aspects of uncertainty such as the imbalance size (which is the same as capacity needed to mitigate the imbalance) and generation ramping requirement must be taken into account. The latter unique features make this work a significant step forward toward the objective of incorporating of wind, solar, load, and other uncertainties into power system operations.

Some of the existing works are also targeting similar objectives. For instance, AWS Truewind [1] and 3TIER [2] companies developed the wind generation forecasting tools with build-in capability to assess the wind generation production uncertainty. Similar works are performed in Europe. In the framework of the European Union project, ANEMOS, a tool for on-line wind generation uncertainty estimation based on adapted resampling or quantile regression is developed [3]. The German company Energy and Meteo Systems developed a tool for wind generation forecasting and assessing the uncertainty ranges associated with wind forecast and also capable to predict the extreme ramping events [4]. Interval forecast of wind generation using quantile method is given in [5]. Prediction error of wind generation forecast using standard deviation based statistical analysis is used in [6]. These works primarily concentrate on the wind generation uncertainties, whereas the other important sources of uncertainty are not addressed. This limited consideration could be misleading to power system operators responsible for system reliability and control performance characteristics.

In this project, the uncertainties associated with wind power generation forecasting, load demand forecasting, and generation supply interruptions caused by forced outages are taken into account in the evaluation of uncertainty ranges for the required generation performance envelope, including balancing capacity, ramping capability and ramp duration. A probabilistic algorithm, based on the proposed histogram analysis to assess the capacity and ramping requirements, is presented. Preliminary simulation was performed using California ISO's system model and data. This report presents these simulation results confirming the validity and efficiency of the proposed solutions.

A probabilistic software tool capable of determining the impact of wind, load and generation uncertainties on the power grid is currently under development. In the research, an assessment of generation capacity requirements means evaluation of uncertainty ranges of generation requirements in order to meet the power system balance.

The objectives of the work reported in this report include the following developments:

- A probabilistic model to evaluate uncertainties of the wind and load forecast errors and to provide rapid (every 5 minutes) look ahead (up to 5-8 hours ahead) assessments of their uncertainty ranges.
- Similar models to evaluate uncertainties caused by generator random forced outages, failures to start up, and contingency activation processes.
- An integrated tool that consolidates abovementioned continuous and discrete random factors contributing to the overall uncertainty to evaluate look ahead worst-case balancing generation requirements (performance envelopes) in terms of the required capacity, ramping capability, and ramp duration.
- A methodology and procedures for self-validation of the predicted performance envelope for each look-ahead interval.

- Visualization displays to communicate information about the expected ramps and their uncertainty ranges.
- A prototype unit commitment program incorporating future uncertainties.
- Integration of the developed tools with the AREVA's EMS system
- Use of the actual California ISO (CAISO) data to perform simulation.
- Review of the actual dispatch scheduling processes in CAISO and Bonneville Power Administration (BPA).

The proposed approach to evaluate the uncertainty ranges for a required generation performance envelope, including the balancing capacity, ramping capability and ramp duration, consists of the following three stages (Figure 1.1):

1. The first stage deals with acquiring statistical data. Retrospective information for a user-specified moving window (e.g., for one month), such as forecasted system load and its actual values, wind and solar generation forecasts and its actual values, as well as generation schedules, are needed to perform the proposed statistical analysis and to build a projection of the balancing requirements into the future.
2. The second stage is a statistical analysis of the retrospective information acquired at the first stage. It consists of the following parts:
   - Capacity requirements analysis based on an empirical statistical analysis of forecast errors
   - Ramping requirements analysis based on the "swinging door" algorithm.
   - Generation forced outage analysis based on the Markov chain reliability model.
3. The third stage is an evaluation of future generation requirements for specified time horizons, e.g., 5 or 8 hours ahead. Examples of generation requirements that can be evaluated are regulation and load following capacity requirements, ramping requirements, contingency reserve requirements, etc., for different confidence levels such as 80, 85, 90 and 95% (as shown in Figure 1.1).These requirements can be compared against the actual generation capability of generators that are currently or will be online within the look-ahead horizon and that are performing relevant services. If the actual generation capability is not matching the requirements, a warning will be issued to system operators. This would constitute a "passive" integration of wind related uncertainties into the system operations. In a proactive approach, the look-ahead generation requirement information will be fed back into the generation commitment and dispatch procedures in order to modify them and to make sure that the generators are committed on time and dispatched to be able to meet the capacity, ramping and ramp duration requirements with certain level of confidence for the entire look-ahead period.

The report is organized as follows. Section 2 evaluates uncertainties associated with the system load forecast and wind generation forecast using different statistical methods. Section 3 presents generator forced outage model recognizing that these are discrete events. Section 4 reviews the current operating processes and schedules followed by the CAISO and the BPA. Section 5 shows how the probabilistic tool developed in Sections 2 and 3 can be integrated with an EMS system. Three modes of integration have been developed. These are "passive," "active," and pro-active integration. It also offers ISOs a choice while integrating the probabilistic tool with their security constrained unit commitment program. Section 6 presents a unit commitment method based on genetic algorithm optimization technique used in this study to simulate EMS integration techniques. Section 7 presents software prototype design and testing, Section 8 provides conclusions and future work, and a list of references is provided in Section 9.

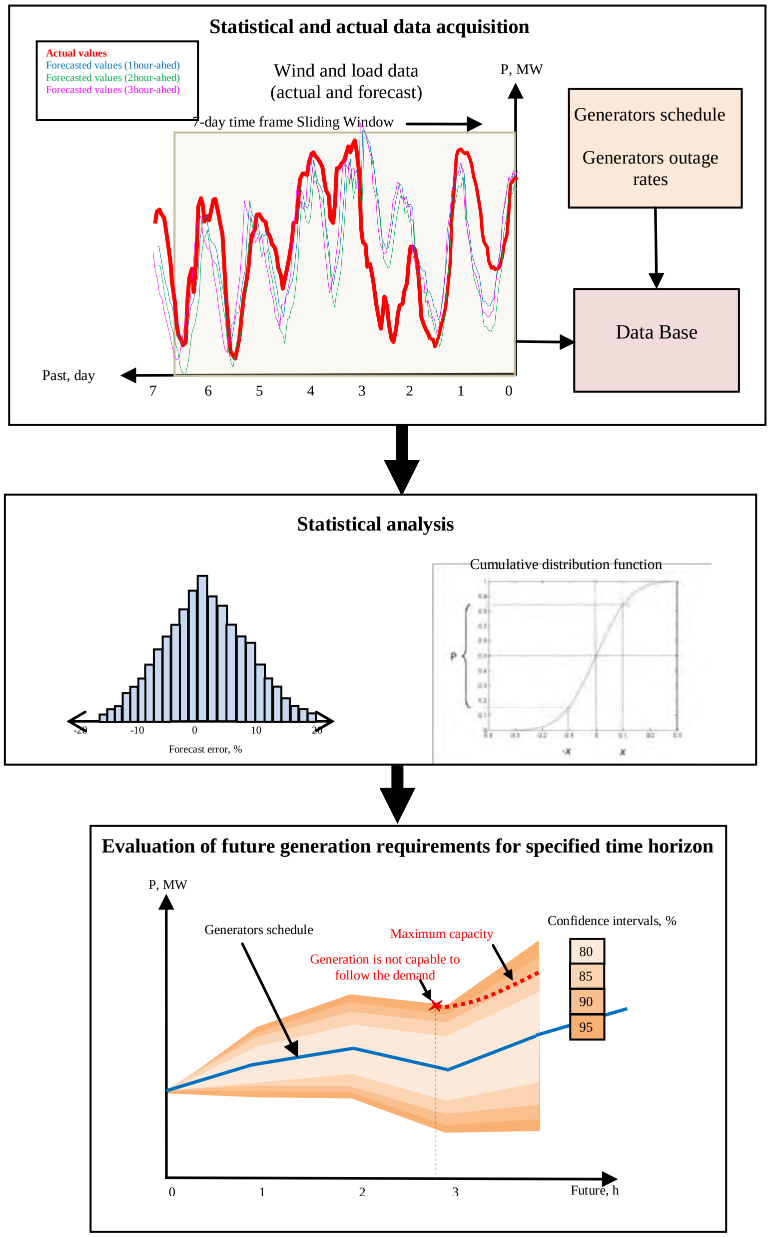

Figure 1.1. Methodology Concept

2.0 Load and Wind Generation Uncertainties Evaluation

This section describes an innovative methodology that is capable of evaluating future generation requirements including the required capacity, ramping capability, and ramp duration capability (these characteristics form the so-called performance envelope). The methodology incorporates uncertainties caused by wind generation and load forecast errors as well as (potentially) uninstructed generation deviations of conventional generation. These tools meet the industry need in a more robust (that is, more reliable for a range of possible future operating conditions) assessment of the balancing reserves required in a control area.

The previous works discussed in the introduction [1]–[6], address only a single source of uncertainty: the one related to wind generation. Because the influence of the other sources of uncertainty is not reflected in the assessment, the resulting confidence intervals could be misleading for the system operators. Unlike these existing approaches, the methodology developed in this report addresses all sources of uncertainty including the uncertainties surrounding the load forecasts, uncertainties associated with the forced generator outages, and uncertainties caused by forced generation outages (see Section 3.0).

A “flying brick” method was developed in this study to assess the look ahead worst-case performance envelope requirements and to be able of ensuring the system capability to balance against the uncertainties with certain specified degree of confidence. The “flying brick” approach idea is to include the ramp rate, ramp duration, and capacity requirements simultaneously and directly into the balancing process, and then look for the worst combinations of these parameters located along the vertices’ trajectories of the “flying brick.”

2.1 Generation Reserves

According to the Western Electricity Coordinating Council (WECC), standard power systems are required to maintain the following types of reserves [7]:

Operating reserve – is the generation capacity above the one needed to supply firm system demand that is required to provide for regulation, to balance against the load forecasting error and equipment forced and scheduled outages, and to maintain local area reliability. It consists of spinning reserve and non-spinning reserve.

Spinning reserve – Unloaded generation that is synchronized, automatically responsive to frequency deviations, and ready to serve an additional demand. It consists of regulating reserve and contingency reserve.

Non-spinning reserve – 1. The generating reserve, which is not connected to the system but capable of serving the demand within a specified time from its activation. 2. Loads or exports that can be removed from the system in a specified time.

Regulating reserve – An amount of reserve responsive to automatic generation control (AGC), which is sufficient to provide normal regulating margin.

Contingency reserve – The capacity available to be deployed by a balancing authority (BA) to meet the North America Electric Reliability Corporation (NERC) and WECC contingency reserve requirements. Increasing penetration of wind and solar generation leads to growing uncertainties in the reserve requirements.

In the study, the term "assessment of generation capacity requirements" refers to the evaluation of uncertainty ranges for generation requirements needed to achieve the power system balance. These uncertainty ranges define intervals within which the future generation requirement is expected to lie with a specified level of confidence.

Uncertainties associated with wind and solar intermittency, electrical load variability, and unexpected generation outages are considered in this report. These uncertainties affect the load following needs as well as regulating and contingency reserve requirements. Details regarding the load and wind/solar generation uncertainties are given in this section; description of the generation forced outage model is presented in Section 3.0. In general, the generation capacity allocation is performed by the unit commitment (UC) process, as shown in Figure 2.1 [8].

To integrate the probabilistic tool into an EMS system, it is necessary to take into account the operating practices of the given power system. In Section 4.0 details of the operating practices in CAISO and BPA are presented.

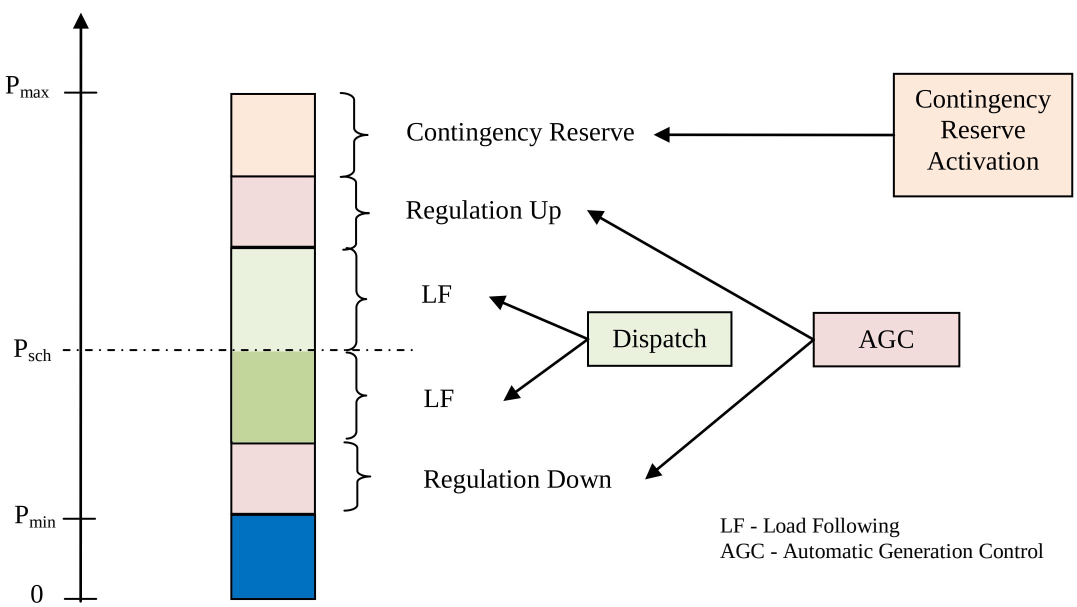

Figure 2.1. Allocation of Generation Unit Capacity

2.2 Load Forecast Uncertainty

The uncertainty associated with the load forecast is one of the most influential factors influencing the resulting uncertainty. In Figure 2.2, the load forecast uncertainty for one of the balancing authorities is shown. The solid blue curve shows the hourly average demand over one month, while the red curve shows the day-ahead load forecast for the same time period - Figure 2.2(a). The load forecast error is presented in Figure 2.2(b). One can see that day-ahead load forecast varies within the ±8% range. What is also important is the fact that the system load is normally more significant than wind or solar generation, so that even if the load forecast is more accurate than the forecast for the intermittent resources (in terms of the percentage error), the MW values of the errors can be quite comparable.

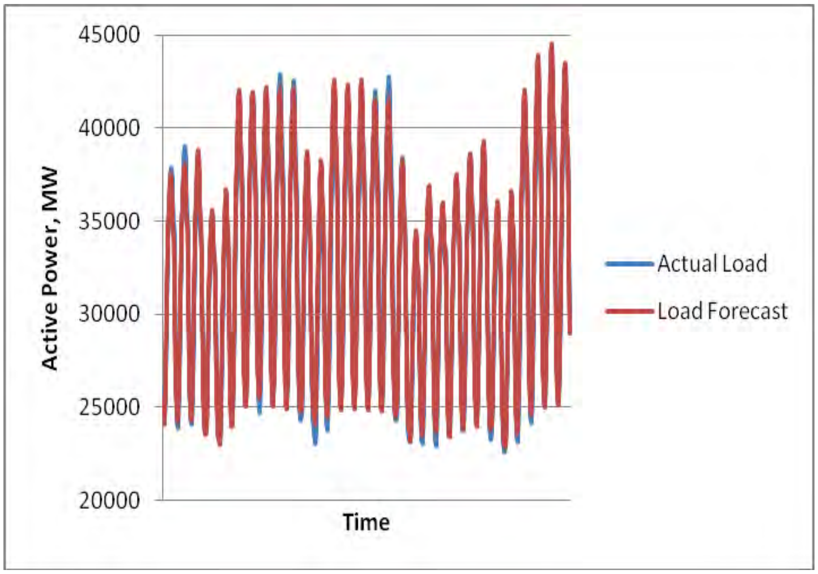

a)

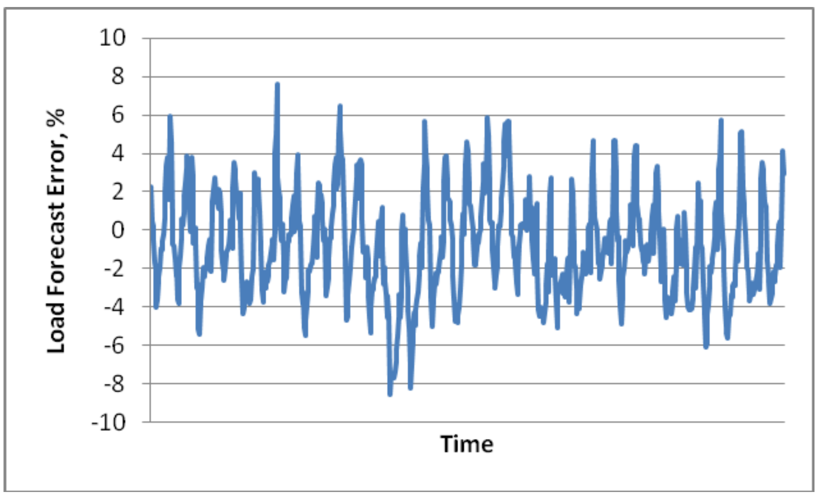

b)

Figure 2.2. Load Fluctuation and Uncertainty: a) Load Forecast vs. Actual Load; b) Load Forecast Error

2.3 Net Load Uncertainty

Wind and solar generation and power system load demand have a number of similar features:

- Wind/solar generation and most of the load are non-dispatchable resources;
- They both have cycling behavior;
- They both depend on the weather conditions;
- They deviate from the forecast, etc.

Actually, wind generation has more in common with electrical load, than with traditional (dispatchable) generation. Therefore, wind generation can be considered as a negative load. At the same time, electrical load and wind/solar generation cannot be considered as independent statistical variables. The correlation between load and wind generation forecast errors is shown in [9], [10]. To address this issue, the net load concept is commonly used in wind integration studies to assess the impact of load and wind generation variability on the power system operation. The net load has the following definition: net load is total electrical load minus total wind generation output minus total solar generation output plus the interchange.

2.4 Statistical Methods to Evaluate the Forecast Uncertainty

There are different approaches that can be used for the uncertainty analysis of the forecast errors. In this work, we analyzed two methods in terms of their applicability for the purpose of this project: distribution fitting and empirical probability.

2.4.1 Distribution Fitting Approach

Probability distributions are based on assumptions about a specific standard form of random variables; for example, normal, uniform or Poisson distributions. Based on the standard distributions and selected set of its parameters, they assign probability to the event that the random variable takes on a specific, discrete value, or falls within a specified range of continuous values, [11].

Selecting a distribution model means choosing a standard probability distribution and then adjusting its parameters to fit the data [11]. For example, in [9] it is assumed that the load and wind forecast errors are described by the truncated normal distribution (TND).

The probability density function (PDF) of the truncated normal distribution is:

$$PDF_{TND}(x;\mu,\sigma,a,b)=\frac{\frac{1}{\sigma}PDF_N\left(\frac{x-\mu}{\sigma}\right)}{CDF_N\left(\frac{b-\mu}{\sigma}\right)-CDF_N\left(\frac{a-\mu}{\sigma}\right)} \tag{2.1}$$

where μ is the mean value of the non-truncated normal distribution;
σ is the standard deviation of the non-truncated normal distribution;
a, b are upper and lower limits of the non-truncated normal distribution;

$x \in (a,b), -\infty \le a < b \le \infty$;

$PDF_N\left(x;\mu,\sigma\right) = \frac{1}{\sigma\sqrt{2\pi}} e^{-\frac{(x-\mu)^2}{2\sigma^2}}$ is the probability density function of the standard normal distribution, and

$CDF_N(\cdot)$ is the cumulative distribution function (CDF) of the standard normal distribution.

The cumulative distribution function of the truncated normal distribution is:

$$CDF_{TND}(x;\mu,\sigma,a,b) = \frac{CDF_N\left(\frac{x-\mu}{\sigma}\right) - CDF_N\left(\frac{a-\mu}{\sigma}\right)}{CDF_N\left(\frac{b-\mu}{\sigma}\right) - CDF_N\left(\frac{a-\mu}{\sigma}\right)}, \quad a \le x \le b \tag{2.2}$$

An example of the load forecast error distribution is presented in Figure 2.3. The blue bars represent the histogram of the real load forecast error. The red curve depicts the TND of the load forecast error.

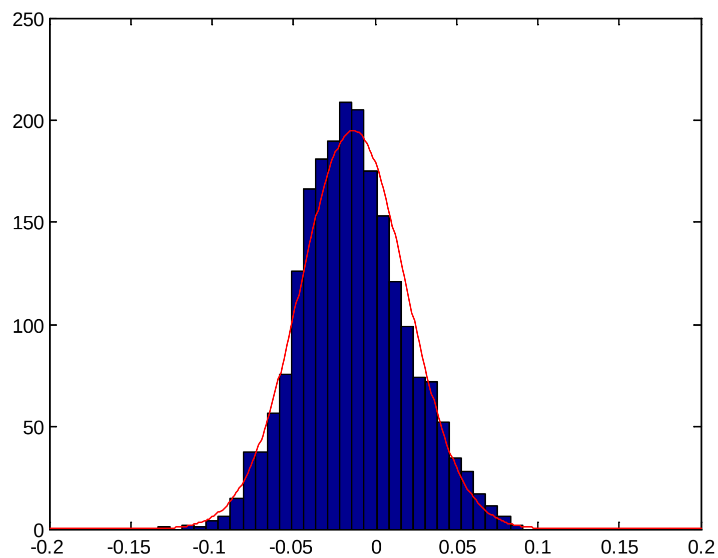

Figure 2.3. Load Forecast Error Histogram

2.4.2 Empirical Probability Approach

When data or statistics do not follow any standard probability distribution, so-called nonparametric models based on empirical probability distribution models become more appropriate. These models make no assumptions about the form of the underlying distribution, so no parameter estimates are needed [11]. An advantage of estimating probability distributions using the empirical modeling approach is that this procedure is relatively free of assumptions.

The idea behind building the empirical CDF is relatively simple. This is a function that assigns probability 1 over *n* to each of *n* observations in the analyzed dataset. The CDF for any specific parameter's value in the analyzed dataset is calculated by adding all probabilities for the samples with smaller values of the parameter of interest. Its graph has a stair-like appearance. If a sample comes from a parametric distribution (such as a normal distribution), its empirical CDF will resemble the parametric distribution. If not, the empirical distribution still gives an estimate of the CDF for the distribution [11]. An example of an empirical distribution (net load forecast error distribution and empirical CDF) are presented in Figure 2.4.

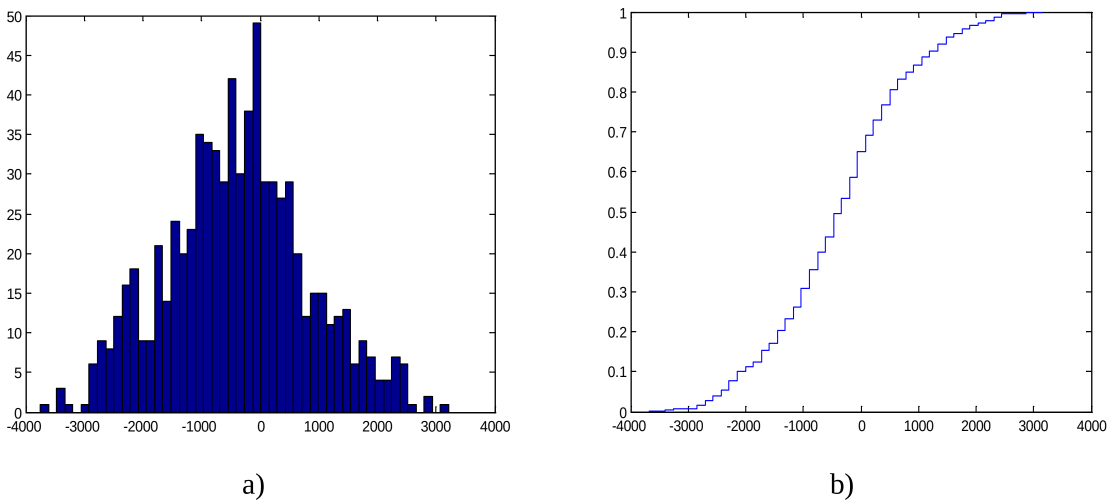

Figure 2.4. Net Load Forecast Error Distribution (CAISO data, June-August, 2007): a) Histogram; b) Empirical CDF

2.5 Assessment of the Generation Capacity Uncertainty

A statistical approach based on the time-varying empirical probability density function (PDF) is used in the study to determine the combined uncertainty ranges of the wind/solar and load forecast errors, as well as the effect of the forced generation outages. In this section, we only consider the wind and load forecast error uncertainties. The solar forecast error can be included into the consideration in the same way as the wind forecast error. The methodology to incorporate the generator forced outages uncertainty will be given in the following sections.

In our approach, wind and load forecast errors are summed together for each dispatch interval in the past within a sliding window. The sliding window size is selected to collect sufficient statistical information regarding the forecast errors. The information can be accumulated separately for each forecast horizon; for instance, for the hour-ahead forecast, two hours ahead forecast, and so on. Based on the collected statistics, the approach evaluates the percentile intervals (also called confidence intervals or uncertainty ranges) for each forecast horizon and different level of confidence. These intervals are assumed to be the same in the future dispatch interval; that is, for the next hour, the hour after that, and so on.

An example of wind generation forecast statistical characteristics for different look-ahead dispatch intervals (1, 2, 3, 4, and 5 hours ahead) for a real power system is presented in Figure 2.5. Figure 2.5 (a) shows the empirical probability density function and Figure 2.5 (b) shows the empirical CDF.

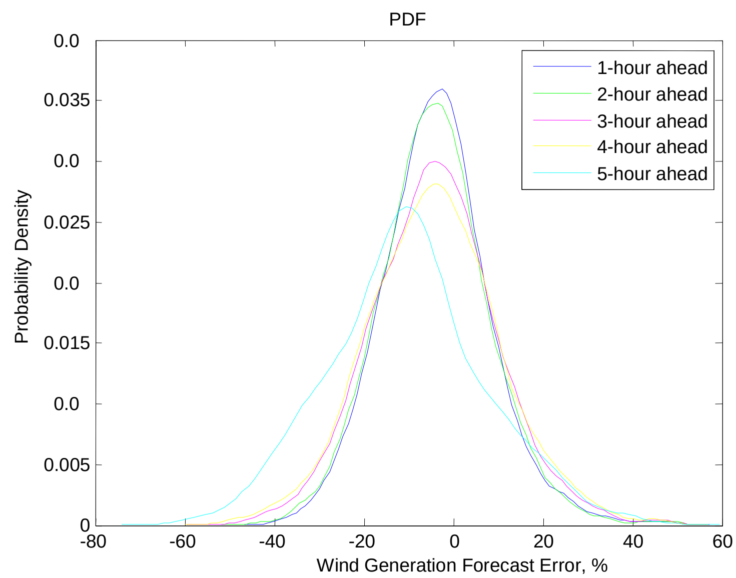

a)

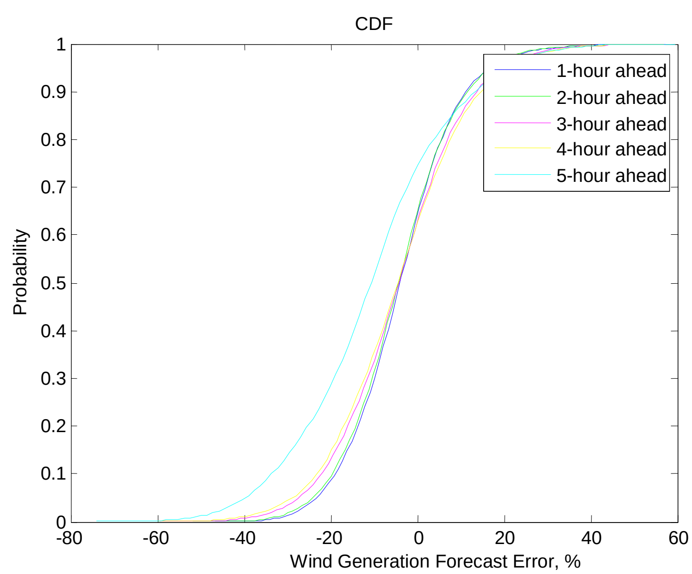

b)

Figure 2.5. Wind Generation Forecast Statistical Characteristic for Different Look-Ahead Period: a) PDF; b) Empirical CDF

The uncertainty range defines an interval within which a random parameter is expected to lie with a specified level of confidence. To determine an uncertainty range, it is necessary to find two solutions of the inverse CDF function corresponding to the desired percentiles on both ends of the distribution. The definition of the inverse CDF is the following:

If the CDF is strictly increasing and continuous, then the inverse CDF function $CDF^{-1}(p),\ p \in [0,1]$ is the unique real number *x* such that *CDF(x) = p*. The inverse of the CDF is called the quantile function. An evaluation of the quantile functions often involves special numerical methods.

Our task is to find the forecast error range $x_1 \ldots x_2$ to the given level of confidence *P*

$$CDF(x_2) - CDF(x_1) = p(x_1 \le X \le x_2) = \int_{x_1}^{x_2} PDF(x)dx \tag{2.3}$$

Inverse CDF functions for wind generation forecast errors for different look-ahead periods are presented in Figure 2.6. The uncertainty ranges are evaluated at 95% confidence level. The 95% uncertainty range corresponds to the 2.5 to 97.5 percentile of the distribution reflecting the uncertainty (Figure 2.6). It is obvious that the size of uncertainty ranges depends on the look-ahead time. It can be seen from Figure 2.6 that for the longer look-ahead periods, the uncertainty range becomes larger.

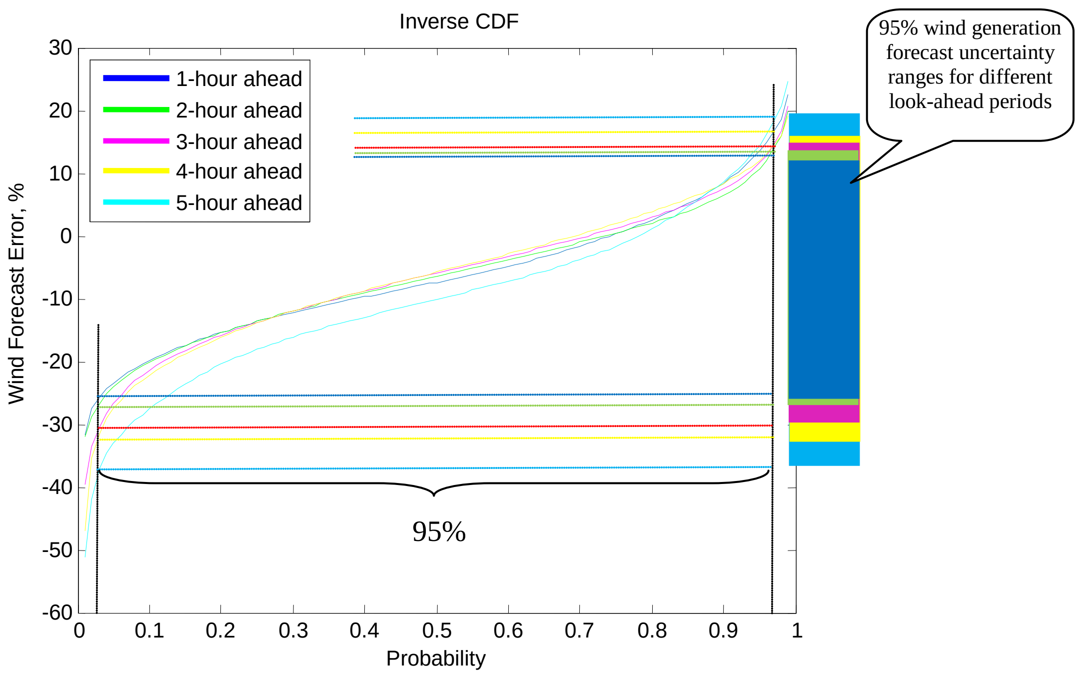

Figure 2.6. Wind Generation Forecast Inverse CDFs for Different Look-Ahead Intervals and 95% Uncertainty Ranges

2.5.1 Enhancement of Capacity Uncertainty Assessment

Statistical characteristics of wind generation forecast essentially depend on the level of predicted wind generation. For simplicity, all levels were combined in Figure 2.5. Therefore, the accuracy of uncertainty ranges evaluation model can be improved if the level of predicted wind generation is taken into account.

To enhance the uncertainty analysis methodology described above, the wind generation forecast can be divided into several intervals, depending on the level of predicted wind power production. The empirical statistical analysis is performed separately for each wind production level. Figure 2.7 shows an example of inverse CDFs of wind generation forecast errors calculated for different levels of wind generation forecast. Five intervals of wind generation forecast are considered: ”low wind,” ”below average wind,” ”average wind,” ”above average wind,” and ”high wind” levels.

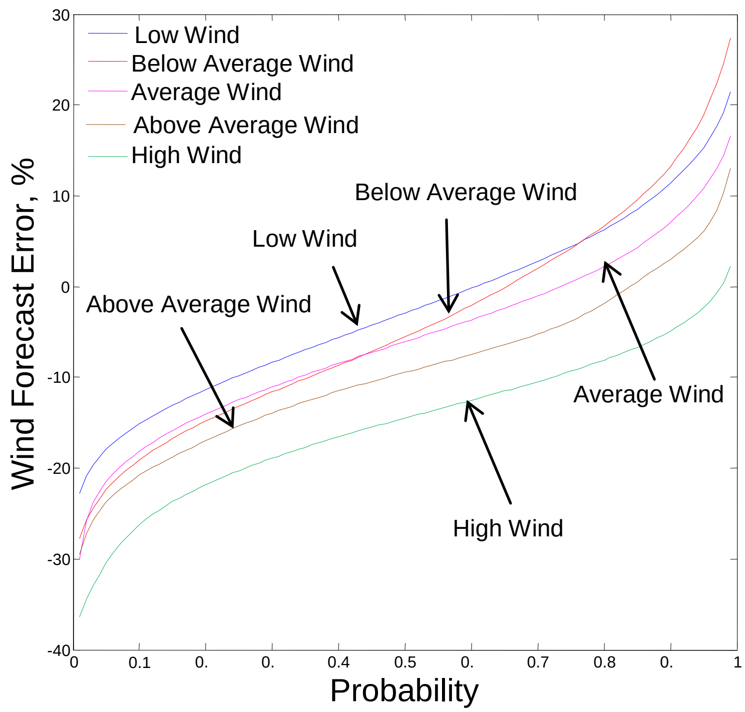

Figure 2.7. Inverse CDFs for Different Levels of Wind Generation Forecast

It can be observed from Figure 2.7 that the error distribution of the “low wind” forecast is close to the normal distribution, and that is varying within a ±20% range. The error distribution of the “high wind” forecast is biased. This fact can be explained by the observation that the actual wind generation cannot exceed the maximum installed wind generation capacity. Therefore, for the “high wind” forecast, the actual wind generation is mostly less than forecasted.

2.6 Assessment of Ramping Uncertainties

Assessment of ramping requirements is very important in case of integration of high amounts of wind generation into a power system. Sudden wind generation ramps can happen frequently and cause additional need in fast responsive generation units available on-line.

The required ramping capability needed to follow the net load curve, which covers all system imbalances, can be derived from the shape of the regulation and load following curves – see details in [10]. The “swinging door” algorithm is proposed for this purpose [10].

Figure 2.8 demonstrates the idea of the “swinging door” approach. A point is classified as a “turning point” whenever, for the next point in the sequence, any intermediate point falls out of the admissible accuracy range $\pm\varepsilon_{\Delta G}$. For instance, for point 3, one can see that point 2 stays inside the “door” *abcd*. For point 4, both points 2 and 3 stay within the “door” *abef*. But for point 5, point 4 goes beyond the ”door,” and therefore, point 4 is marked as a turning point.

Based on this analysis, we conclude that points 1, 2, and 3 correspond to the different magnitudes of the regulation signal, π_1, π_2 and π_3, whereas the ramping requirement at all of these points is the same, $\rho_{1\text{-}3}$ (see Figure 2.9) The swinging door algorithm also determines the ramp duration δ.

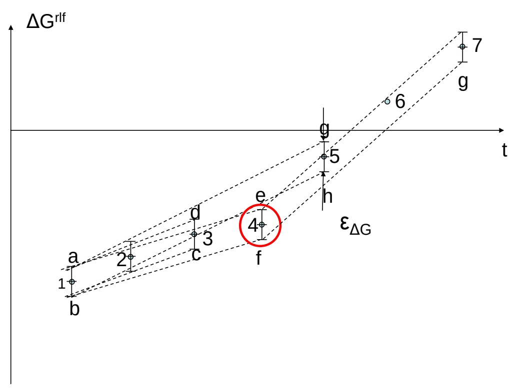

Figure 2.8. The Idea of "Swinging Door" Algorithm

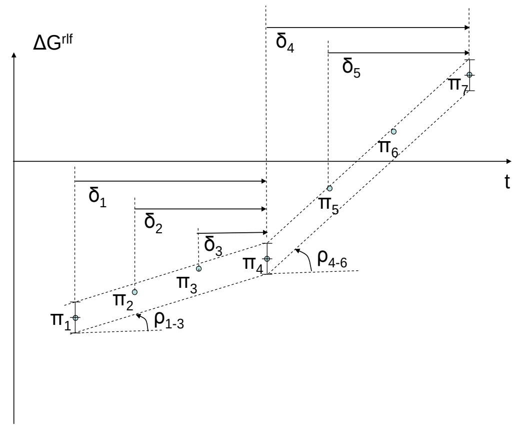

Figure 2.9. "Swinging Door" Algorithm – Obtaining Capacity, Ramps, and Their Duration

The regulation capacity and ramping requirements are inherently related. Insufficient ramping capability could cause additional capacity requirements. A multivariable statistical analysis can be applied to provide a concurrent consideration of the regulation and load following capacity, ramping, and ramp duration requirements. For the regulation/load following requirement curve, the "swinging door" algorithm is applied to determine the sequences of its magnitudes and ramps, $\pi_1, \pi_2, \ldots$, $\rho_1, \rho_2, \ldots$, and $\delta_1, \delta_2, \ldots$. The triads $(\pi_i, \rho_i, \delta_i)$ can be used to populate the three-dimensional space of these parameters (Figure 2.10). Let us define a rectangular box in the space that contains certain percentage of the points. If a point lies outside the box, the regulation/load following requirements are not met at this point. We will require that this probability must be below a certain minimum probability, $P_{\min}$. Our task is to find a position of the walls of the probability box that corresponds to a given $P_{\min}$. For given ranges of these three parameters, $\Delta\pi, \Delta\rho$ and $\Delta\delta$, a box can be plotted in this space, so that some triads are inside the box (N_{in}), some are outside (N_{out}). This approach helps determine the probability of being outside the box,

$$p_{out} = \frac{N_{out}}{N_{out} + N_{in}} \tag{2.4}$$

For example, assume that the confidence level for the analysis is established at 94%. Then for each dimension of the box, we can request that the probability of finding a point outside the box due to any of several possible reasons such as insufficient generation capacity (incremental or decremental), insufficient ramping capability (upward and downward), or insufficient ramp duration capability, is equal. This results in a requirement that only 1% of the points should be left on the outside on both sides of the box along any of the analyzed coordinates while adjusting its walls. Of course, it is desirable to eliminate double or triple counting of points that are found outside of the box due to more than one reason. The resulting size of the box determines the ranges of the generation requirements for the capacity, ramp, and ramp duration characteristics that are sufficient to meet the system needs in 94% of the cases.

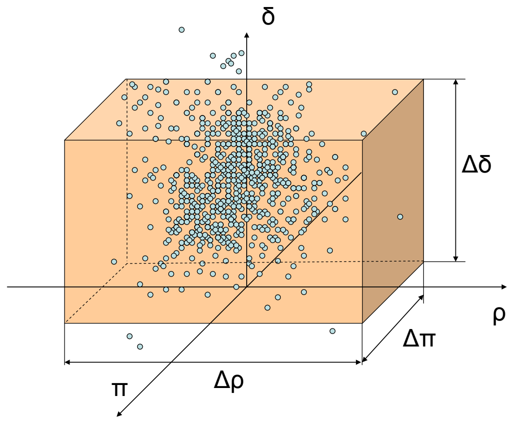

Figure 2.10. Concurrent Consideration of the Capacity, Ramping and Duration Requirements

2.6.1 "Flying Brick" Method

A method called "flying brick" is proposed in this study to analyze the time-varying extreme (worst-case) requirements applied to the look-ahead generation capacity, ramping capability and ramp duration. The "flying brick's" idea is to include a worst-case (for a given confidence level) combination of the ramp rate, ramp duration, and capacity requirements into the generation scheduling and dispatch processes. The three requirements are visualized as a three-dimensional probability box. Figure 2-11 demonstrates the idea of the "flying brick" method. The blue curve in the center is the expected generation requirement curve that meets the expected net load. The pink is the actual net load, which can deviate from its expected values. The generator requirement ranges with 95% and 93% confidence levels are also shown in Figure 2.11.

Suppose t_0 is the current time point. At this point, we apply the probability box algorithm to the 1-hour-ahead forecast errors. The three dimensions of the box are the capacity, ramp rate, and ramp duration requirements' ranges. The worst combinations of these parameters shown by the vertices of the probability box set a criterion for the generation characteristics needed to meet the system needs with a certain level of confidence. For example, the edge could correspond to the maximum capacity, maximum ramp, and maximum ramp duration within the covered uncertainty range for these parameters. For each time interval, the "flying brick" box is built based on the three-dimensional CDFs reflecting the ranges of the analyzed parameters induced by the forecasting errors.

Figure 2.12 presents the ramping requirement PDFs for different ramp durations. Inverse CDF functions of the ramp rate distribution for different ramp durations, obtained using the "flying brick" approach, are presented in Figure 2.13. Uncertainty range evaluation for ramping requirements is similar to capacity requirement evaluation (see Figure 2.6). Ramping requirement uncertainty ranges evaluated at the 95% confidence level are shown in Figure 2.13. It can be observed that the ramping ranges depend on ramp durations, and ramping requirements become lower for longer ramp durations.

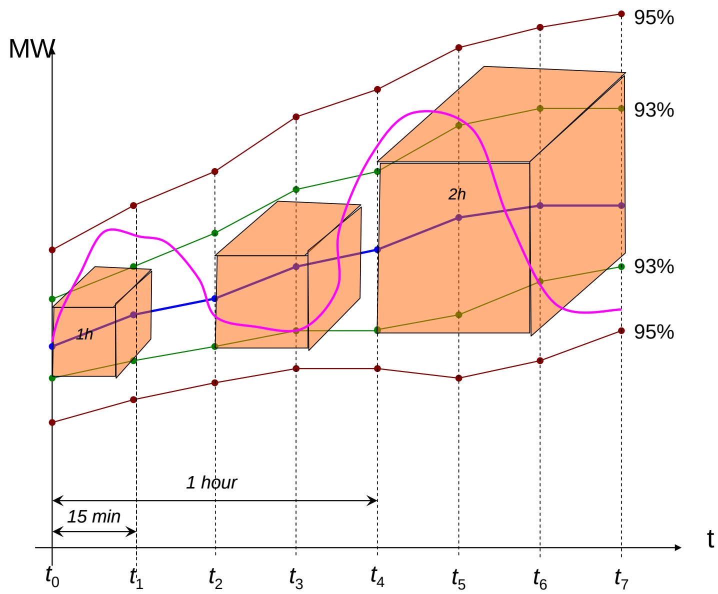

Figure 2.11. Idea of the “Flying Brick” Method

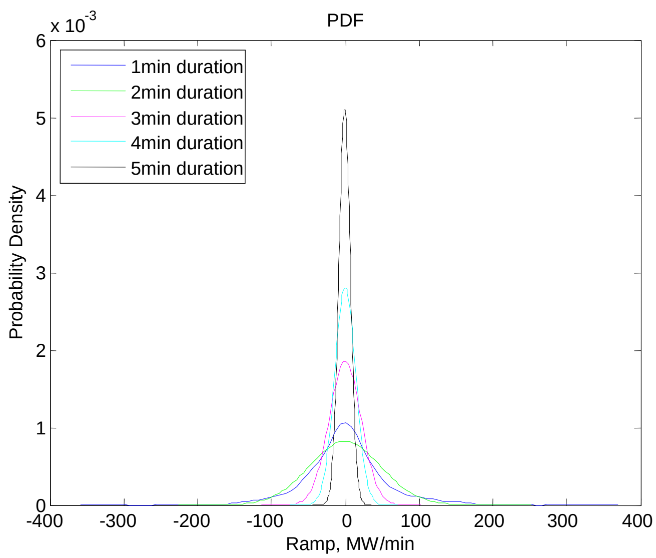

Figure 2.12. Ramping Requirement PDFs for Different Ramp Durations

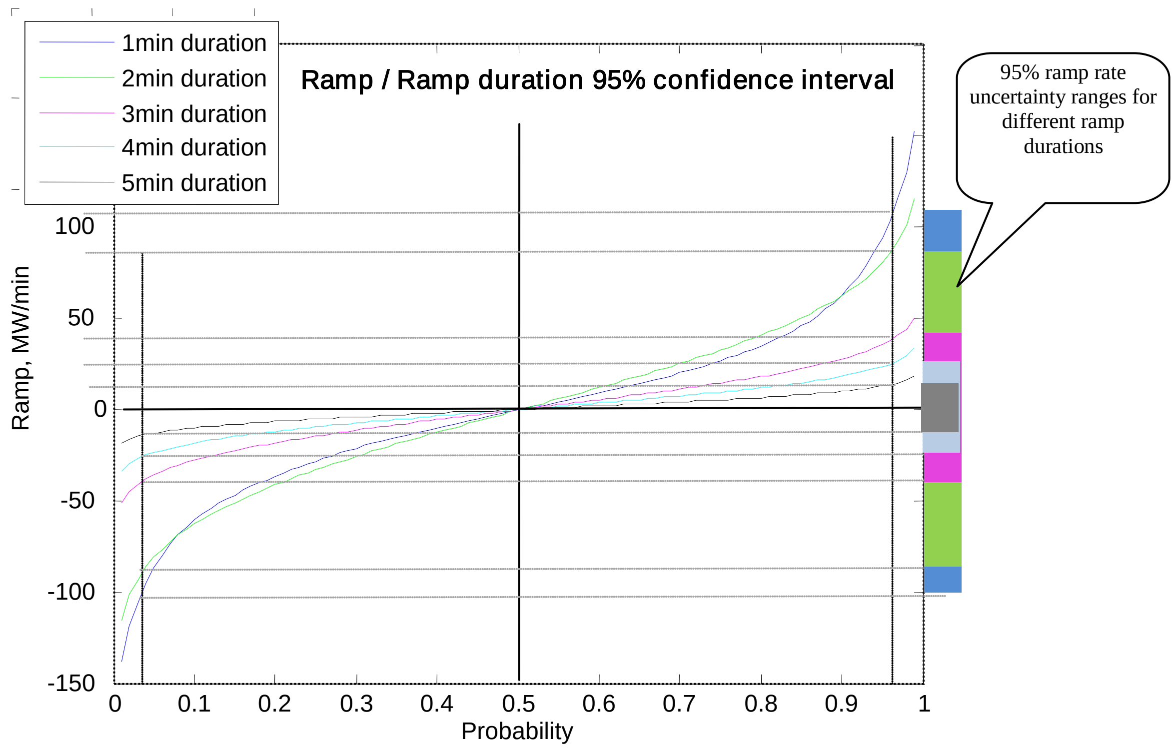

Figure 2.13. Ramping Requirement Inverse CDFs for Different Ramp Durations and 95% Confidence Intervals

2.7 Evaluation of Generation Requirements

Evaluation of generation requirements includes an assessment of generation capacity requirements and generation ramping requirements. Evaluation of balancing capacity requirements is shown in. The blue line corresponds to the generation schedule. The hour-ahead schedule with 1-hour resolution is considered in this example. Uncertainty ranges are calculated for each scheduling (dispatch) interval using individual statistical characteristics for a specified look-ahead horizon and taking into account the level of predicted wind generation, as it is obtained by the statistical analysis of retrospective information.

The following information, taken from a real system, was used in the example:

- Load
  - Actual load
  - 1(2,3,4,5)-hour-ahead load forecast
- Wind generation
  - Actual wind generation
  - 1(2,3,4,5)-hour-ahead wind generation forecast
- Hour-ahead generation schedule.

The process of building the resulting uncertainty characteristics is a repetitive process. The generation schedule, load and wind generation forecasts, and statistical characteristics of the retrospective data are updated each hour. A sliding window with a 1-hour refreshment rate was used to acquire continuously updated statistical information. Details on the data acquisition process and data requirements are given in Section 5.2 of the report. The uncertainty ranges are also updated hourly, taking into account changing generation schedules, load forecast, and wind generation forecast and their statistical characteristics.

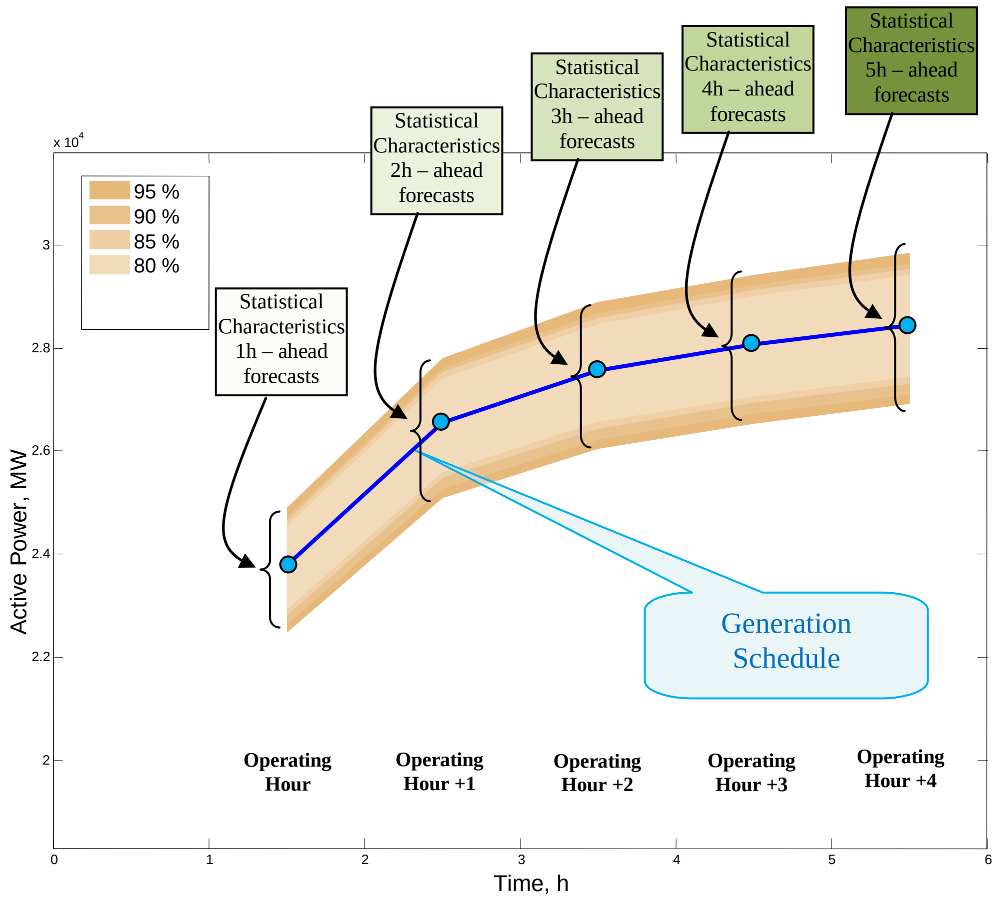

Figure 2.14. Evaluation of Capacity Requirements

2.8 Uncertainty Range Validation Approach

To validate the accuracy of the generation requirements uncertainty model, a validation approach is developed in this project. It is based on comparing the predicted uncertainty ranges against the actually observed ranges for the same dispatch intervals. The algorithm includes the following steps.

1. Acquire retrospective statistical information using the sliding window technique. The sliding window is updated hourly (or according to some other specified refreshment rate). Details can be found in Section 5.2

2. Perform a statistical analysis of the data acquired at step 1. The derived statistical characteristics are also updated hourly (or according to some other specified refreshment rate). See Sections 2.5 for details.

3. Evaluate uncertainty intervals for the future generation requirements using the statistical characteristics obtained at step 2. Uncertainty intervals are also updated according to a specified refreshment rate. See Section 2.7 for details.

4. When the predicted dispatch interval is reached, overlay the actual generation values over the previously forecasted uncertainty intervals, as shown in Figure 2.15, and determine which predicted uncertainty interval the actual generation value belongs to. Put this information into the validation table (Table 2.1). Note that for different look-ahead forecasted intervals, different tables should be used.

At the end of simulation, the following calculations are made:

1. Count how many points belong to the predicted intervals with a specified confidence level, and calculate the percentage of points found within the intervals (Table 2.1).

2. Compare the obtained percentages with targeted percentage values. The targeted percentages correspond to the confidence level of the interval. For example, for the 0 to 80% confidence interval, the targeted value is equal to 80%, and for 80 to 85% uncertainty interval, the targeted value is equal to 5%, etc (see Table 2.1).

The uncertainty algorithm is validated if the calculated percentages and the targeted percentages are close.

Table 2-1. Example of Validation Table (1- Hour Ahead Forecast)

	Day 1						…			Day N							Objective
Interval	1h	2h	3h	4h	….	24h	…	…	…	1h	2h	3h	…	24h	Total Points	Percentage, %	Values, %
0-80%	✓	✓					✓		✓	✓	✓			✓	803	80.3	80
80-85%			✓			✓						✓			46	4.6	5
85-90%				✓									✓		51	5.1	5
90-95%					✓										49	4.9	5
95-100%								✓							51	5.1	5
Total															**1000**	**100%**	

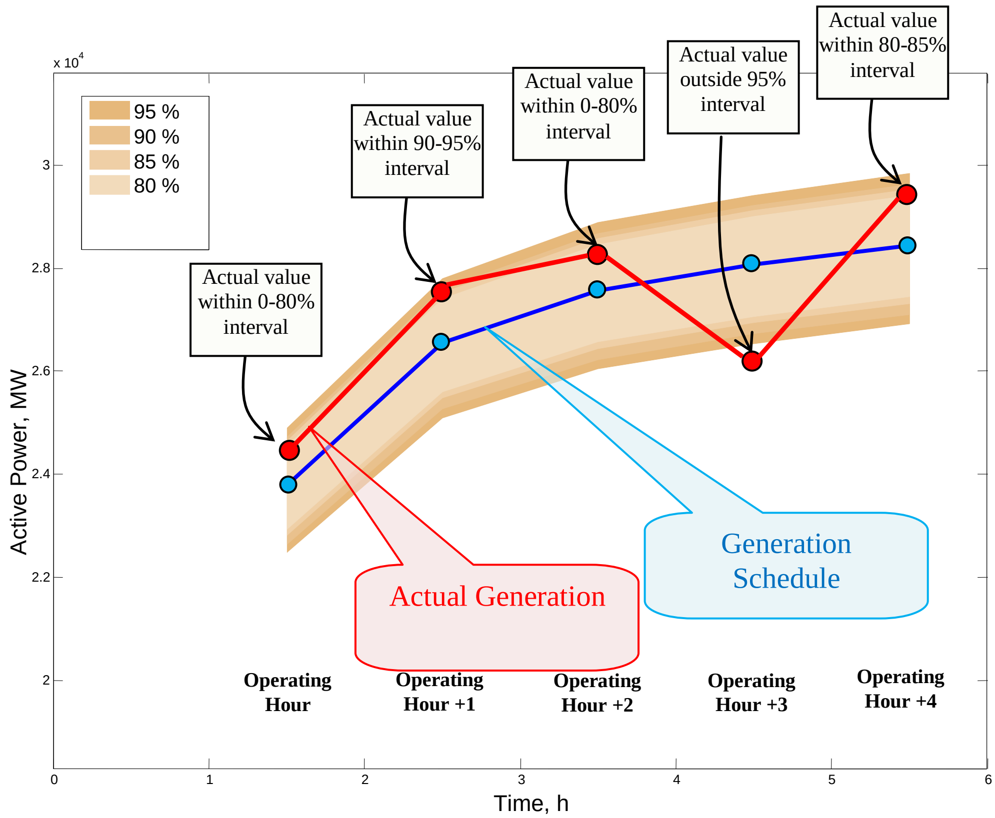

Figure 2.15. Validation Procedure

2.9 Simulation Results for Capacity Requirements

Simulations were performed using a probabilistic prototype tool developed in MATLAB [11] based on the validation approach presented in previous section. The MATLAB prototype interface is presented in Figure 2.16.

The actual system data from the Western interconnection were used.

- Simulation period: 70 days
- Sliding window length: 21 days
- Sliding window refreshment rate: 1 hour
- Generation schedule: Hour-ahead schedule (one hour resolution)
- Wind and load forecasts: 1 hour resolution, updated hourly, over a 5-hours time horizon

Results of the model validation runs for a real system are presented in Figure 2.17. The percentage numbers, labeled on the pie chart, are the confidence intervals. The targeted percentages are the intervals indicated in the legend. The blue slice of the pie has a targeted percentage of 80%, and the other colored portions correspond to 5% each. It can be seen from Figure 2.17 that the uncertainty validation procedure confirms the fact that the developed uncertainty prediction method provides a quite an accurate prediction of uncertainties.

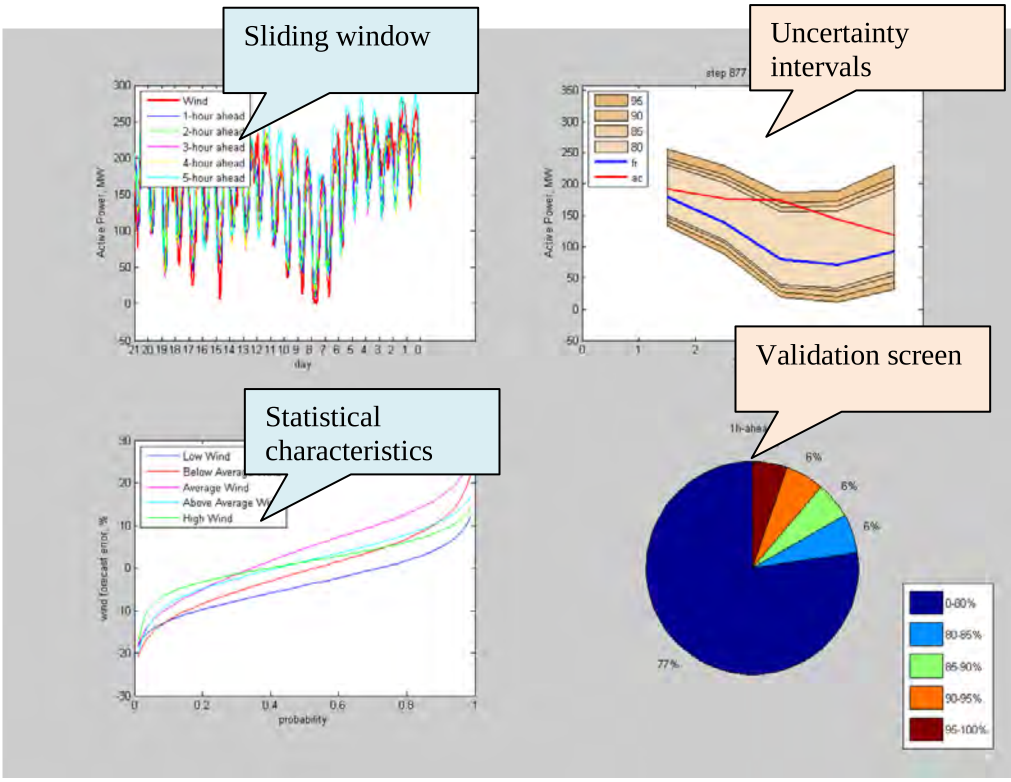

Figure 2.16. MATLAB Prototype Interface

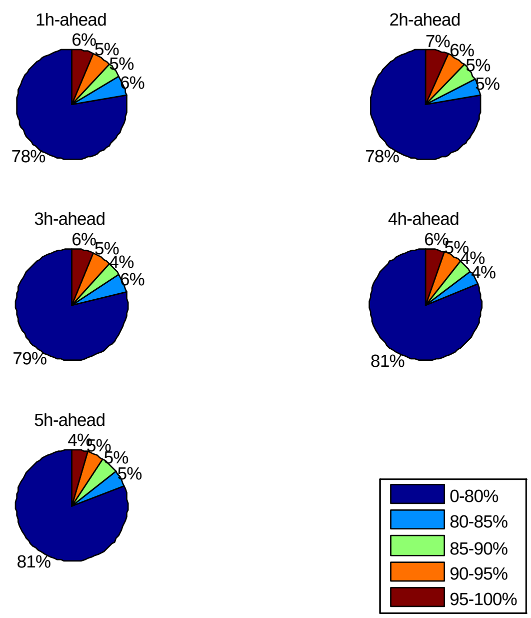

Figure 2.17. Results of Model Validation

3.0 Generator Forced Outage Model

This Section presents the generator forced outage model. The term “generator forced outage” usually refers to the shutdown of a generating unit for emergency reasons or a condition in which the generator unit is unavailable for supplying the load because of an unanticipated breakdown. Generator outage is a discrete event and may or may not happen in any given dispatch interval. This characteristic contrasts with the continuous nature of wind and load variations. Also, the size of the power mismatch caused by a forced outage depends on the generator that is disconnected and the generators’ load at the moment of the event. Any of the generators that are online within a dispatch interval could be forced out. The main challenge that has been overcome in this development was to combine the uncertainty information on continuous parameters (such as the generation capacity requirement) with discrete information (such as forced generation outages). This challenge has been successfully met in this project.

Forced outages of system generators cause temporary imbalances that must be eliminated within 10 minutes by activating the contingency reserve. Within this 10-minute interval, the system is exposed to an imbalance that can be as much as 1000 MW (the size of the largest generation unit in the system). The system inertia, governor response, and automatic generation control act to minimize the system power mismatch during the first seconds and minutes after the disturbance. Therefore, the generation controls and generation characteristics needed to balance the system must be sufficient to mitigate these possible mismatches. Again, there is an uncertainty associated with this process because the timing and the size of the forced outages are not known ahead of time and the contingency reserve activation process is not a deterministic process (for example, it depends on the characteristics of activated generators and type of activated reserve – spinning or non-spinning).

The project develops a methodology that evaluates additional uncertainty caused by forced generator outages and incorporates this information into the overall framework. This advanced feature constitutes a significant step forward in handling the uncertainty information in the modern EMS systems. As a result, the system reliability and control performance can be additionally improved.

Generator forced outages are stochastic events. Modeling statistical characteristics of generator forced outages is important for a correct evaluation of the future generation requirement. In the following sections, two types of generator forced outage models, i.e., the two-state Markov model and four-state Markov model, are described. The capacity outage probability table (COPT) and an example of COPT calculation are provided. Simulation results on forced outage model are also provided. The forced outage model is incorporated in the contingency reserve activation model developed by the University of Washington team subcontracted by PNNL in this project (Dr. Richard D. Christie and Scott D. James Macpherson). Details of the contingency reserve activation model can be found in Appendix B.

3.1 Forced Outage Rate Calculation

A generator outage is a discrete event and may or may not happen in any given hour. This feature contrasts with the continuous nature of the wind and load variations [12].

The simplest type of the generation unit model is a two-state Markov model as shown in Figure 3.1. Here the unit is assumed to always be in one of the two states: “up” – fully available, running, and subject to a possible failure; or “down” – totally unavailable, not running, and undergoing repair [13], [14].

Here, μ (repairs/year) is the repair rate, $r=1/\mu$ (years) is the mean downtime due to a forced outage (mean time to repair - MTTR), λ is the failure rate, (failures/year), and $m=1/\lambda$ is the mean up time between failure events (mean time to failure - MTTF). The unit’s forced outage rate (FOR) is the probability that the unit is down:

$$FOR = \frac{\lambda}{\lambda + \mu} = \frac{r}{m + r} = \frac{FOH}{SH + FOH} \tag{3.1}$$

where FOH is the forced outage duration within a year, (hours), and SH is the service hours within a year.

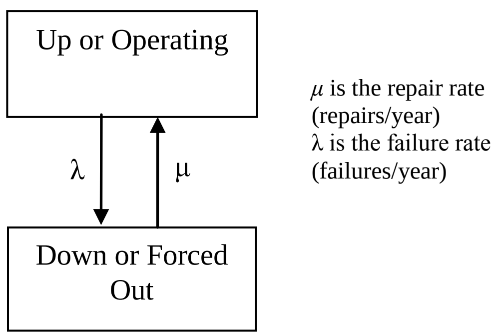

Figure 3.1. Two-State Markov Model

The two-state model is a valid representation for base load units but does not adequately represent intermittent operating units used to meet peak load conditions. The two-state model for a base load unit has been extended to the four-state peaking unit model shown in Figure 3.2, which is widely used in practice [14],[15]. The model assumes that the generating unit is either fully available or totally unavailable, but also considers that the unit may be either needed or not needed [14].

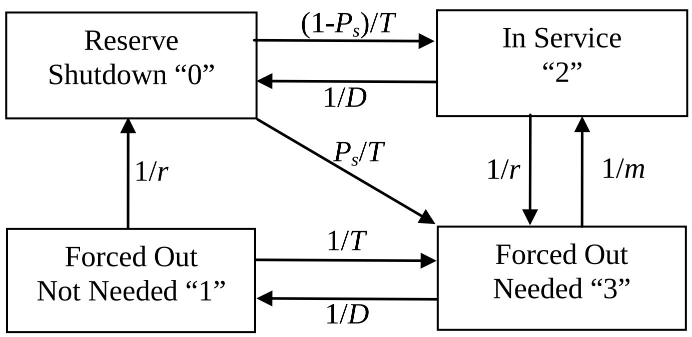

D is the average in-service time per occasion of demand;
T is the average reserve shutdown time between periods of need;
r is the average repair time per forced outage occurrence;
m is the average in-service time between occasions of forced outage when needed;
P_s is the probability of a starting failure resulting in inability to serve load during all or part of a demand period.

Figure 3.2. IEEE Four-State Markov Model

The frequency balance equations for the four-state model shown in Figure 3.2 are as follows [13], [14]:

$$\begin{cases} P_2 \times \left(\dfrac{1}{D} + \dfrac{1}{m}\right) = P_0 \times \dfrac{1-P_s}{T} + P_3 \times \dfrac{1}{r} \\ P_3 \times \left(\dfrac{1}{r} + \dfrac{1}{D}\right) = P_2 \times \dfrac{1}{m} + P_1 \times \dfrac{1}{T} + P_0 \times \dfrac{P_S}{T} \\ P_1 \times \left(\dfrac{1}{T} + \dfrac{1}{r}\right) = P_3 \times \dfrac{1}{D} \\ P_0 + P_1 + P_2 + P_3 = 1 \end{cases} \tag{3.2}$$

where P_i is the probability of the state i, $i = 0 \ldots 3$.

According to [14], P_1 and P_3 can be calculated using the following equations:

$$P_1 = \frac{r^2 T(D + mP_s)}{M} \tag{3.3}$$

$$P_3 = \frac{rD(D+r)(D+mP_s)}{M} \tag{3.4}$$

Demand factor f can be expressed as the function of the parameters given in Figure 3.2 as follows [14]:

$$f = \frac{P_3}{P_3 + P_1} = \frac{\frac{1}{r} + \frac{1}{T}}{\frac{1}{D} + \frac{1}{r} + \frac{1}{T}} \tag{3.5}$$

The factor f serves to weight the FOH to reflect the time the unit was actually on forced outage when in demand by the system [13].

Forced outage rate demand (FORd) can be evaluated as follows:

$$FORd = \frac{f \times FOH}{f \times FOH + SH} \tag{3.6}$$

FORd is the probability that a generating unit will not be available when required.

Equivalent forced outage rate demand (EFORd) [13]:

$$EFORd = \frac{f \times FOH + f_p \times EFDH}{f \times FOH + SH} \tag{3.7}$$

where f_p is the partial outage factor and EFDH is the equivalent forced derating hours.

EFORd can be found in the NERC Generating Availability Data System (GADS) [17],[18]. The difference between EFORd and FORd is that EFORd also includes derated states of the generator.

The full outage probability (FOP) of a unit is the probability that the unit will stop providing all of its current output in an hour period. Here, it is assumed that the trip causes the unit's output to be instantaneously unavailable. The hourly FOP of a unit can be related to the FOR and MTTR as follows [12]:

$$FOP_i = \frac{FOR_i}{MTTR_i} \tag{3.8}$$

In the case of peaking units, EFORd can be used instead of FOR in (3.8).

3.2 Capacity Outage Probability Table

The capacity adequacy evaluation of generation systems requires the creation of a generation capacity model, known as the capacity outage probability table (COPT). COPT gives the probability of occurrence for each possible outage capacity level [13].

Let us assume that the system has n independent generating units and that unit i has m_i discrete states with outage capacity C_{ij} and individual probability $p_{ij} = p(X_i = C_{ij})$, where $j = 1 \ldots m_i$ [16]. Outage states of unit i are arranged in ascending order. The COPT contains $N + 1$ discrete states, where $N = C_{max}/\Delta$, C_{max} is the installed capacity of the system and Δ is the resolution of the COPT. The new individual state probabilities, after unit i is added to the system, can be calculated using the following recursive algorithm [16]:

$$p(k) = \sum_{j=1}^{m_i} p_{ij}\, p'(k - \frac{c_{ij}}{\Delta}), \quad k = 0,1,2,\ldots,N \tag{3.9}$$

where $p(\cdot)$ is individual state probabilities after unit i is added;
$p'(\cdot)$ is individual state probabilities before unit i is added;
k is an index of discrete state.

The recursive convolution process starts with the initial values: $p(0) = 1$ and $p(k) = 0$, $k = 1,2 ,\ldots N$. Note that $p(k) = 0$ if $k < 0$.

In summary, the recursive convolution procedure for building a COPT has the following basic steps [16]:

1. Read unit data, determine Δ and $N = C_{max}/\Delta$;
2. Set initial values: $p(0) = 1$ and $p(k) = 0$, $k = 1,2 ,\ldots N$;
3. Add unit i to the system, calculate $p(k)$, $k = 0,1,2 ,\ldots ,N$ using (3.9);
4. Repeat Step 3 for all the units.

Usually, the table obtained by (3.9) is simplified by rounding the COPT to selected discrete capacity levels. The size of the round-off increment depends on the desired accuracy.

The cumulative probability of having $k\Delta$ MW to be forced out can be calculated using the following equation:

$$P(k) = \sum_{s=0}^{k} p(s) \tag{3.10}$$

3.3 Example of COPT Calculation

Let the system consist of two generators. The first generator has a capacity of 100 MW and outage probability 10%, and the second generator has a capacity of 50 MW and outage probability 20%. Assume that generating units has only two states: operating state and forced out state.

Then, the capacity matrix is:

$$C = \begin{bmatrix} c_{11} & c_{12} \\ c_{21} & c_{22} \end{bmatrix} = \begin{bmatrix} 0 & 100 \\ 0 & 50 \end{bmatrix}$$

where $c_{11} = 0$ and $c_{21} = 0$ – correspond to operating states of generators one and two (no forced outage) and $c_{12} = 100$ and $c_{22} = 50$ – correspond to forced out states (nominal generator capacity).

Individual probability matrix is defined as:

$$P = \begin{bmatrix} p_{11} & p_{12} \\ p_{21} & p_{22} \end{bmatrix} = \begin{bmatrix} 0.9 & 0.1 \\ 0.8 & 0.2 \end{bmatrix},$$

where $p_{11} = 0.9$ and $p_{21} = 0.8$ are probabilities of operating state of generators one and two;

$p_{12} = 0.1$ and $p_{22} = 0.2$ are probabilities of the forced out state.

The installed system capacity is $C_{max} = 150$MW, and the COPT resolution is $\Delta = 50$MW. Therefore COPT contains four discrete states.

Let us set initial probability values *p(k)*in the COPT (Table 3.1).

Table 3-1. COPT (Initial Values)

State, *k*	Capacity, *c(k)* (MW)	Probability, *p(k)*
0	0	1
1	50	0
2	100	0
3	150	0

Now we will add unit one to the system and calculate new capacity outage probabilities using (3.9) - see Table 3.2.

$$k = 0: \quad p(0) = p_{11} \cdot p'(k - \frac{c_{11}}{\Delta}) + p_{12} \cdot p'(k - \frac{c_{12}}{\Delta}) = 0.9 \cdot p'(0 - \frac{0}{50}) + 0.1 \cdot p'(0 - \frac{100}{50}) =$$
$$= 0.9 \cdot p'(0) + 0.1 \cdot p'(-2) = 0.9 \cdot 1 + 0.1 \cdot 0 = 0.9$$

$$k=1: \quad p(1) = p_{11} \cdot p'(k - \frac{c_{11}}{\Delta}) + p_{12} \cdot p'(k - \frac{c_{12}}{\Delta}) = 0.9 \cdot p'(1 - \frac{0}{50}) + 0.1 \cdot p'(1 - \frac{100}{50}) =$$
$$= 0.9 \cdot p'(1) + 0.1 \cdot p'(-1) = 0.9 \cdot 0 + 0.1 \cdot 0 = 0$$

$$k=2: \quad p(2) = p_{11} \cdot p'(k - \frac{c_{11}}{\Delta}) + p_{12} \cdot p'(k - \frac{c_{12}}{\Delta}) = 0.9 \cdot p'(2 - \frac{0}{50}) + 0.1 \cdot p'(2 - \frac{100}{50}) =$$
$$= 0.9 \cdot p'(2) + 0.1 \cdot p'(0) = 0.9 \cdot 0 + 0.1 \cdot 1 = 0.1$$

$$k=3: \quad p(3) = p_{11} \cdot p'(k - \frac{c_{11}}{\Delta}) + p_{12} \cdot p'(k - \frac{c_{12}}{\Delta}) = 0.9 \cdot p'(3 - \frac{0}{50}) + 0.1 \cdot p'(3 - \frac{100}{50}) =$$
$$= 0.9 \cdot p'(3) + 0.1 \cdot p'(1) = 0.9 \cdot 0 + 0.1 \cdot 0 = 0$$

Table 3-2. COPT (Unit One Added)

State, *k*	Capacity, *c(k)* (MW)	Probability, *p(k)*
0	0	0.9
1	50	0
2	100	0.1
3	150	0

The next step is adding the unit two and update values of COPT (Table 3.3):

$$k=0: \quad p(0) = p_{21} \cdot p'(k - \frac{c_{21}}{\Delta}) + p_{22} \cdot p'(k - \frac{c_{22}}{\Delta}) = 0.8 \cdot p'(0 - \frac{0}{50}) + 0.2 \cdot p'(0 - \frac{50}{50}) =$$
$$= 0.8 \cdot p'(0) + 0.2 \cdot p'(-1) = 0.8 \cdot 0.9 + 0.2 \cdot 0 = 0.72$$

$$k=1: \quad p(1) = p_{21} \cdot p'(k - \frac{c_{21}}{\Delta}) + p_{22} \cdot p'(k - \frac{c_{22}}{\Delta}) = 0.8 \cdot p'(1 - \frac{0}{50}) + 0.2 \cdot p'(1 - \frac{50}{50}) =$$
$$= 0.8 \cdot p'(1) + 0.2 \cdot p'(0) = 0.8 \cdot 0 + 0.2 \cdot 0.9 = 0.18$$

$$k=2: \quad p(2) = p_{21} \cdot p'(k - \frac{c_{21}}{\Delta}) + p_{22} \cdot p'(k - \frac{c_{22}}{\Delta}) = 0.8 \cdot p'(2 - \frac{0}{50}) + 0.2 \cdot p'(2 - \frac{50}{50}) =$$
$$= 0.8 \cdot p'(2) + 0.2 \cdot p'(1) = 0.8 \cdot 0.1 + 0.2 \cdot 0 = 0.08$$

$$k=3: \quad p(3) = p_{21} \cdot p'(k - \frac{c_{21}}{\Delta}) + p_{22} \cdot p'(k - \frac{c_{22}}{\Delta}) = 0.8 \cdot p'(3 - \frac{0}{50}) + 0.2 \cdot p'(3 - \frac{50}{50}) =$$
$$= 0.8 \cdot p'(3) + 0.2 \cdot p'(2) = 0.8 \cdot 0 + 0.2 \cdot 0.1 = 0.02$$

Table 3-3. COPT (Unit Two Added)

State, k	Capacity, $c(k)$ (MW)	Probability, $p(k)$
0	0	0.72
1	50	0.18
2	100	0.08
3	150	0.02

Figure 3.3 and Figure 3.4 show the capacity discrete outage PDF and CDF based on the calculated COPT.

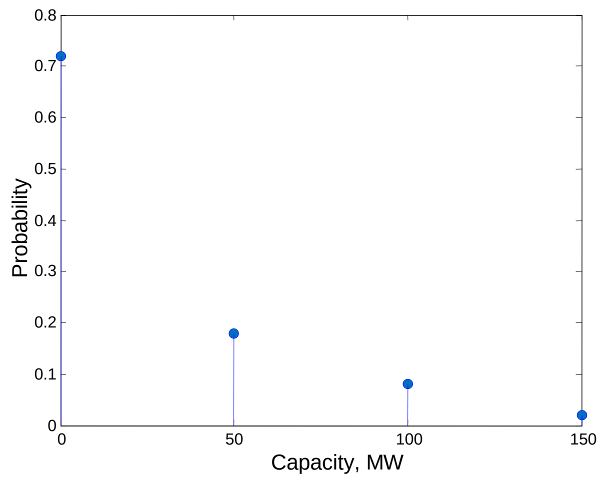

Figure 3.3. Discrete Probability Density Function

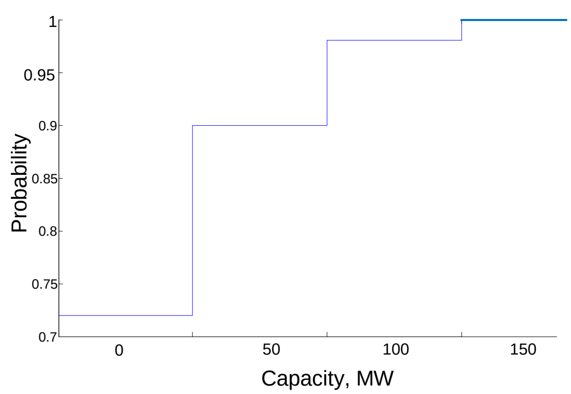

Figure 3.4. Cumulative Distribution Function

3.4 Preliminary simulation results (Forced Outage Model)

An example of a CAISO generation schedule is presented in Table 3.4, and generation unit performance statistical characteristics taken from GADS [17] are presented in Table 3.5.

COPTs are calculated to each hour, taking into account the generators' schedule. Figure 3.5 and Figure 3.6 show the capacity outage PDF and CDF functions for a 1-hour look-ahead period.

Table 3-4. Generation Schedule

Number	UNIT_ID	Unit Type	1h	2h	3h	4h	5h
1	Unit1	STUR	16	16	16	16	16
2	Unit2	STUR	20	20	20	20	20
3	Unit3	HYDR	16	16	16	16	16
4	Unit4	GTUR	0	0	0	0	0
…..	…	……	…	…	…	…	…
516	Unit516	STUR	3	3	3	3	3
517	Unit517	WIND	10	10	10	10	10
	Total Generation		17792.916512.0616113.2215813.1515811.15				
	Wind		1344	1310.28	1313.55	1299.14	1256.3

Table 3-5. Annual Unit Performance Statistic

GEN_TYPE	GEN_TECH	FUEL_TYPE	FOR	Service Hours	Number of Occurrences
T	STUR	GEOT	0.5	8500	3.6
T	GTUR	GAS	46.33	270	3
T	STUR	GAS	8.29	2750	4
H	HYDR	WATR	4.92	4981	3
T	WIND	WIND	-	-	-
T	CCYC	GAS	7.33	3673	9
H	PTUR	WATR	3.71	2634	3.86

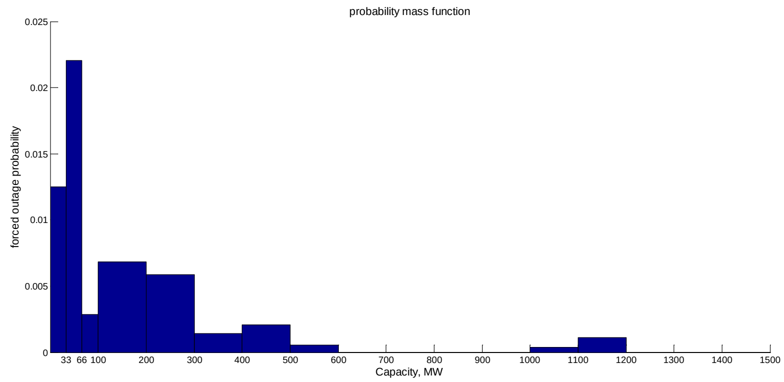

Figure 3.5. Capacity Outage Discrete PDF

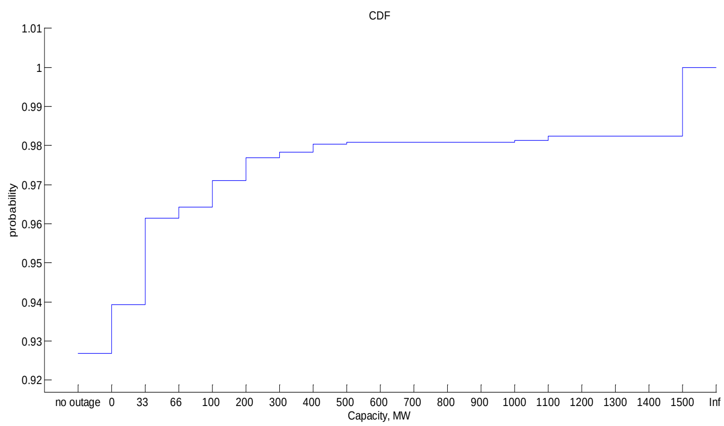

Figure 3.6. Capacity Outage CDF

4.0 Review of Current Operating Practices at CAISO and BPA

To incorporate the proposed probabilistic tool into the real EMS systems, we need to know the actual generation scheduling and dispatch procedures used by the balancing authorities where this integration can take place. In this Section, the operating practices at the CAISO and BPA are briefly reviewed.

CAISO runs different generation schedules in their day-ahead market and real-time market to make sure that the energy and reserve requirements including regulating up, regulation down, and ramping requirements are ultimately met in real-time operation. BPA's generation scheduling, load following and regulation requirements as well as hydro optimization procedures are also reviewed here.

4.1 Scheduling Process at CAISO

Figure 4.1 shows the CAISO market timeline. The CAISO scheduling process includes day-ahead market (DAM), real-time unit commitment (RTUC), short-term unit commitment (STUC), and real-time economic dispatch (RTED). Although regulation (REG) capacity is procured in the day-ahead market, it is controlled by the EMS AGC system, rather than the market software [19].

The regulation capacity is procured day-ahead for each operating hour of the next operating day. The additional ancillary services (AS) also can be procured in the real-time market (RTM) to meet additional AS requirements. The AS include: regulation up reserve, regulation down reserve, spinning reserve and non-spinning reserve. Temporal characteristics of the scheduling and dispatch processes are given in Table 4.1.

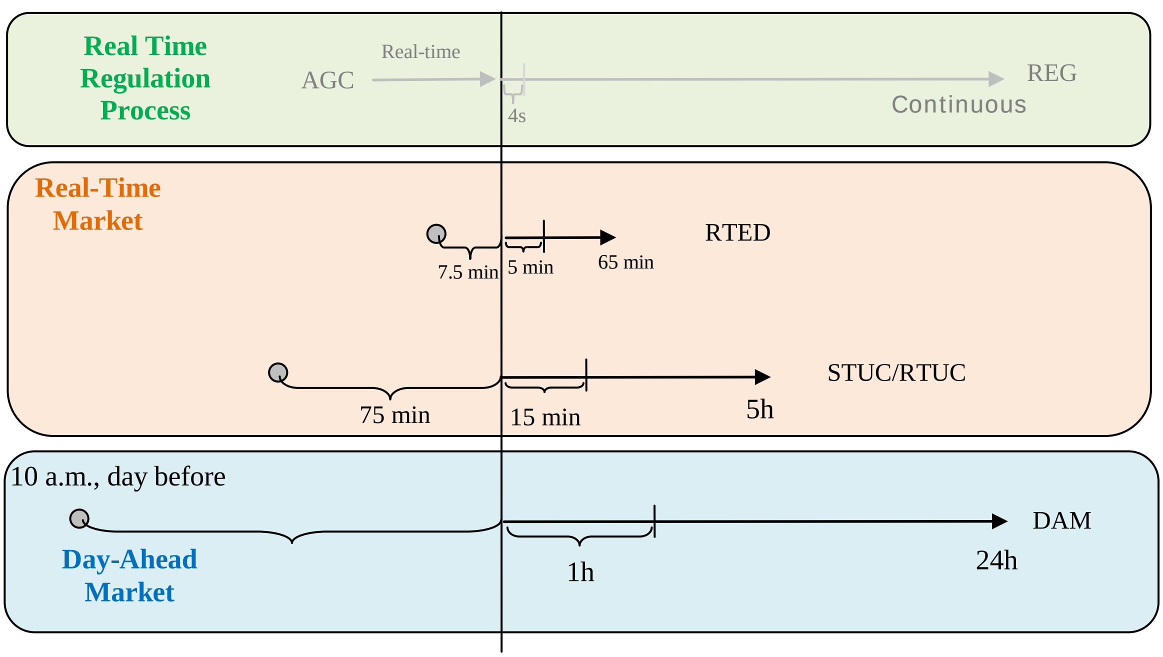

Figure 4.1. CAISO Timelines

Table 4-1. Time Characteristics of the Scheduling Process at CAISO

Element	Acronym	Start time	Interval	Frequency	Time horizon
Day-Ahead Market	DAM	Closes at 10:00 on the day before	1h	Every day	24h
Short-Term Unit commitment	STUC	75 min before	15 min	hourly	5 hours
Real-Time Unit commitment	RTUC	-	15 minute	15 minutes	4 to 7x15 minute interval
Real-Time Economic Dispatch	RTED	7.5 min before	5 min	Every 5 min	65 min
Regulation	REG	-	4s	4s	-

The CAISO RTM consists of several applications, three of which including STUC, RTUC, and RTED, work together. The STUC and RTUC applications ensure there is enough on-line capacity to meet a 5-minute demand. The STUC is performed in the RTM to commit units and balance the system resource and demand while enforcing transmission constraint. STUC is run once an hour and looks out 5 hours to commit resources that have start up times greater than 90 minutes.

The RTUC application runs every 15 minutes and looks out between four and seven 15-minute intervals to determine if short-start and fast start units need to be committed or de-committed.

The RTED process runs every 5 minutes to meet the imbalance energy requirements of the CAISO. This process looks ahead 65 minutes to ensure that enough capacity is on-line to meet real-time demand. It is expected that wind variability and the lack of accurate wind forecast could create challenges for the RTED application. RTED is the lowest granularity of dispatch in the ISO market except for regulating reserves, which is procured in the RTM, but is dispatched through the EMS AGC system every 4 seconds.

Figure 4.2 represents the CAISO market design generation schedules. In the day-ahead (DA) timeframe, wind and solar resources are not required to bid directly into the CAISO markets. This fact can significantly impact the unit commitment process in the DA timeframe because the CAISO must forecast the expected hourly production in the DA to ensure that enough resources are committed for next day operation. Similarly, the CAISO load forecast is done in the DA and RT timeframes. In the DAM, the forecast of the CAISO's hourly demand is done for three days in advance. The DA schedule is an hourly block energy schedule that includes 20-minute ramps between hours. It is provided at 10.00 a.m. the day prior to the operating day. The real-time schedule is based on STUC/RTUC timelines. The RTM closes 75 minutes before the actual beginning of an operating hour as shown in Figure 4.1. RTED is provided 7.5 minutes before the dispatch operating target (DOT) and is based on real-time forecasts. Symmetrical ramping is used, which means that by dispatching for the average, the DOT ends in the center of the interval. In the RTM, the CAISO automatic load forecasting system (ALFS) provides a load forecast for each 15-minute and 5-minute interval. Load and wind forecasting errors can cause the RTM application to dispatch incorrect amounts of imbalance energy needs. RTED results are 5-minute dispatch instructions and advisory notices for the look-ahead timeframe.

Thus, the load following or supplemental energy dispatches are the difference between RTED and STUC/RTUC curves. This is an instructed deviation caused by real time dispatches. Regulation is the difference between the actual demand and the RTED curves (see Figure 4.2).

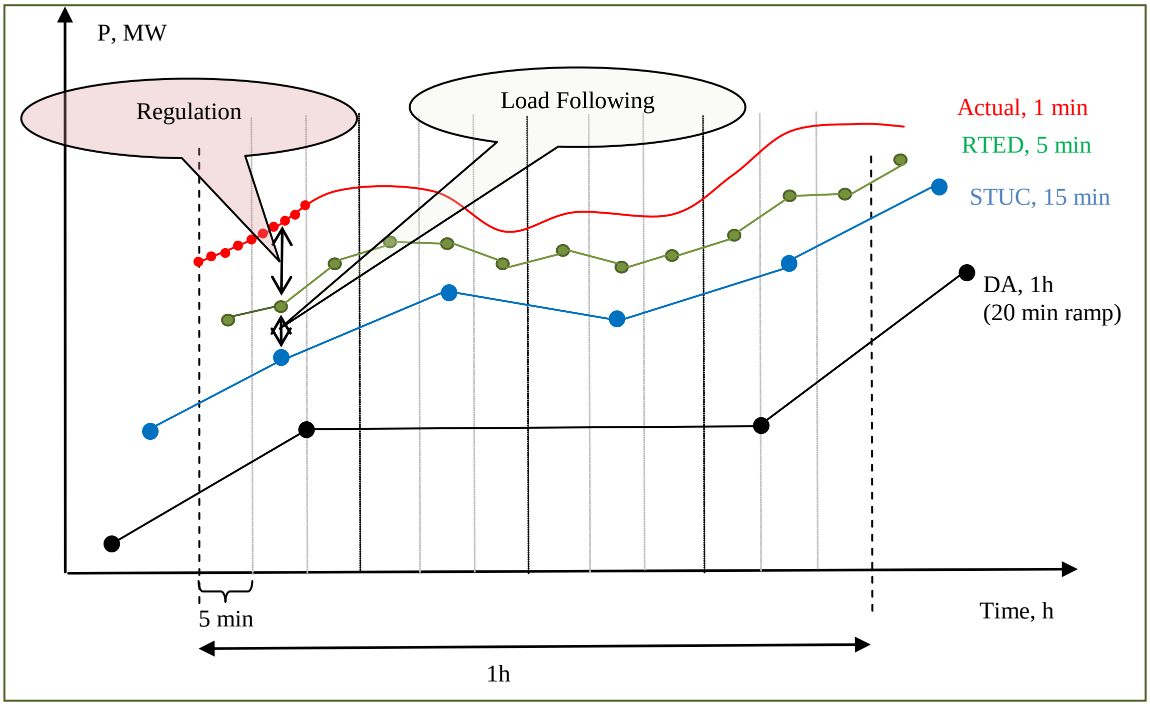

Figure 4.2. Generation Dispatch Components

Because of the load and wind (as well as solar) forecasts errors, there are uncertainties in the ranges of regulation and load following requirements. Figure 4.3 and Figure 4.4 show regulation and load following uncertainty ranges, where the actual demand (dotted line) is unknown.

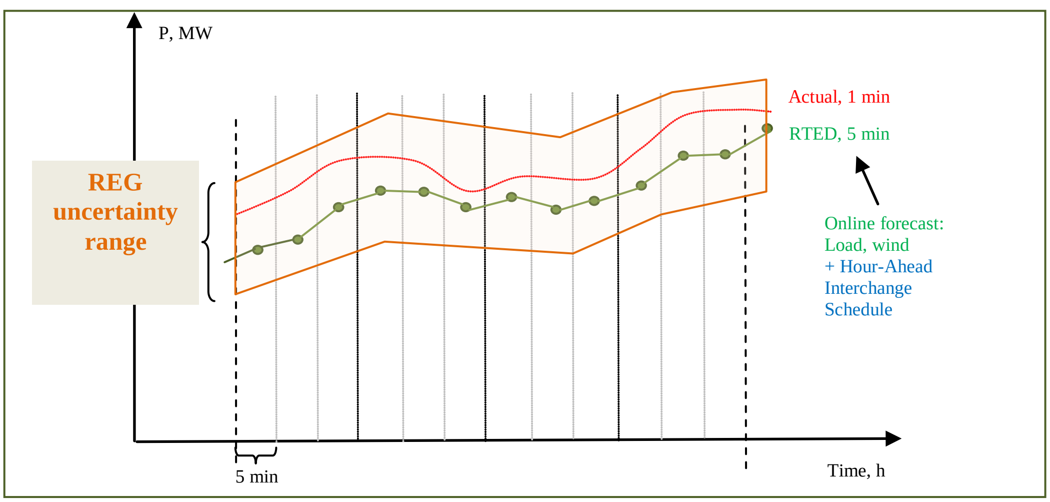

Figure 4.3. Regulation Uncertainty

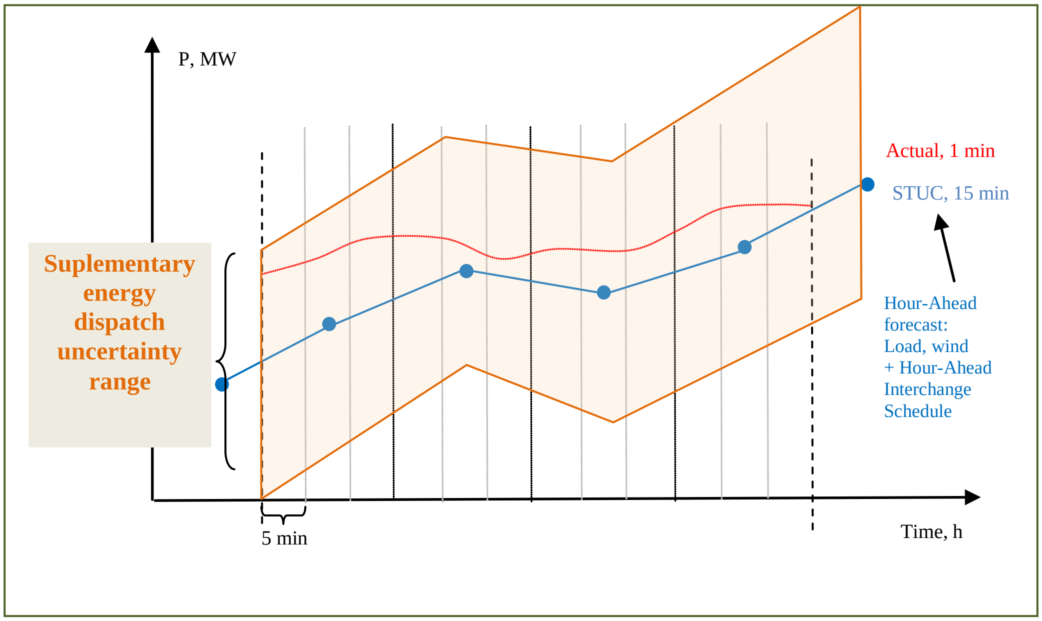

Figure 4.4. Load Following Uncertainty

4.2 Operating Practices at BPA

BPA normally has a sufficient range of load following, regulation, and ramping capabilities under many conditions but not at all times. Because of the constraints of the hydro system, BPA could run out of available range under the following conditions:

- During spring runoff, load following, and regulation down is limited.
- Throughout summer, range on the lower Columbia River is limited due to salmon run requirements.

4.2.1 Generation Schedules

The generation scheduling process at BPA is based on bulk hourly energy schedules and includes 20-minute ramps between the hours (beginning 10 minutes before the end of an hour and ending 10 minutes after the beginning of an hour). The pre-schedule is based on the day-ahead forecast and completed before 2 pm the day before the day of delivery. The real-time schedule is based on an hour-ahead forecast completed 20 minutes before the hour of delivery and implemented by adjusting generation units base point settings. Figure 4.5 shows the timeline for the pre-schedule and real time schedule procedures.

Within-hour load balancing is achieved mainly through the adjustment of several federally owned hydro plants responding to AGC signal. There is not yet a separate automated load following process to dispatch generations following intra-hour load variations.

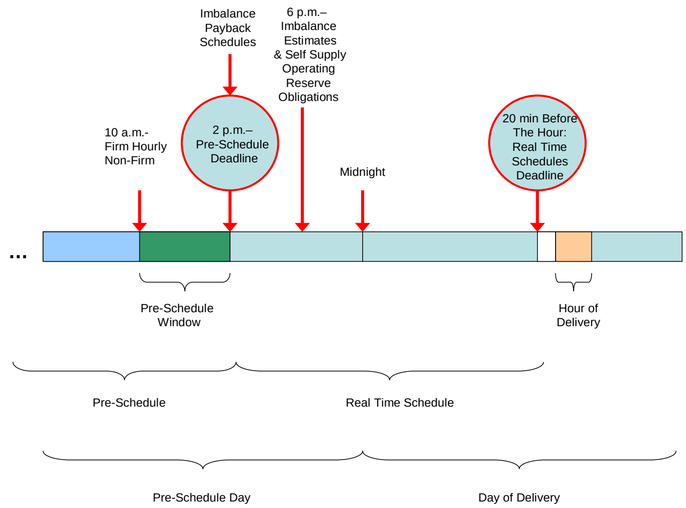

Figure 4.5. BPA Scheduling Timeline

4.2.2 Load Following

Load following is the use of online generation equipment to track the intra- and inter-hour changes in customer loads. There is not a within-hour scheduling process, or load following, in the BPA system presently. Load following in the current BPA system may be interpreted as the process of manual adjustment of the generation base points when the deviation of the regulating units from their base points exceeds certain threshold. This adjustment can be repeated any 30 minutes by BPA real-time dispatches if needed. A within-hour scheduling process with 10-minute intervals is being considered for implementation in the BPA system in the future.

4.2.3 Regulation

Regulation service in the BPA system, which follows the moment-to-moment changes in load, is accomplished by committing on-line generators responding to the AGC signal. The outputs of these generators are raised or lowered based on the difference between generation schedule and actual load. The transmission customers must either purchase this service from the BPA or make alternative arrangements to satisfy its regulation and frequency response obligation.

4.2.4 Hydro Optimization

BPA has two hydro optimization models: Columbia Vista, which optimizes generation and loads the next hour, next day, weekly and seasonally and the near real time optimizer (NRTO) that optimizes generation to meet loads within the hour [20].

Columbia Vista is primarily used by short-term planners to determine:

- Use of H_2O (Basin optimization)
- Use of machines (Plant optimization).

Vista is the software system for hydropower scheduling. It determines the global optimum generation schedule for a cascade or group of cascades over the long term (one or more years) as well as the short-term planning horizon of one to two weeks on a one-hour time resolution [21].

The NRTO is primarily used by plant operators and duty schedulers to determine use of machines (plant optimization). NRTO has been developed by Synexus Global Inc. in cooperation with the BPA [22]. The software tool enables hydropower operators and schedulers to assess system parameters and optimize operations on a near real-time basis. NRTO now serves as a tool to evaluate the Columbia River hydro system's distribution of generation on a within-hour basis.

NRTO works as a stand-alone application or in conjunction with the Synexus Vista decision support system ("Columbia Vista"), which has recently been installed and customized for BPA. The NRTO model allows users to evaluate unit dispatch options while simultaneously meeting generation requests and observing imposed operating constraints. For example, a project operator can look half an hour ahead (in six 5-minute “snapshots”) and determine the best way to meet the distinct generation requirements anticipated for each interval while minimizing the number of unit-commitment changes that would be required over the half-hour period. Factors such as constraints on unit dispatch order, unit operating efficiencies, and the effects on head of the generation decision are all taken into account [22].

5.0 EMS Integration of Probabilistic Tools

This Section describes how the developed probabilistic tool (see Sections 2 and 3) can be integrated with existing EMS systems consistently with their application designs and requirements (as discussed in Section 4). Depending on the desired sophistication level, three modes of integration have been proposed: “passive,” “active,” and “proactive.” “Passive” integration is the first step of integration, which brings awareness of wind and load forecast uncertainties into control center software tools through information visualization and alarming. “Active” integration uses the uncertainty information to modify existing grid operation functions such as unit commitment. “Proactive” integration develops new grid operation functions enabled by the uncertainty information. For example, a new probabilistic unit commitment process can be defined with the wind and load forecast uncertainty being an additional constraint. As part of the integration, choices are offered regarding how the balancing authorities prefer to integrate the probabilistic tool with their security constrained unit commitment program and other tools.

5.1 Conceptual Design of Probabilistic Tool Integration

Integration of probabilistic tools with an EMS system should take into account operating practices of specific power systems. Figure 5.1 shows the conceptual view of the capacity requirements uncertainty evaluation based on the CAISO scheduling process. The RTED, STUC, and DAM scheduling tools (described in Section 4.1) use various forecasts, such as those that provide forecasts with different dispatch intervals for different time horizons, and those with different resolutions. Therefore, these forecasts have different accuracies, statistical characteristics, and uncertainty ranges associated with them. Figure 5.1 shows the uncertainty ranges as color bars for different time horizons. Different shades of colors indicate different levels of confidence. For the first 65-minute time horizon, when the scheduling is done by RTED, the uncertainty range is smaller as the forecast is more accurate compared to longer-term forecasts such as those for the 5-hour horizon and the 24-hour horizon, when the scheduling is done by STUC and DAM, respectively. RTED runs every 5 minutes, so the uncertainty needs to be evaluated at a 5-minute interval. For the 5-hour STUC and the 24-hour DAM, uncertainty can be evaluated for a look-ahead interval of 30 minutes up to hours. To ensure reliable supply of generation, scheduling or dispatch at different time horizons needs to cover the predicted uncertainty ranges.

Figure 5.2 shows a conceptual view of capacity requirements evaluation based on the BPA operating practices. BPA has day-ahead and hour-ahead scheduling processes that are based on day-ahead and hour-ahead forecasts, respectively. BPA’s scheduling process looks relatively simpler because most of the scheduling is for its hydro units. But again, at the two different time horizons – hour-ahead or day-ahead–the uncertainty associated with wind and load forecasts as well as other factors needs to be evaluated at different intervals.

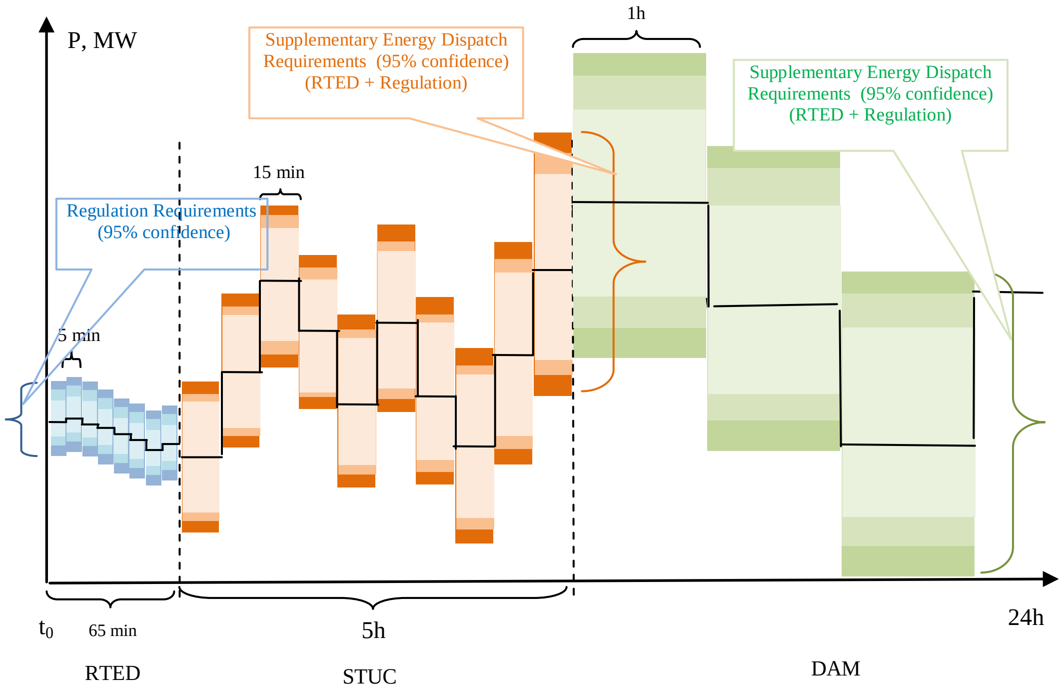

Figure 5.1. CAISO Generation Schedule and Capacity Requirements Uncertainty Evaluation

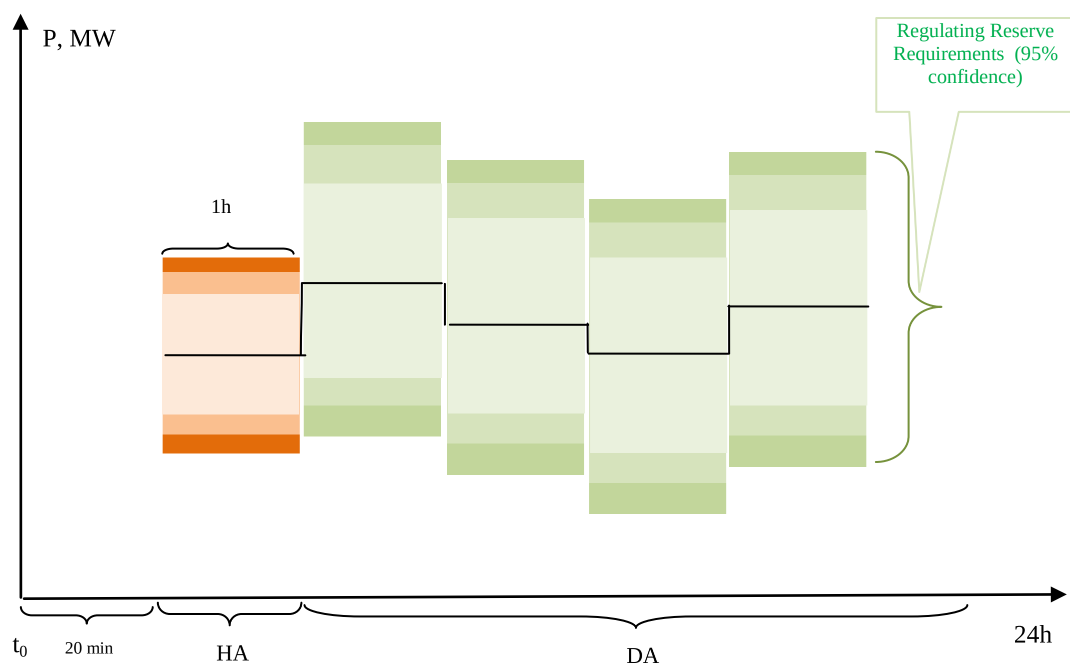

Figure 5.2. BPA Generation Schedule and Capacity Requirements Uncertainty Evaluation

A conceptual flow chart for software implementation is presented in Figure 5.3, which shows three possible levels of integration.

1. Level I - “Passive” Integration.

Passive integration is the initial step and the simplest way of integration. In this case, the probabilistic uncertainty will be only visualized as part of the desktop application for grid dispatchers. Displays with look-ahead capacity and ramping requirements are provided to a real-time dispatcher. The displays help the dispatcher to assess balancing needs in real time so as to take right actions to mitigate potential energy deficit or surplus situations. The decision on actions to take is part of the short-term generation scheduling. Details on visualization screen design are given in Section 5.5.

2. Level II - “Active” Integration

Active integration of the tool is a more advanced level of integration. The uncertainty tool interacts with the EMS environment, especially the unit commitment and economic dispatch processes. The uncertainty information is used as a constraint in the unit commitment and economic dispatch processes, which results in different generation schedules to meet different confidence levels. In addition to uncertainty visualization displays, the uncertainty tool also displays alerts about potential threats to the power system due to deficit in reserve or over-generation and provides advisories to the dispatcher what actions can be taken to avoid any undesirable scenarios. Details on active interaction with unit commitment are given in Section 5.3.1.

3. Level III - “Proactive” Integration

Proactive integration is the most advanced level of integration. It requires not only interaction with the EMS, unit commitment, economic dispatch and other systems; it also requires modification of current operating practices and algorithms. For instance, new constrains based on uncertainties evaluations can be incorporated into the unit commitment process, or probabilistic unit commitment can be developed based on the uncertainty information. Details are given in Section 5.3.2.

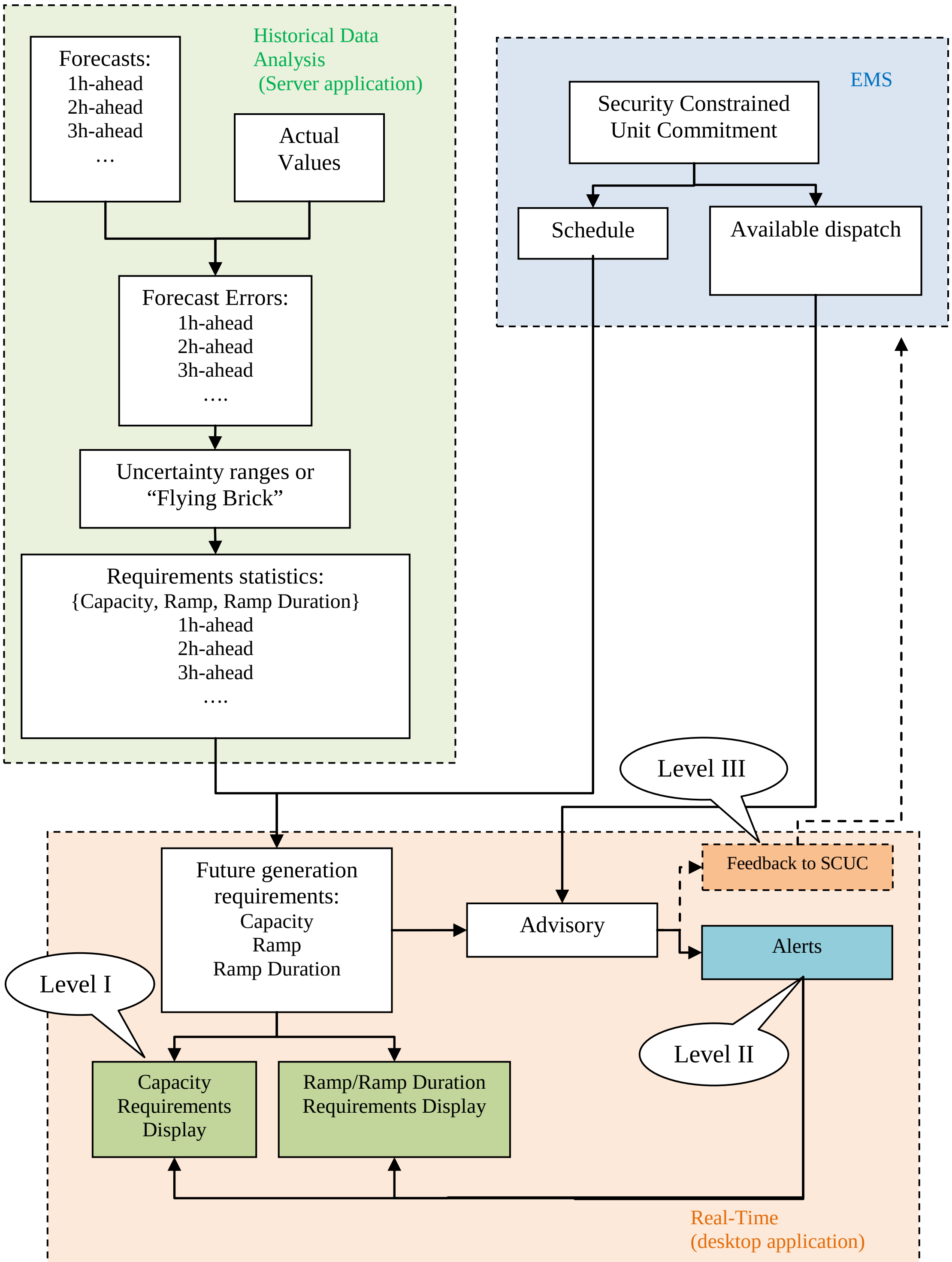

Figure 5.3. Software Flowchart

5.2 Data Acquisition

In order to model the statistical uncertainty information, large volumes of historical and real-time data are needed. As shown in Figure 5.4, a sliding window is used for acquiring continuous statistical information on system load, wind and solar power generation, generation schedules, and so on. Table 5.1 lists the data needed for the uncertainty evaluation process. The time frame size and refreshment rates of sliding windows are tuned for different systems depending on their individual characteristics. This study uses a one- to two-month time frame and a one-hour refreshment rate.

Figure 5.4 represents a typical structure of the load or wind generation forecasts. The forecast resolution is the time interval between two consecutive data records. The time horizon is the length of the look-ahead interval, and the forecast update interval is the time interval for updating the forecast.

Besides the statistical information, actual measurements are also acquired. The full list of required data for the CAISO system is shown in Table 5.1. It includes five categories of data: Category A – conventional generation information; B – load information; C – wind and solar generation information; D – actual measurements; and E – static information.

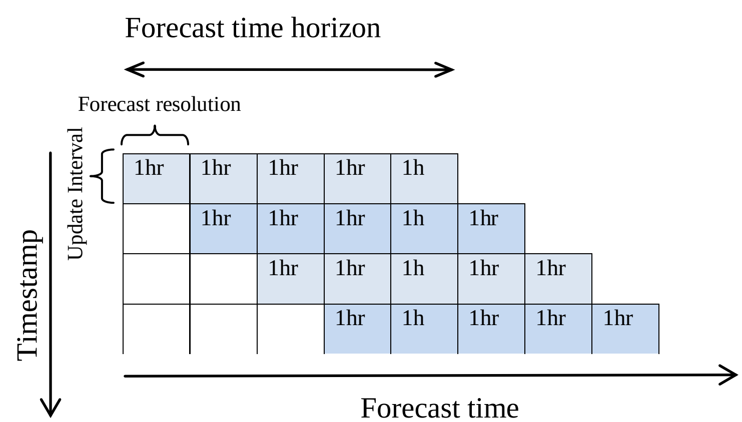

Figure 5.4. Example of Wind Generation or Load Forecast Structure

Table 5-1. List of Required Data for the CAISO System

Items#		Data	Resolution	Time Horizon	Frequency
A					
Generation and Interchange Schedules	A1	Day-ahead Generation Schedule (total and for each individual generator)	1 hr	24 hr	Every day at 10:00 a.m.
	A2	Short-Term Unit Commitment (total and for each individual generator)	15 min	5 hr	Each 15 min , 75 min before
	A3	Pumped Hydro Schedule	1 hr	24 hr	–
	A4	Real-Time Economic Dispatch (total and for each individual generator)	5 min	65 min	Every 5 min, provided 7.5 min before the beginning of a 5-min dispatch interval
	A5	Day-ahead Interchange Schedule (total)	1hr	24 hr	–
	A6	Hour-ahead Interchange Schedule (total)	15 min	5 hr	–
Dynamic Schedules	A7	Day-ahead (total and for each individual generator)	1 hr	24 hr	Every day at 10:00 a.m.
	A8	Short-Term Unit Commitment (total and for each individual generator)	15 min	5 hr	Each 15 min , 75 min before
	A9	Real-Time Economic Dispatch (total and for each individual generator)	5 min	65 min	Every 5 min, provided 7.5 min before the beginning of a 5-min dispatch interval
Operating Reserves (total and for individual generators)	A10	Regulation Up Procurement	1 hr	24 hr	–
	A11	Regulation Up (available)	5 min	–	–
	A12	Regulation Down Procurement	1 hr	24 hr	–
	A13	Regulation Down (currently available)	5 min	–	–
	A14	Spinning Reserve	1 hr	24 hr	Procured day-ahead
	A15	Non-Spinning Reserve	1 hr	24 hr	Procured day-ahead

Table 5.1. (contd)

Items#		Data	Resolution	Time Horizon	Frequency
B					
Load Forecast	B1	Day-Ahead Load Forecast	1 hr	24 hr	Every day before 10 am
	B2	Hour-Ahead Load Forecast	30 min	24 hr	30 min
	B3	Real time Load Forecast	5 min	60 min	5 min
C					
Wind Generation Forecast (total and per generation zone)	C1	Day-ahead Wind Forecast	1 hr	24 hr	Every day before 10 am
	C2	Hour-ahead Wind Forecast	5 min	8 hr	5 min
	C3	Real Time Wind Forecast	5 min	65 min	5 min
Solar Generation Forecast	C4	Day-ahead Solar Forecast	1 hr	24 hr	Every day before 10 am
	C5	Hour-ahead Solar Forecast	5 min	8 hr	5 min
	C6	Real Time Solar Forecast	5 min	65 min	5 min
D					
D1		Actual Load	5 min	–	5 min
D2		Actual Generation (total and for each individual generator)	5 min	–	5 min
D3		Actual Wind Power Generation (total and per generation zone)	5 min	–	5 min
D4		Actual Solar Power Generation (total and per generation zone)	5 min	–	5 min
D5		Actual Interchange (total)	5 min	–	5 min
D6		Actual Regulation (total and for each individual generator)	1 min	–	1 min
D7		Actual Load Following (total and for each individual generator)	5 min	–	5 min

Table 5.1. (contd)

Items#	Data	Resolution	Time Horizon	Frequency
E				
E1	Generator Type (Hydro, Nuclear, Gas Turbine, Combined-cycle, Wind, Solar, …)	–	–	–
E2	Ramp Rate	–	–	–
E3	Regulation Ramp Rate	–	–	–
E4	Startup Time	–	–	–
E5	Startup Cost	–	–	–
E6	Maximum Capacity	–	–	–
E7	Minimum Capacity	–	–	–
E8	Minimum Run Time	–	–	–
E9	Minimum Down Time	–	–	–
E10	Failure to Start Up (% of startups)	–	–	–
E11	Production Cost Characteristic (piecewise linear characteristics)	–	–	–
E12	Force Outage Rate (FOR)	–	–	–
E13	In Service Hours	–	–	–
E14	Out of Service Hours (due to Forced Outages)	–	–	–
E15	Number of Occurrences (per year for forced outages)	–	–	–
E16	Must-Run Units (Yes/No)	1 hr	24 hr	Determined before 10 am for the next operating day
E17	Availability for Redispatch (Yes/No)	1 hr	24 hr	Determined before 10 am for the next operating day
E18	Availability for Unit Commitment (Yes/No)	1 hr	24 hr	Determined before 10 am for the next operating day

Figure 5.5 shows an example (a snapshot) of forecasted and actual wind power generation. The red bold line represents the actual wind generation during a three week period. The other curves represent the forecast wind generation with different look-ahead time horizons (1,2,3,4,5- hours ahead) for the same time period. It can be observed that the longer the horizon is, the less accurate the forecast becomes. The statistical analysis can be applied to the forecast errors, and histograms for different look-ahead time horizons can be used to generate forecast PDFs and CDFs.

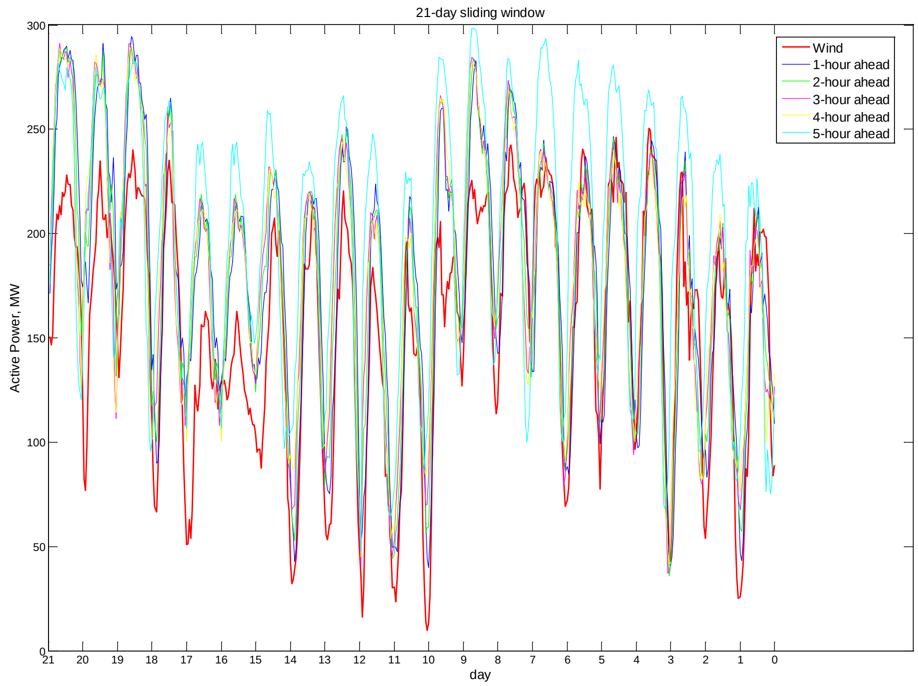

Figure 5.5. Example of Forecast and Actual Wind Generation in a Three-Week Period

5.3 Integration with Unit Commitment

In restructured power systems, security-constrained unit commitment (SCUC) is utilized by an independent system operator/regional transmission organization (ISO/RTO) to clear the day- or week-ahead market. The objective of SCUC is to minimize the system operating cost while meeting the prevailing constraints such as power balance, system spinning and operating reserve requirements, minimum on/off time limits, ramping up/down limits, limits on state and control variables including real and reactive power generation, controlled voltages, settings of tap-changing, and phase-shifting transformers [23]. Wind and load forecast uncertainty information adds to the complexity of the unit commitment process as the system also needs to mitigate the variations in wind and load. One way to achieve that is to commit the right units at the right time so the system has enough margins for ramping up or ramping to balance energy needs. This section uses the unit commitment process to demonstrate the concept of “active” and “proactive” integration of uncertainty information.

5.3.1 "Active" Integration

The active integration approach with the unit commitment (UC) procedure does not imply any modification in current operating practices. In this approach, the uncertainty evaluation tool will interact with and use the existing UC engine with the objective to monitor the sufficiency of available balancing resources within the uncertainty range of system requirements and to generate alternative generating schedules (advisories) in case of potential threats to the power system reliability.

A simple example of how the active integration with UC could be achieved is given below.

1. Run unit commitment and economic dispatch (standard UC) optimization problems with nominal forecast values of wind generation and load demand.
2. An existing UC engine uses various input information such as demand forecasts, generating unit characteristics, different constraints, market bids, as input (see Figure 5.6). As a result of the UC problem, a generation schedule is produced. In Figure 5.7, an example of generation schedule is presented. The hour-ahead schedule (HAS) shown in the figure corresponds to BPA's scheduling process.
3. Perform an evaluation of the generation requirement according to the methodology proposed in Section 2.0. As a result, we get the uncertainty ranges for the generation requirements.
4. Figure 5.8 shows the uncertainty range as colored blocks.
5. Evaluate currently available balancing capacity, including regulating reserves and available redispatch ranges[1] from the generation schedules determined in step 1.
6. No actions are needed if a sufficient balancing capacity is available (i.e., if the uncertainty range is found within the available redispatch range). Otherwise, if balancing capacity is not sufficient, i.e. there is probability that the system would experience balancing problems, proceed to the next step.

In Figure 5.8, one can see that at the hour ending by 2:00 (HE2) and HE4 there is no sufficient available balancing capacity to meet the demand with the 95% confidence.

[1] Operating practices of specific power systems (balancing authorities) should be taken into account.

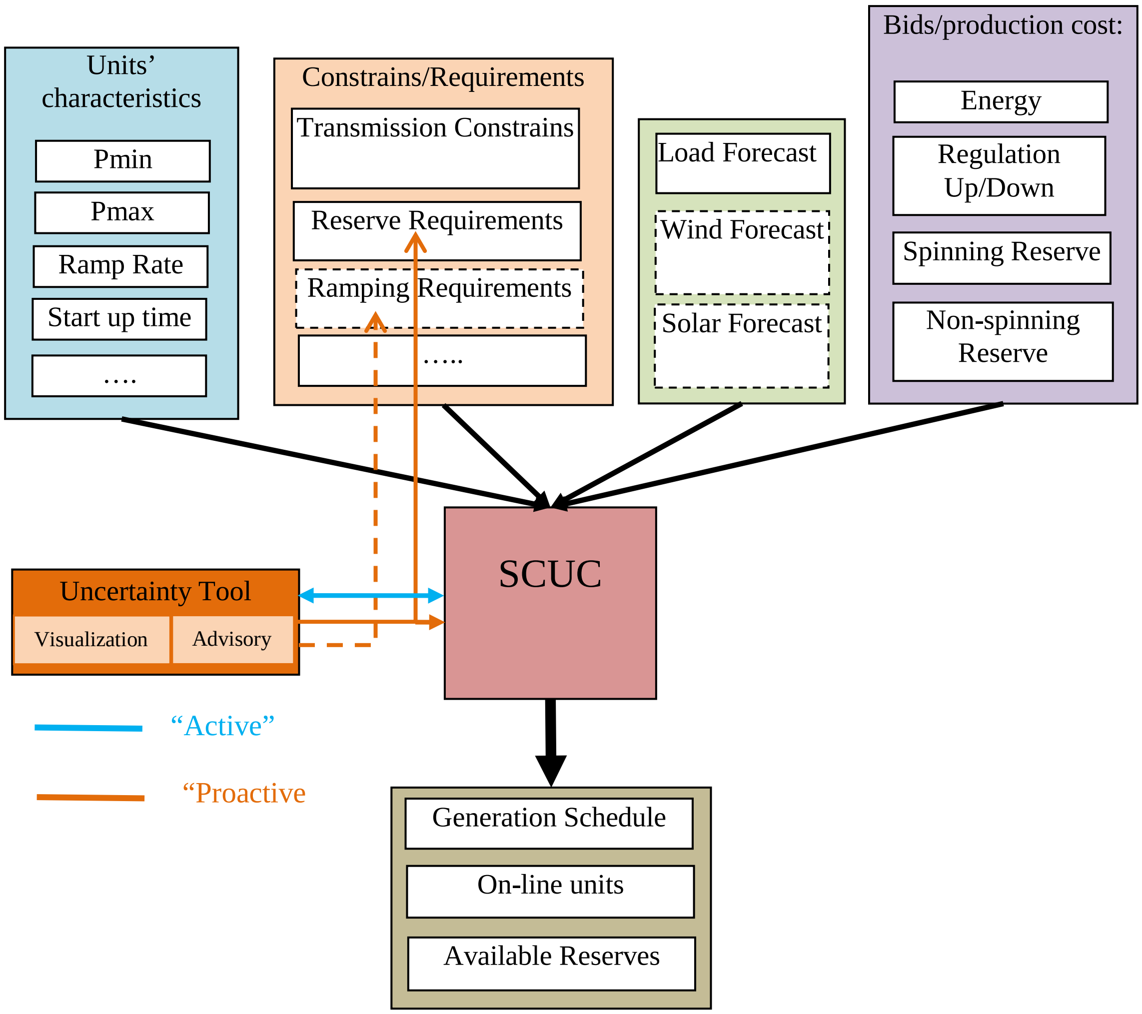

Figure 5.6. Flowchart of a Unit Commitment Process Considering Wind and Load Uncertainties for the "Active" and "Proactive" Integration Approaches

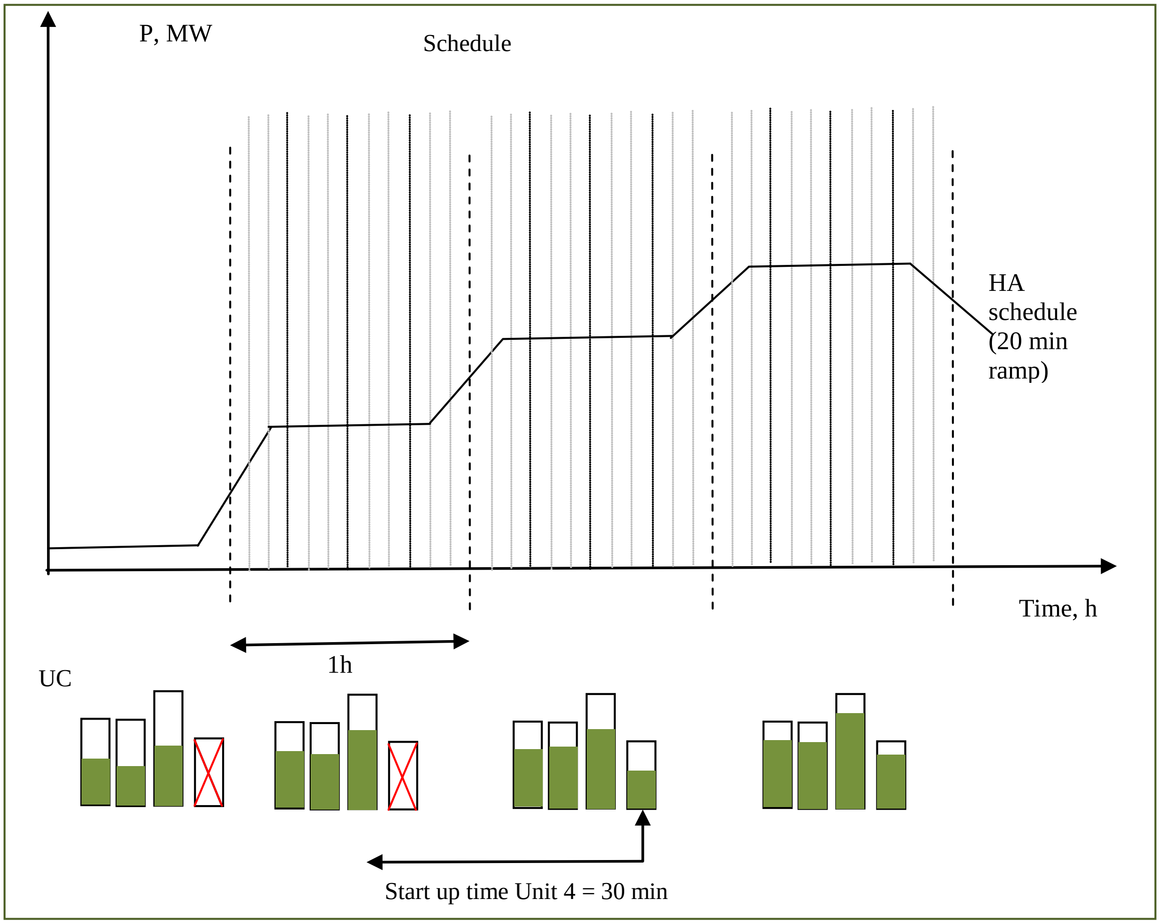

Figure 5.7. Unit Commitment for the Case With Nominal Wind and Load Forecast Values

1. Run UC optimization again (UC2) to follow the upper bound of the desirable confidence interval.

- The same UC engine is run again to attempt to follow the extreme generation requirement, corresponding to the boundary of the confidence interval. A specific aspect of the UC optimization process for uncertainty range boundaries is that the available on-line generators committed during standard UC optimization should be taken into account. UC2 only commits additional units if there is insufficiency of balancing resources or de-commits some units in case of potential over-generation. CAISO uses the similar UC engine in RTUC/STUC optimization process.
- Figure 5.8 shows that to provide a sufficient balancing capacity at HE2, it is necessary to start up an additional unit (unit 4) 30 minutes before the HE2 begins. At HE4, UC2 optimization could not find any solution. This means that it would be necessary to curtail a part of the load or procure additional balancing services from other balancing authorities.

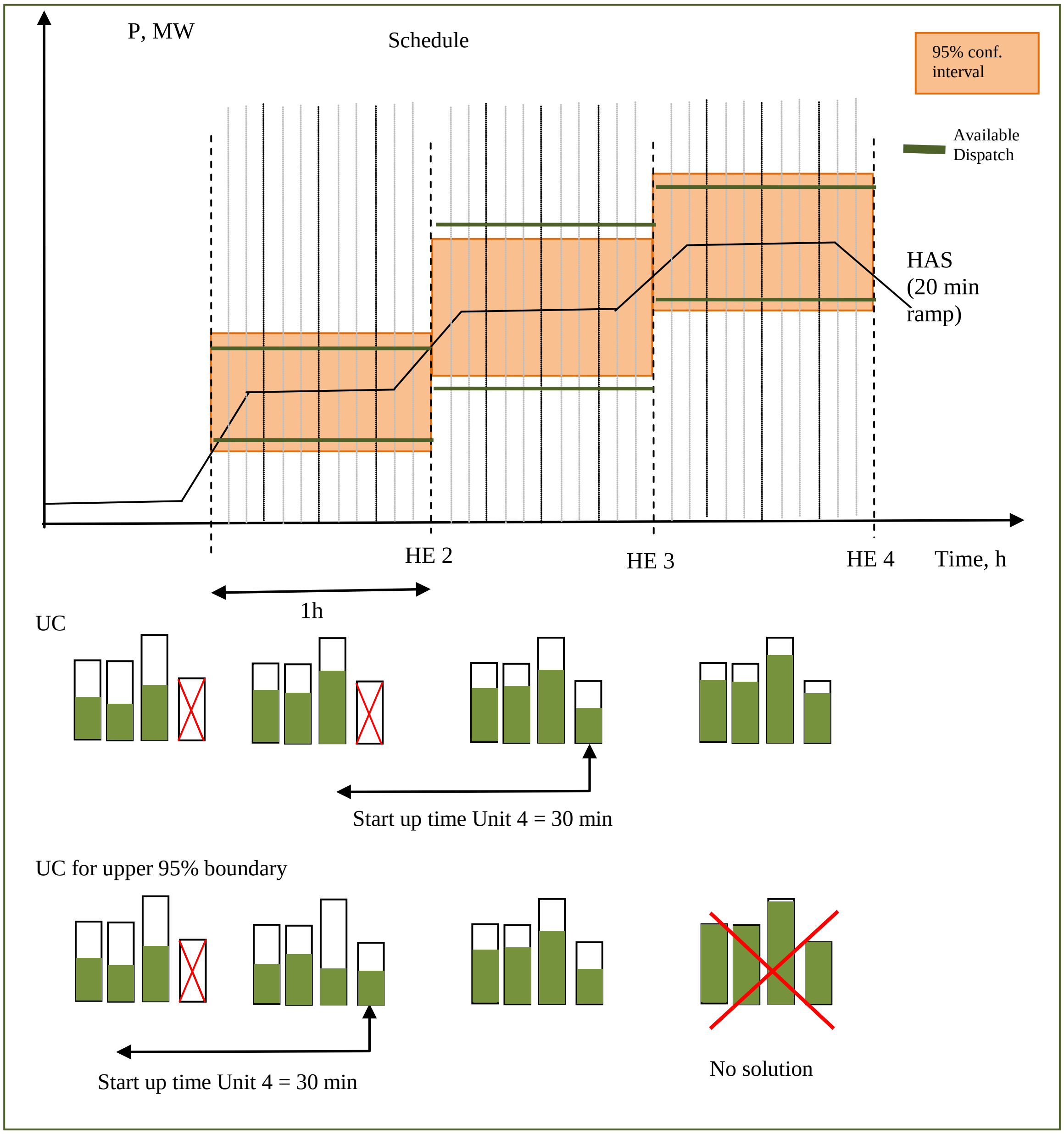

Figure 5.8. Unit Commitment for the Upper Uncertainty Range Boundary

1. Display real-time alerts and advisories to the dispatcher.

Different advisories and alerts can be shown on the dispatcher's screen. Alerts can have different grades reflecting the level of risk to the system.

In Figure 5.9, two examples of advisories are presented:

- At HE2, there is a 10% chance that the balancing resources will not be sufficient, and the recommended solution would be to start up unit 4 at hour 00:30.

- At HE4 there is a 15% chance that the balancing resources will not be sufficient. The recommended solutions are to procure 100 MW of additional capacity or be ready to curtail 100MW of load.

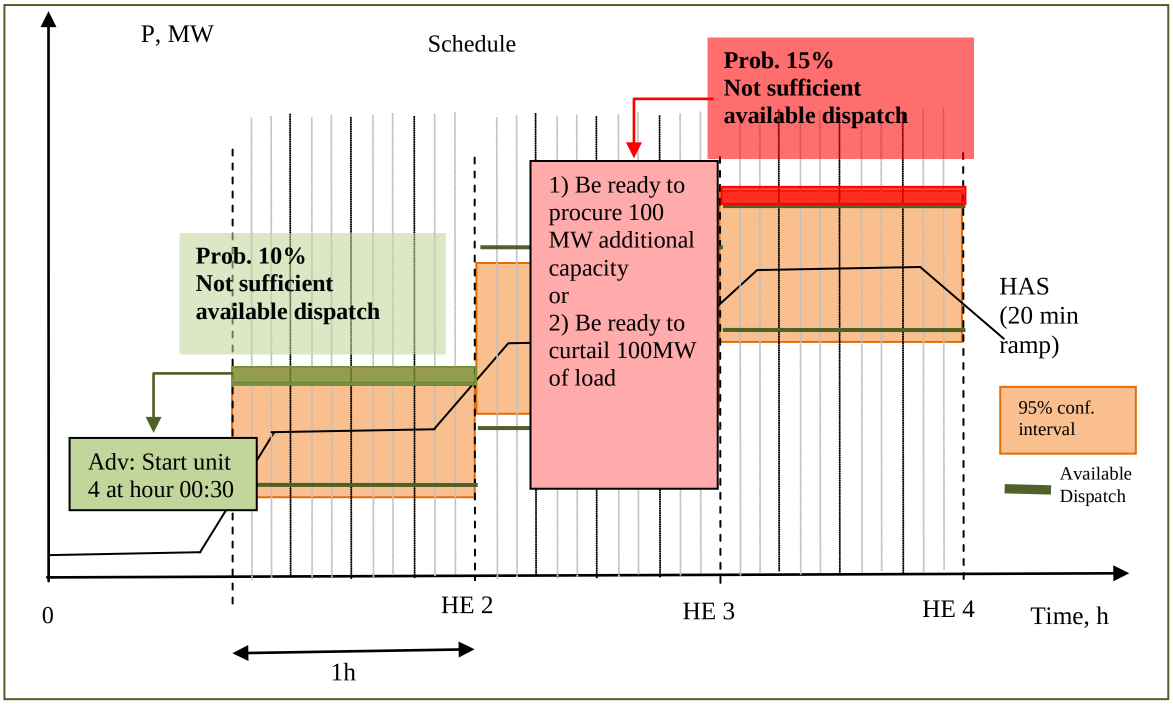

Figure 5.9. Example of Advisories

5.3.2 "Proactive" Integration

Proactive integration approach requires some modifications of the current UC optimization procedures and potentially the operating practices. This is the most comprehensive type of integration. Only initial studies are performed in the course of this work. Further research is required in the next phase of this project.

The initial idea of proactive integration is to use the output of the uncertainty tool as a new constraint in the existing unit commitment process, or as an input to run a probabilistic unit commitment process. For example, the uncertainty range of the capacity requirement can be used as part of the reserve requirements in the UC optimization procedure (see Figure 5.6). In addition, the uncertainty range of the ramping requirement could be incorporated into the UC process. Today's SCUC process considers ramps between consecutive hours, but within-the-hour ramping requirements are not part of SCUC yet. Therefore, a modification of the SCUC optimization engine will be required. Generally, the proactive integration of uncertainty information into the UC process results in fundamental changes to the unit commitment algorithm.

5.4 EMS Integration Design

We developed the framework for integrating the probabilistic uncertainty evaluation tool with EMS systems. Figure 5.10 shows the overall design of the integration. The uncertainty evaluation tool (labeled as "Wind/Load Uncertainty Assessment") is a standalone module outside of the EMS environment. It needs data from the EMS in addition to wind forecast information, as shown in the figure. The output of the uncertainty tool can then be used to drive other grid operation functions such as unit commitment and its associated economic dispatch, which will be our focus of the implementation though other elements such as contingency analysis (CA) and reserve sharing are shown for the completeness of the design. The integration consists mainly of four elements:

1. Data export from the EMS
2. Data management for the uncertainty tool
3. Data import to the EMS
4. Integration with the unit commitment and economic dispatch processes.

The following subsections give detailed specifications of the four elements using AREVA's EMS software as an example. To demonstrate the probabilistic uncertainty evaluation tool and its applicability to actual grid operation environments, we implemented the data export and data management elements as well as integration with unit commitment and economic dispatch. A prototype tool is introduced in Section 7.0. It lays a solid foundation for future full integration with EMS systems.

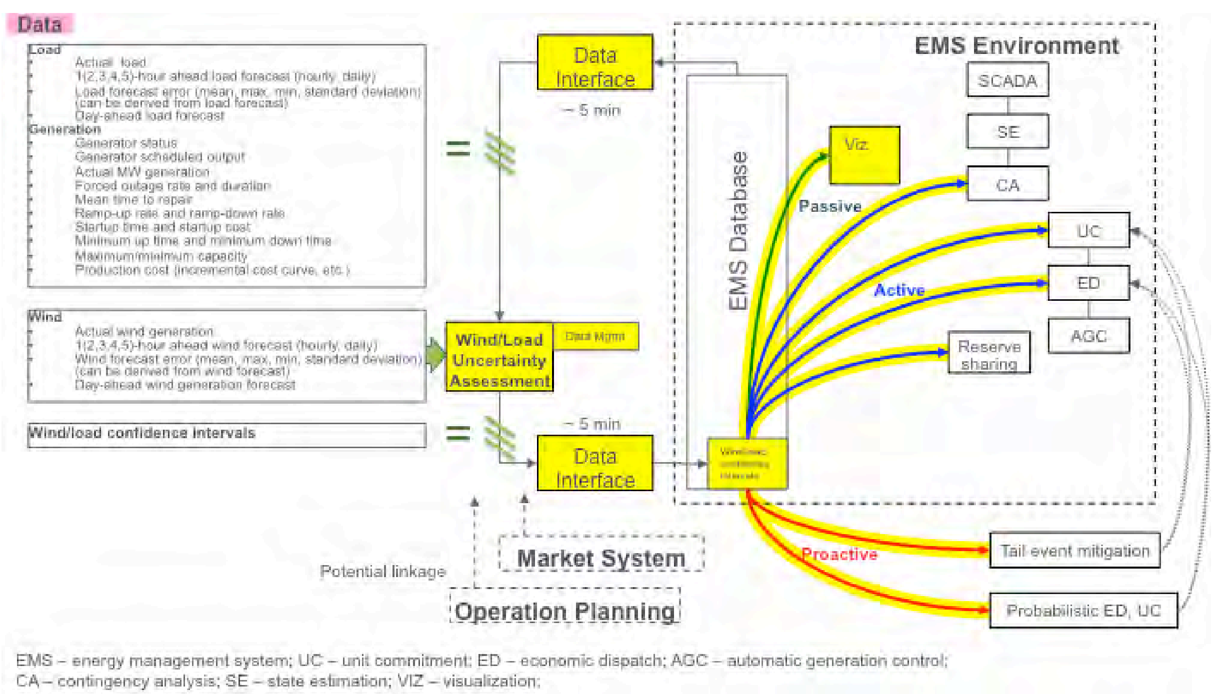

Figure 5.10. Concept of PNNL Tool Integration with EMS systems

5.4.1 Data Export from the EMS Environment

The data export interface is based on HABConnect, an interface provided in the suite of AREVA's EMS tools. A flat buffer structure will be used for data export. The data to be exported from the EMS are shown in Figure 5.10.

The wind forecast data are shown to be provided by a third-party forecast service company external to the EMS. This is based on the fact that current EMS environments do not have interface to wind forecast information. However, considering wind forecast would be directly linked to the EMS in the future, the design can be slightly altered to have the uncertainty tool receives wind forecast information using the same HABConnect-based data export interface.

Load forecast information is generated by **e-terra***loadforecast* module, containing hourly mid-term load forecast data for seven days and short-term load forecast data at a 5-minute interval for next hour. For the purpose of uncertainty evaluation, only the mid-term load forecast data are required,so the HABConnect buffer only provides the mid-term load forecast. Unit commitment results are from **e-terra***commit* module and will be part of the HABConnect structure. Actual measurement data are available from the SCADA module. Specific data points will be identified in the HABITAT database during the implementation phase.

The data export interface is designed to be configurable regarding transfer rate, forecast window length, forecast interval, number of confidence intervals and their percentages. The configuration and data exchange sequence numbers and timestamps are used to ensure that the data exchanged between the EMS and the uncertainty tool is properly synchronized.

5.4.2 Data Management for the Uncertainty Tool

As stated in the previous subsection, significant amounts of data will be received from the EMS through the HABConnect-based interface. These data need to be stored in a structured manner for a certain length of history so the statistical analysis can be preformed. Data exported from the EMS will be read into a specially designed Microsoft SQL Server database structure. Interface between the SQL database and the uncertainty tool will be designed so historical data of a specified length can be retrieved for analysis. Output from the uncertainty tool will be sent to the SQL database for archiving and for packaging into XML format for import to the EMS.

A display of the uncertainty information will be developed in associated with the database table. The display can be generated externally by the uncertainty evaluation tool and integrated into the EMS through an active serve page mechanism, or it can generated internally as part of the EMS.

5.4.3 Data Import to the EMS Using an XML Interface

The data to be imported back to the EMS HABITAT database include confidence intervals and associated uncertainty ranges as well as derived ramping requirements. The data import is done via a FTP transfer of an XML file. The format of the XML file will be designed during the implementation phase.

Once the data reaches the HABITAT database, a specially designed table will be used to store the data. This database table will have an interface to other functions in the EMS environment, such unit commitment and economic dispatch. The economic dispatch is part of the UC optimization process, which is different from the real-time economic dispatch at a 4-second interval.

The data export interface is designed to be configurable regarding transfer rate, uncertainty evaluation time horizons and resolutions, number of confidence intervals, and their percentages. The configuration and data exchange sequence numbers and timestamps are used to ensure that the data exchanged between the EMS and the uncertainty tool is properly synchronized.

5.4.4 Integration with the Unit Commitment and Economic Dispatch Process

This phase of the project will implement the active level of integration stated in Section 5.3. The UC optimization process including unit commitment and economic dispatch is performed in the **e-terra***commit* module. The existing UC engine is not modified but run multiple times for multiple uncertainty boundaries at different confidence levels as well as for the nominal forecast wind and load values. The process is repeated at a configurable interval such as an hour or five minutes. Special attention will be paid to the fact that **e-terra***commit* is unaware of the distinctions between these different runs. The **e-terra***commit* solution will always be written back to the same buffer in the HABITAT database, so it is important to handle multiple outputs within the database to ensure they are not overwritten. The output of the multiple UC runs will then be exported to the uncertainty tool to produce alerts or advisories as stated in Section 5.3. The displays of the alerts and advisories can be either external to the EMS or integrated into the EMS through an active serve page mechanism.

The final outcome of the implementation is an integrated tool of wind/load uncertainties and improvement of unit commitment and economic dispatch. The tool is to be at a prototype level capable of demonstrating the impact of wind/load uncertainties on power grid operations.

5.5 User Interface Conceptual Design

Information representation is an important aspect in the integration, in order to provide easy-to-understand, real-time information to dispatchers. The design of several displays is presented in this section.

5.5.1 Capacity Requirements Screen

A conceptual view of capacity requirement screen is shown in Figure 5.11. Capacity requirement screen contains the following information:

- Generation schedule to a specified time horizon (five to eight hours);
- Capacity requirements uncertainty ranges with different confidence levels associated with the generation schedule; and
- Alerts and advisories.

The screen is updated in a specified interval, shown hourly in Figure 5.11. It can be as short as five minutes. As the screen is updated, the confidence intervals as well as any alerts or advisories will be updated as well.

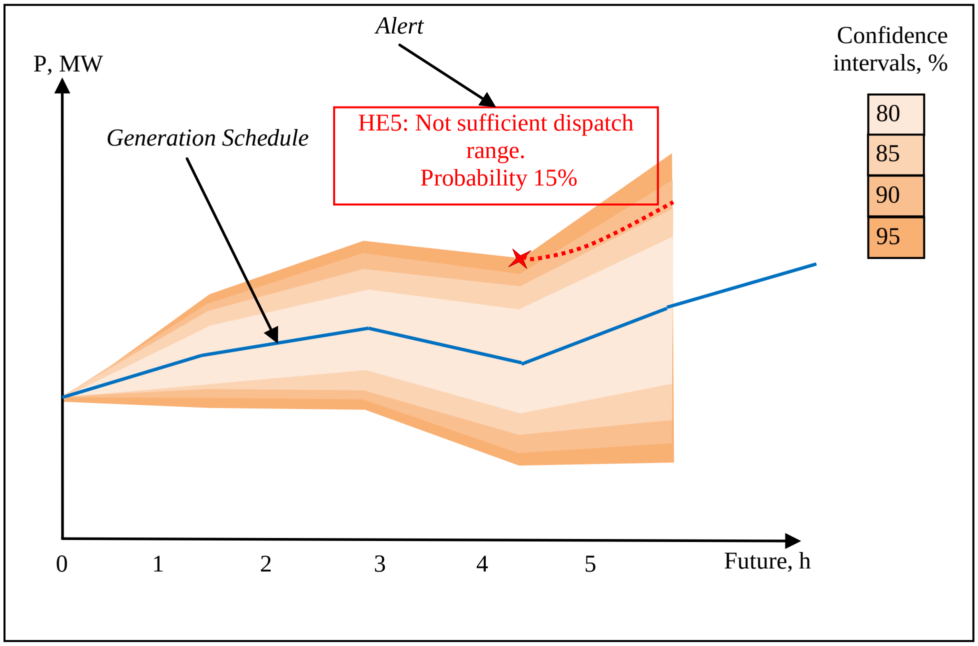

Figure 5.11. Capacity Requirement Screen

5.5.2 Ramping Requirement Screen

There are several options to represent the requirements of ramp rates and ramp durations. Some of them are shown in Figure 5.12. Software interface should be flexible and allow dispatchers to get any desirable representation of the requirements in a real time manner. For example, they should be able to change the number of confidence levels, the percentages of confidence levels, time horizons, and enabling/disabling alerts or advisories.

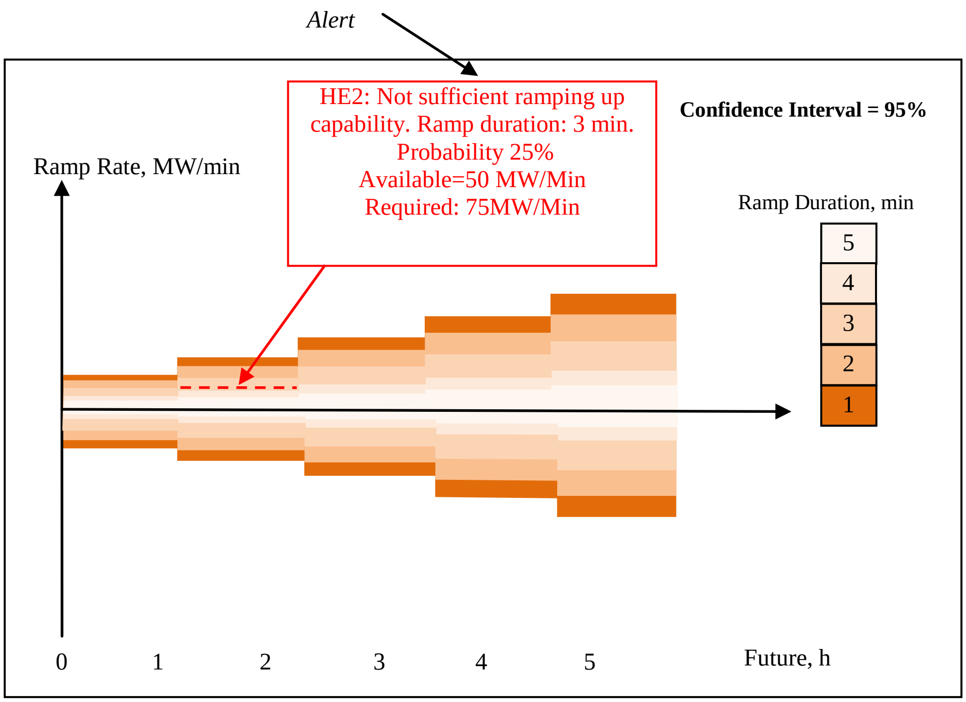

a)

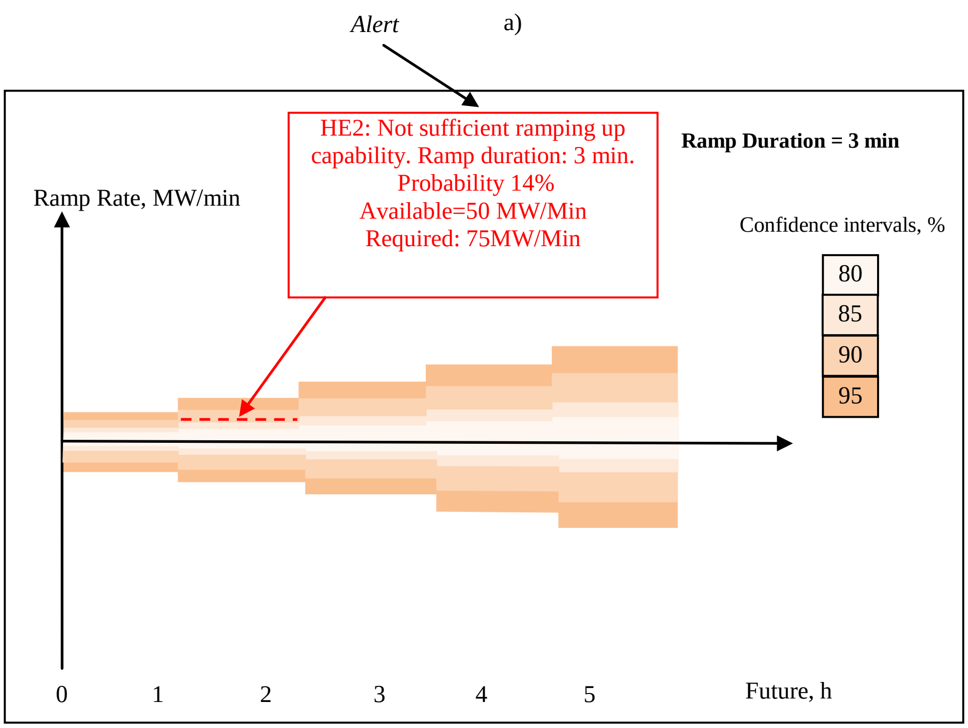

b)

Figure 5.12. Displays of Ramp Rate and Ramp Duration Requirements: A) Ramp Rates vs. Ramp Durations; B) Ramp Rates vs. Confidence Levels

Ramping requirements screen will contain the following information:

- Uncertainty range of ramp rate requirements for a specific time horizon;
- Ramp duration requirements; and
- Alerts and advisories.

5.6 Contingency Reserve Activation Model

Contingency reserve activation model (CRAM) was developed in cooperation with the University of Washington. Detailed information, mathematical model and preliminary simulation results of CRAM are given in the report produced by the University of Washington. This report can be found in Appendix B.

A flowchart reflecting interaction of software tool internal blocks interaction is shown in Figure 5.13. The capacity outage probability table produced by the forced outage model (see Section 3.0 for details) is an input of CRAM.

The output of CRAM is the contingency reserve deficiency probability distribution (histogram). This histogram can be combined with net load uncertainty histogram. As a result the combined probability distribution of generation requirements can be calculated. Based on this information uncertainty ranges for generation requirements with any user-specified confidence level can be produced.

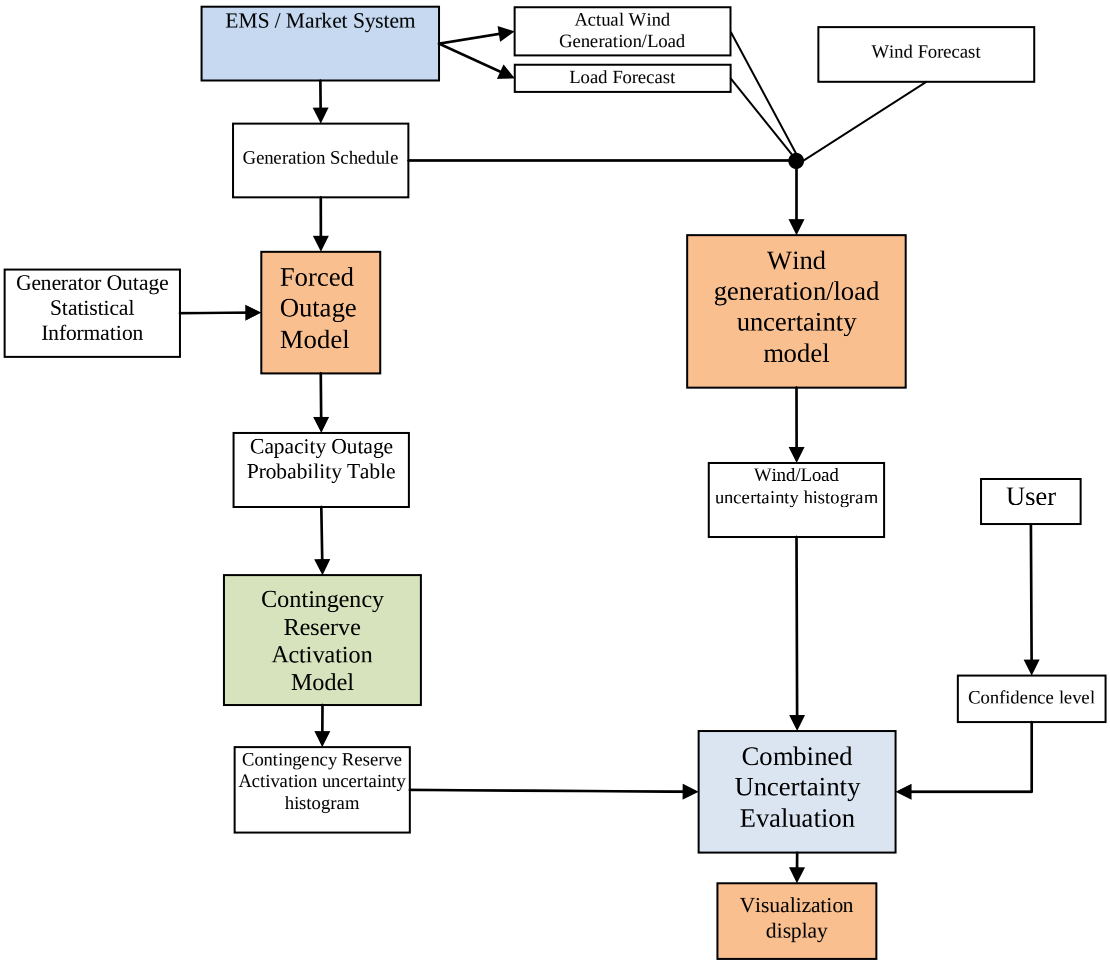

Figure 5.13. Software Blocks Interaction

6.0 Genetic Algorithm Based Unit Commitment

The UC problem is to allocate the start up and shut down schedules of generation units to meet load demand for a future period. The objective is to minimize the system cost while satisfying certain constraints. Various optimization techniques have been applied to solve the US problem. The most frequently used technique is the mixed integer programming method. In recent years, artificial intelligence techniques, such as the genetic algorithm (GA) and the artificial neural network methods have emerged as possible candidate approaches for solving the UC problem. GA is a search algorithm combining genetic operators (such as crossover and mutation) with survival of the fittest genes. In this section, a genetic unit commitment solver is presented. The algorithm has been developed and implemented to autonomously test the proposed uncertainty analysis methodologies, EMS integration ideas, and (in the future) to implement and examine high level integration concepts, namely, the active and proactive integration principles.

6.1 Problem Formulation

6.1.1 Objective Function

The UC determines the optimal commitment and decommittment sequences for generation units. The aim is to minimize the system total costs while satisfying various constraints. The UC problem can be mathematically formulated as a constrained discrete nonlinear optimization problem. The objective function can be given as:

$$\begin{aligned}\min F &= P_{\text{cost}} + S_{\text{cost}} + D_{\text{cost}} \\ &= u_{i,j}\left[\sum_{j=1}^{T}\sum_{i=1}^{M} C_i(P_{ij})\right] + u_{i,j}(1-u_{i,j-1})\left[\sum_{j=1}^{T}\sum_{i=1}^{M} S_{ij}\right] \\ &\quad + u_{i,j-1}(1-u_{i,j})\left[\sum_{j=1}^{T}\sum_{i=1}^{M} D_{ij}\right]\end{aligned} \tag{6.1}$$

where M is the number of units; T is total scheduling period in hours; P_{cost} is the production cost; S_{cost} is the start-up cost; D_{cost} is the shut-down cost; u_{ij} is status of unit i at time j, ON ('1')/OFF ('0'); $C_i(P_{ij})$ is fuel cost of unit i for generating power P_{ij} at time j, where $C_i(P_{ij}) = a_i + a_i P_{ij} + c_i P_{ij}^2$, and a_i, b_i, c_i are cost coefficients of unit i; P_{ij} is output of generator i at time j; S_{ij} is start-up cost of unit i at time j, where $S_{ij} = \sigma_i + \delta_i(1-e^{-T_{ij}^{OFF}/\tau_i})$ and σ_i and δ_i are start-up cost coefficients of unit i; $-T_{ij}^{OFF}$ is the unit off time, and D_{ij} is shutdown cost of unit i at time j. In this study, the shutdown cost is considered as a constant to simplify the problem. The sum of start-up and shut-down cost is the transition cost.

6.1.2 Constraints

Two types of constraints, i.e., system constraints and unit constraints are considered in the unit commitment problem. System constraints include real power balance constraints, spinning reserve constraints, energy constraints, etc. Unit constraints include generation output limits, ramp rate limits, minimum, up- and down-time constraints, turbine and pump operating constraint, unit initial status constraints, unit must-run constraints, etc. Among these constrains, ramp rate limits, minimum, up- and down-time constraints, unit initial status constraints, and unit must-run constraints are time-dependent constraints. Others are time-independent constraints.

In this study, the following constraints are taken into account.

1. Power balance constraints

The total output of on-line generators must be equal to the system load demand in each of the planned time period, i.e.

$$P_{Dj} + P_{loss} \leq \sum_{i=1}^{M} u_{ij} P_{ij} \tag{6.2}$$

where P_{Dj} is system load demand at time j; and P_{loss} is the power losses.

2. Generation output limits

At normal system operation situations, the generation output of each individual unit must be within its allowable lower and upper generation limits, i.e.:

$$P_i^{\min} \leq P_{ij} \leq P_i^{\max} \tag{6.3}$$

where $P_i^{\min}$ is minimum generation limit of unit i; and $P_i^{\max}$ is maximum generation limit of unit i.

3. Unit minimum up time constraints

The unit must maintain on status for a minimum up time period after being started up.

$$MUT_i < T_{ij}^{ON} \tag{6.4}$$

where MUT_i is minimum up time of unit i; and T_{ij}^{ON} : ON period of unit i at time j.

4. Unit minimum down time constraints

The unit must maintain off status for a minimum down time period after being shut down.

$$MDT_i < T_{ij}^{OFF} \tag{6.5}$$

where MDT_i is minimum down time of unit i; and T_{ij}^{OFF} is OFF period of unit i at time j.

5. Ramp rate limits

Because of the physical restrictions on generators, the rate of generation change must be limited within a certain range, which confines unit's power output changes between adjacent hours.

$$P_{i,j} - P_{i,j-1} \leq RU_i \tag{6.6}$$

$$P_{i,j-1} - P_{i,j} \leq RD_i \tag{6.7}$$

Where RU_i is ramp-up rate limit for the unit i; and RD_i is ramp-down rate limit for the unit i.

6. Spinning reserve constraints

If generation forced outages are not considered, the spinning reserve constraint can be given as:

$$P_{Dj} + P_{Rj} \leq \sum_{i=1}^{M} u_{ij} P_i^{\max} \tag{6.8}$$

If the generator outages are taken into account, the spinning reserve constraint is:

$$P_{Dj} + P_{Rj} \leq \sum_{i=1}^{M} p_i u_{ij} P_i^{\max} \tag{6.9}$$

where p_i is probability of unit i operated in normal operating state.

7. Must run/down constraints

The must run/down constraints force units in or out of service due to the fuel factors or short-term maintenance.

8. Unit initial status

Some units may have initially committed as on or off before the planned time period, the unit initial status need to be considered for some situations.

To sum up, the objective of UC problem is to minimize the objective function (6.1), subject to the constraints (6.2)–(6.9).

6.2 Solving Unit Commitment Problem Using Genetic Algorithm

In this study, GA is selected to solve the UC problem. A genetic algorithm contains four main components: choosing chromosome syntax, interpretation of a chromosome, evaluation of a chromosome, and operators on chromosomes.

Figure 6.1 shows the basic procedure of applying the GA to solve the UC problem.

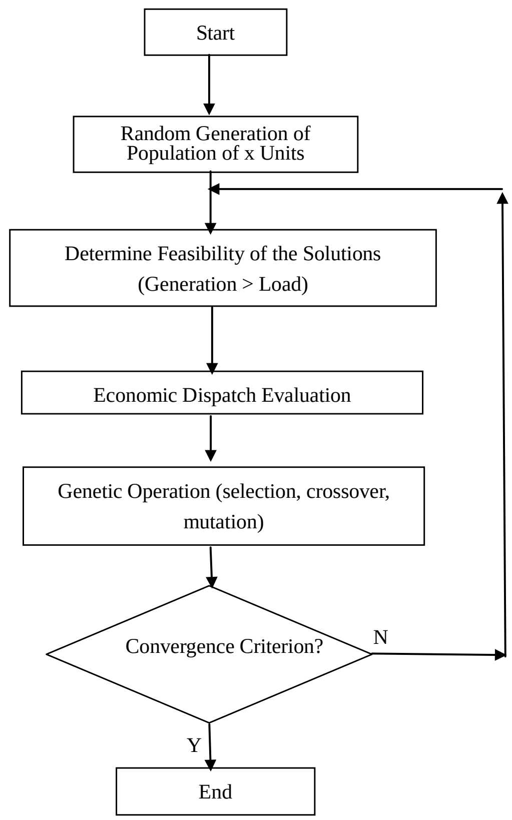

Figure 6.1. Flowchart of the GA-Based UC Solver

Representing chromosomes by binary vectors has been widely used in GA. This is because applying operators to binary vectors, evaluating and interpreting binary chromosomes become easy to implement functions. To convert a chromosome to a solution, an appropriate syntax needs to be applied. The chromosome could be either feasible or infeasible. A feasible chromosome yields a solution that lies in the feasible region (the region where all constraints are satisfied) of the solution space of a given problem. Infeasible chromosomes yield a solution that lies outside of the feasible region. Every chromosome must be evaluated against the objective of the problem. This evaluation is done by calculating the fitness function, that is the UC objective function.

Genetic operators in the reproduction stages of a GA include random operators, crossover operators, and mutation operators. Random operators can be used to create an initial population. The crossover operators combine features of any two parent chromosomes to form two offspring by swapping corresponding segments of the parents. The mutation operators are used to generate new populations by changing two or more bits of the chromosome. The selection process is used to choose the chromosomes to produce offspring based on the fitness assignment. Each chromosome in the selection pool receives a reproduction probability depending on their fitness, and the fitnesses of all other individuals in the selection pool. Roulette wheel selection is used in this paper.

6.3 Simulation Results

In this section, the UC solver based on GA is applied to solve a unit commitment problem of committing and decommitting 10 generators in a period of 24 hours. Crossover (also called recombination) and/or mutation is used to generate a second generation population of solutions from those selected through genetic operators. These processes ultimately result in the next generation population of chromosomes that is different from the initial generation. If the difference between current solution and the previous one is less than the converge criterion, the GA stops. If the number of iterations is greater than the maximum number, the GA stops.

The genetic algorithm uses the following parameters:

Selection scheme	: Roulette wheel
Population size	: 25
Crossover rate	: 0.6
Mutation rate	: 0.001
Converge criterion	: 0.0001
Number of iterations	: 3000

The unit commitment problem uses the following parameters:

Number of generators	: 10
Scheduled hours	: 24 hours
Startup cost	: $2900
Shutdown cost	: $1600
Ramp rate	: 200 MW/hr
Reserve percentage	: 10% of load demand
Startup/shutdown time	: 4 hours

All the parameter settings are saved in a configuration file. The C++ program reads the parameters from the configuration file.. Users can solve their own UC problem by modifying the file. The structure of the configuration file is described as follows.

Line 1: Total number of generation units (int)
Line 2: Total number of stages (int)
Line 3: Mutation rate (double)
Line 4: Crossover rate (double)
Line 5: Population size (int)
Line 6: Convergence criterion (double)
Line 7: Number of iterations (int)
Line 8: Percentage of reserve (double)
Line 9: Generator start-up cost (double)
Line 10: Generator shut-down cost (double)
Line 11: Ramp rate (double)

Line 12: Load demand offset, control the GA converge speed (double)
Line 13: Consider generator start up/shut down time constraint? (1 - yes, 0 - no) (int)
Line 14: Consider generator initial status constraint? (1 - yes, 0 - no) (int)
Line 15: Consider generator must-run constraint? (1 - yes, 0 - no) (int)
Line 16: Consider ramp rate constraint? (1 - yes, 0 - no) (int)
Line 17: Write the GA results into files? (1 - yes, 0 - no) (int)
Line 18: Generators' start up/shut down time (hrs), (2, 3, or 4)
Line 19: Generators' initial status, (1 - on, 0 - off) (int)
Line 20: Generators' must run flag, (1 - must run, 0 - no) (int)
Line 21: Generating units' coefficients - cost function factors, "a" (double)
Line 22: Generating units' coefficients - cost function factors, "b" (double)
Line 23: generation unit coefficients - cost function factors, c (double)
Line 24: Minimum generation output (double)
Line 25: Maximum generation output (double)
Line 26: Load demand (double)

Table 6.1 shows the generator initial status and must-run status. The initial status refers to the on and off status of generators at the end of previous scheduling plan. Must-run flags demonstrate whether the generator must be kept "ON" during the scheduled period. In this case study, generators 1, 2, 3, and 4 are scheduled as must-run during the 24 hour period. Table 6.2 shows the load demand in the 24 hour period. Usually, the future load demand is predicted by load forecasting procedures. Table 6.3 shows the unit commitment solution obtained by the developed GA-based UC solver. In

Table 6.3, the scheduled generation for each generator unit in 24 hour period is provided. The total generation is obtained by taking into account both the load demand and contingency reserve. Total cost is calculated by the objective function of the GA-based UC solver.

Table 6-1. Generator Settings

Units	1	2	3	4	5	6	7	8	9	10
Unit Initial Status	on	on	on	on	on	on	off	off	on	on
Must-run (Y/N)	yes	yes	yes	yes	no	no	no	no	no	no
Max Generation	625	625	600	500	625	525	500	550	605	625
Min Generation	100	100	75	75	100	100	85	85	90	90

Table 6-2. Load Demand (MW)

Hours	1	2	3	4	5	6	7	8	9	10	11	12
Demand	1200	1295	1490	1530	1690	1730	1900	1930	2090	2230	2200	2190
Hours	13	14	15	16	17	18	19	20	21	22	23	24
Demand	2210	2090	1950	1880	1710	1680	1550	1500	1285	1210	1285	1490

Table 6-3. Unit Commitment Solution

Units → Hours ↓	1	2	3	4	5	6	7	8	9	10	Total Generation (MW)	Total Cost ($)
1	121.1	105.1	88.3	84.6	330.4	252.5	0	0	173.6	173.7	1329.2	16963.18
2	212.4	160.6	201.8	199.6	272.4	109.1	0	0	132.3	142.3	1430.5	17729.91
3	105.6	341.7	145.3	131.9	322.7	129.5	0	139.5	95.0	235.4	1646.8	23357.64
4	236.0	267.8	177.1	226.6	187.2	149.4	0	157.7	177.1	108.8	1687.9	20370.38
5	361.2	160.0	354.2	342.5	0	0	0	175.5	208.3	257.4	1859.1	26253.00
6	560.9	348.4	293.6	290.6	0	0	133.7	279.5	0	0	1906.7	29564.68
7	586.5	356.6	404.0	314.7	0	0	162.1	267.7	0	0	2091.6	26171.05
8	608.6	499.8	305.9	214.6	0	0	183.6	317.7	0	0	2130.2	26733.64
9	477.2	464.9	383.4	361.2	134.4	175.6	307.7	0	0	0	2304.5	36457.67
10	391.5	437.7	338.8	465.5	277.1	318.9	0	0	107.6	116.1	2453.2	38227.04
11	283.2	328.4	186.9	422.7	403.3	374.2	0	0	203.3	226.5	2428.4	30372.35
12	173.4	358.7	95.5	302.2	582.9	461.9	0	0	201.3	238.5	2414.4	31530.16
13	339.7	198.0	161.7	170.1	416.6	409.1	0	185.0	379.9	173.7	2433.9	33747.76
14	204.2	133.4	313.6	156.8	244.2	312.7	162.9	318.6	458.0	0	2304.5	34040.30
15	297.6	171.8	303.9	233.3	410.5	0	155.2	160.5	413.2	0	2145.9	29752.22
16	294.5	109.8	336.7	383.3	191.3	0	155.6	167.7	435.9	0	2074.8	27417.69
17	401.8	112.3	295.1	270.3	0	0	234.7	0	570.8	0	1885.0	29565.93
18	500.8	172.4	217.7	142.3	0	0	233.1	0	588.4	0	1854.6	26298.82
19	600.9	151.3	81.2	296.4	0	0	0	0	390.0	186.2	1706.1	27452.17
20	476.7	272.9	226.4	280.2	0	105.0	0	0	0	293.4	1654.7	24703.01
21	545.5	131.8	168.9	264.0	0	158.6	0	0	0	153.8	1422.6	17608.37
22	414.6	145.7	78.6	289.4	0	152.3	0	132.3	0	126.6	1339.5	19145.98
23	227.8	270.9	116.1	157.7	174.4	127.0	0	236.8	0	110.4	1421.0	19761.67
24	341.7	118.0	160.7	203.4	283.7	0	133.7	184.5	0	215.5	1641.2	24663.61

In this section, a genetic algorithm based unit commitment solver is described. The developed genetic algorithm based unit commitment solver is incorporated in the EMS Wind Integration system. In the unit commitments solvers, the considered constraints include power balance, generation output limits, unit minimum up time, unit minimum down time, ramp rate limits, spinning reserve, must run/down and unit initial status constraints. A unit commitment case study of 10 machines 24 hours is applied to show the effectiveness of the unit commitment solver.

7.0 Software Prototype Design and Testing

The software prototype of generation requirements uncertainty evaluation tool has been developed within the framework of the CAISO project sponsored by CEC. The plan is to install the prototype at the CAISO control room. The tool is based on the methodology developed in this project.

At the first phase the prototype is planned to be operated in the testing mode as a stand-along tool for approximately 6 months. It corresponds to the passive level of integration (see Section 5.0 for details). During the testing period, the CAISO specialists will evaluate the efficiency and the usefulness of the tool. Testing will be based on analysis of retrospective data collected from different sources of information, like CAISO's SCADA/EMS systems, CAISO's market system, CAISO's master file, CAISO's wind forecast provider, etc. The prototype can help CAISO to evaluate the balancing capacity needed to mitigate negative impacts, caused by unpredicted deviations of wind generation, as well as due to inaccurate load forecast and generation forced outages. In case of successful testing, a decision will be made by the CAISO on a possibility of the actual integration of the tool into the CAISO's EMS system.

7.1 Prototype Design and User Interface

Microsoft Visual Studio 2008 was used for the tool development. The developed tool is deployed on the Microsoft Windows platform and .NET Framework. The prototype consists of three major modules: the database, the uncertainty evaluation module and the display for results and alerts. The database is implemented in Microsoft SQL Server. Data exchange with CAISO systems will be performed via the XML protocol. Flowchart reflecting the interactions among different prototype blocks, database and EMS system is presented in Figure 7.1.

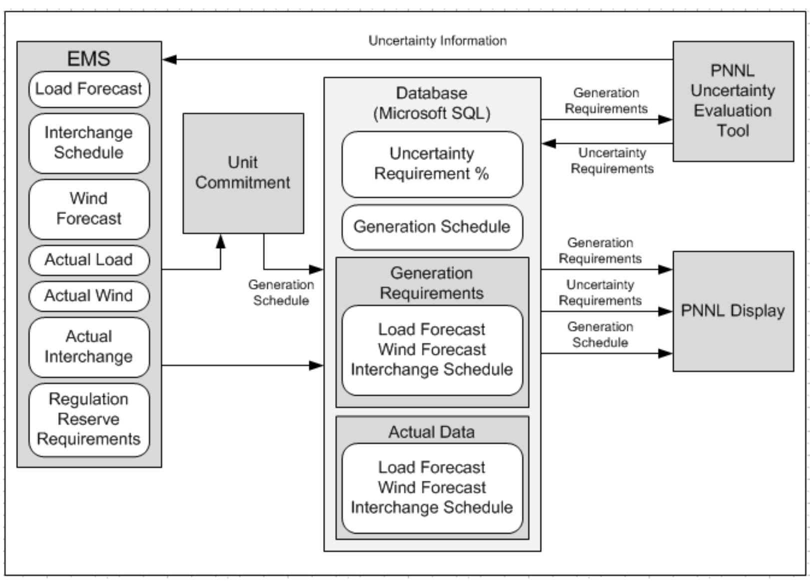

Figure 7.1. Software Flowchart

At the first phase of integration the used CAISO data are shown in Table 7.1. Database structure details are given in Appendix A.

Table 7-1. CAISO Data Used in the First Phase of the Project

	Day-ahead Forecast(schedule)	Hour-Ahead forecast(schedule)	Real-time forecast(schedule)	Actual
Load	✓	✓	✓	✓
Wind Generation	✓	✓	✓	✓
Interchange	✓	✓		✓
Generation	DAM	STUC	RTED	✓

Currently, the prototype can operate in three modes:

1. Static mode

- In the static mode, the user can select any required date and time to display information on the forecasted and actual parameters in the tabular or graphical form. This information includes:
  - Load forecast
  - Wind Generation forecast
  - Interchange schedule
  - Generation requirements forecast – Load forecast minus wind generation forecast and minus interchange schedule.
  - Generation schedule
  - Actual load
  - Actual wind generation
  - Actual interchange
  - Actual generation requirements
- The user can select the desired uncertainty ranges with any required level of confidence. The ranges are reflecting the uncertainty in generation requirements caused by different sources: wind, load, etc. Screenshots shown in Figure 7.2–Figure 7.4 are examples of the software user interface. In Figure 7.2 the uncertainty visualization display is given. Uncertainty analysis display is shown in Figure 7.3. Using this tool, one can analyze statistical characteristics of forecast errors, plot different histograms and CDF functions. Figure 7.4 shows the database display that provides access to the SQL database for the user.

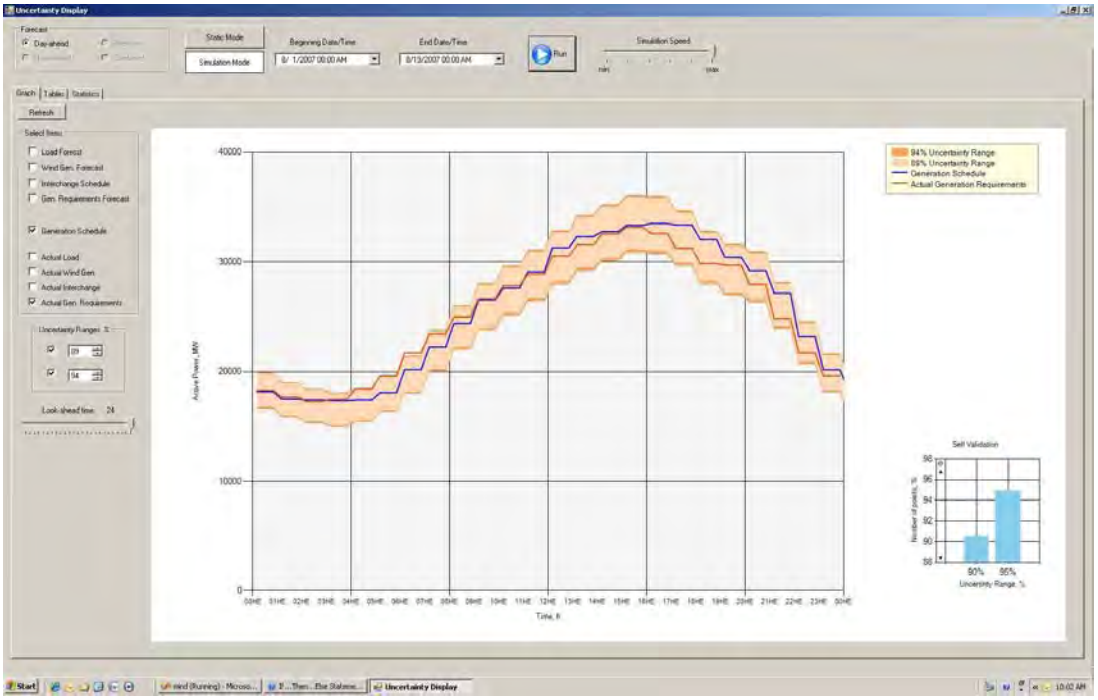

Figure 7.2. Screenshot of Uncertainty Visualization Display

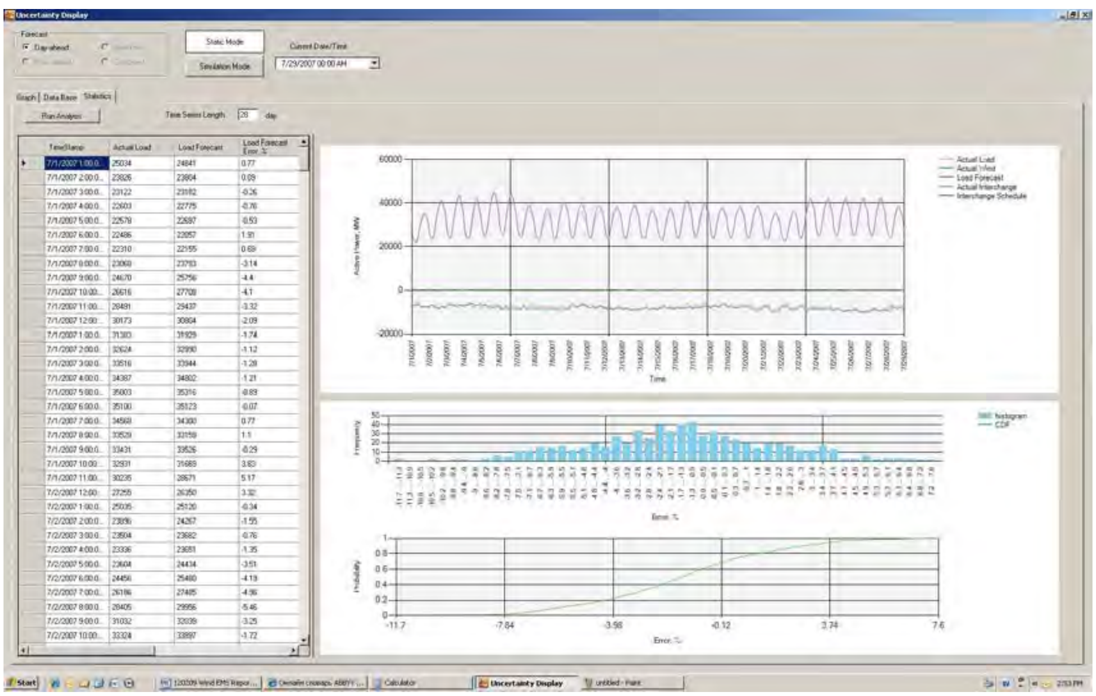

Figure 7.3. Screenshot of Uncertainty Analysis Display

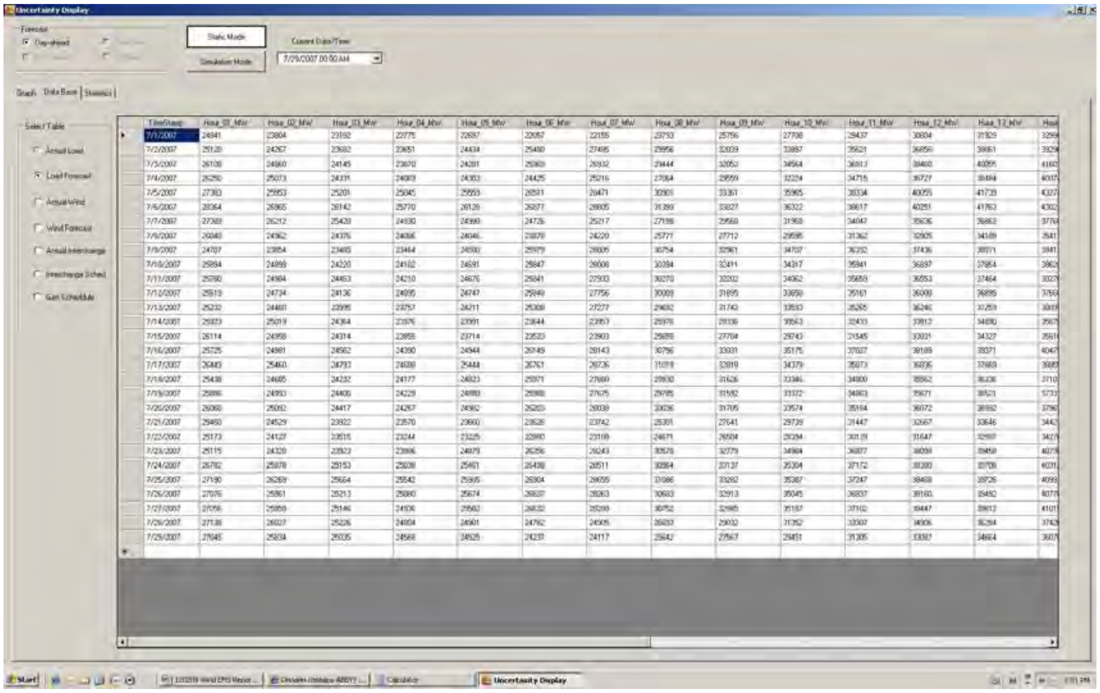

Figure 7.4. Screenshot of Database Display

2. Simulation mode

In the simulation mode an hour by hour simulation for a specified time interval can be performed. It is needed to validate the accuracy of uncertainty evaluation model. Details of self validation algorithm are given in Section 2.8.

During the simulation, the user sees an animated picture reflecting changing of the current conditions of the system. The speed of simulation can be specified by the user.

3. Real-time mode (under development)

In real-time mode the prototype will link to the real-time system operation. The tool will receive information in real-time and update the uncertainty prediction every 5 minutes.

7.2 Test Plan for the Ramp Tool Prototype

A comprehensive plan to test the tool prior to release has been developed. It includes functional, requirements and performance testing of the database, database loading, analytical, and GUI.

A server will be initialized by installing the test database with no data. It will then be updated using the data loading software and examined for correct loading. One or more standard PC workstations, configured with needed supporting software, in accordance with the Prototype Hardware and Software Requirements and Prototype Data Specification, will then be loaded and tested using procedures in the test tool.

Testing will be performed using the database running on a separate workstation as a server and with the database running on the local workstation. TestLink reporting tools will be used to generate testing repots. TestLink enables easily to create and manage test cases as well as organizes them into test plans [24]. These Test plans allow team members to execute test cases and track test results dynamically, generate reports, trace software requirements, prioritize and assign tasks.

Items to be tested:

- Prototype analytics and GUI.
- SQL database loading tool.
- SQL database performance testing.

Features to be tested:

All user controls will be tested. Conformance with software requirements will be tested. Details of the testing will be included in the TestLink test project.

7.2.1 Statistical Analysis Module Test

To validate the statistical analysis module developed by PNNL using Visual Studio 2008 IDE, results produced by this module were compared with standard results obtained from a professional statistical package. MATLAB statistical toolbox was used as the standard statistical package [11].

Figure 7.5 depicts the day-ahead net load forecast error. The length of time series is 30 days. This test time series is used as an input for the statistical analysis module. A comparison of histograms and empirical CDFs for the test time series, obtained using PNNL tool and MATLAB statistical toolbox are presented in Figure 7.6–Figure 7.7. One can see that results produced by PNNL tool coincide with the MATLAB toolbox results.

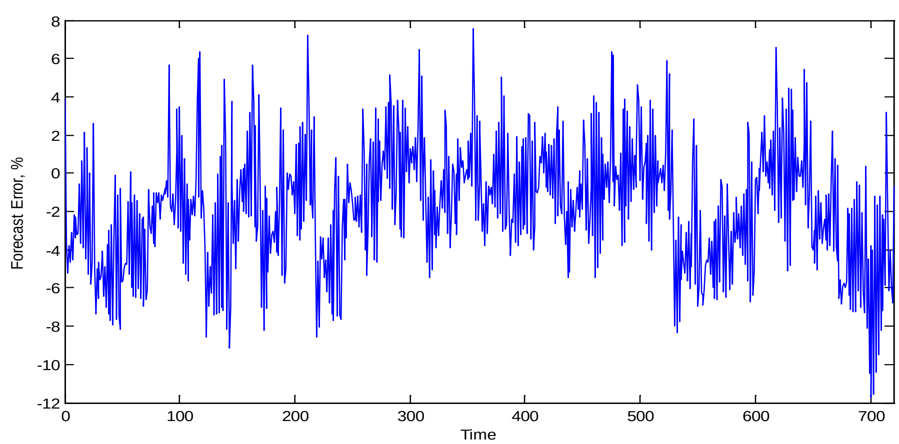

Figure 7.5. Net Load Error Forecast (Day-Ahead)

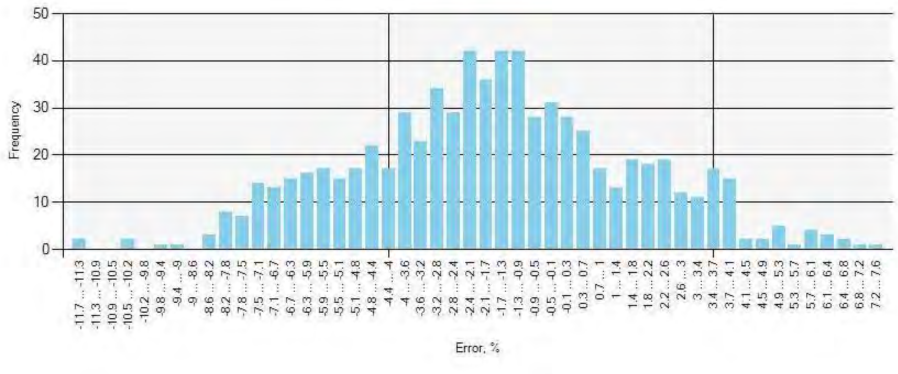

a)

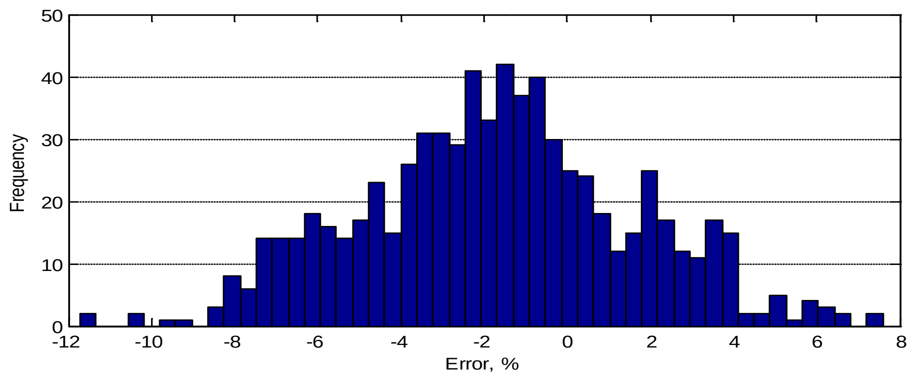

b)

Figure 7.6. Histograms Comparison: a) PNNL Tool; b) MATLAB Statistical Toolbox

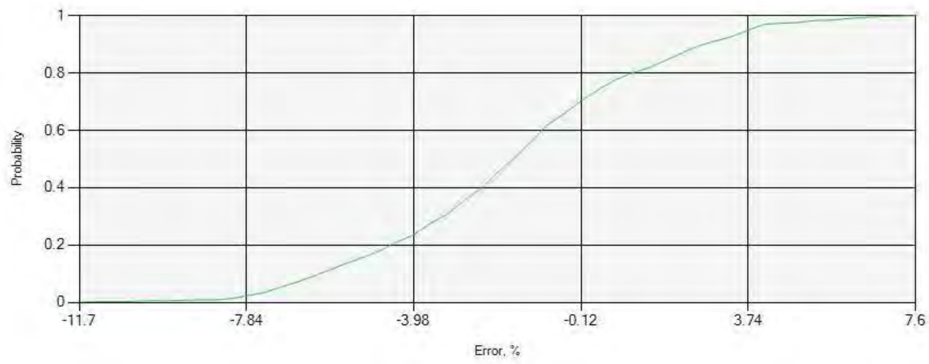

a)

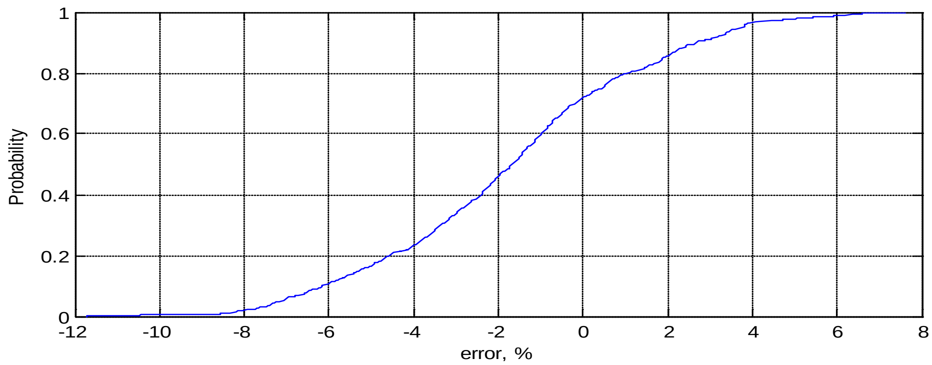

b)

Figure 7.7. Empirical CDFs Comparison: a) PNNL Tool; b) MATLAB Statistical Toolbox

7.2.2 Uncertainty Evaluation Model Test

To validate the accuracy of the uncertainty evaluation model, a self validation algorithm was developed and used (see Section 2.8 for details). CAISO's real statistical information for year 2007 was used in this test. Figure 7.8 shows the uncertainty range evaluation for the day-ahead schedule produced on August 1st, 2007, at 6 a.m. The ranges for 90% and 95% level of confidence are shown. Blue curve represents the day-ahead generation schedule. The red curve represents the actual generation requirements (actual load minus actual wind generation and minus actual interchange).

The developed set of self validation tests were performed. Different time periods were analyzed. The length of studied intervals is 1 month. Some results of self validation test are presented in Figure 7.9. For example, in Test I (Figure 7.9), the uncertainty ranges with 90% and 95% confidence were evaluated for the time period from August 1 until August 30. The percentage of the actual generation requirements points found within 90% confidence interval is about 91%, and within 95% confidence interval is about 95%. Similarly, Test II and Test III compare the results for 70, 85, 99, and 100% confidence levels. Thus the uncertainty evaluation model tests have confirmed the adequacy of the proposed uncertainty evaluation algorithm as well as the proper operation of developed prototype tool.

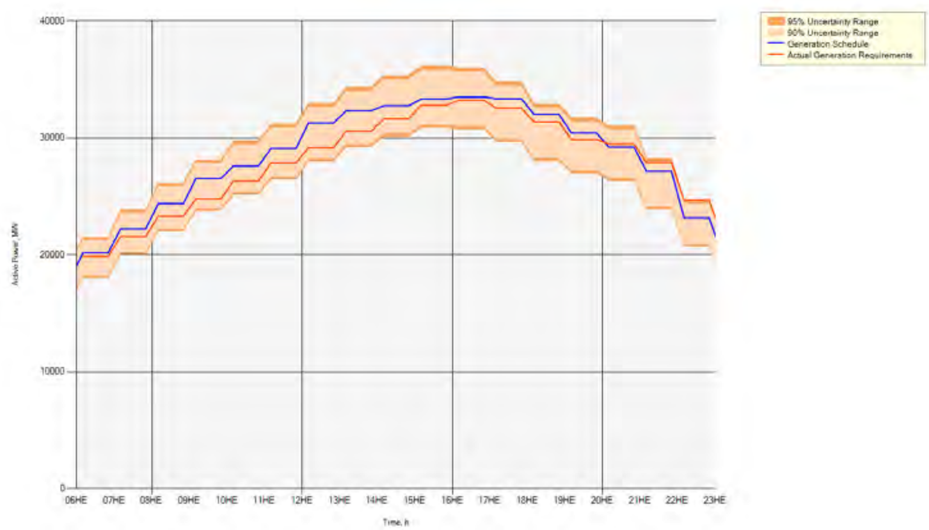

Figure 7.8. Example of Uncertainty Ranges Evaluation (August 1, 2007 at 6 am)

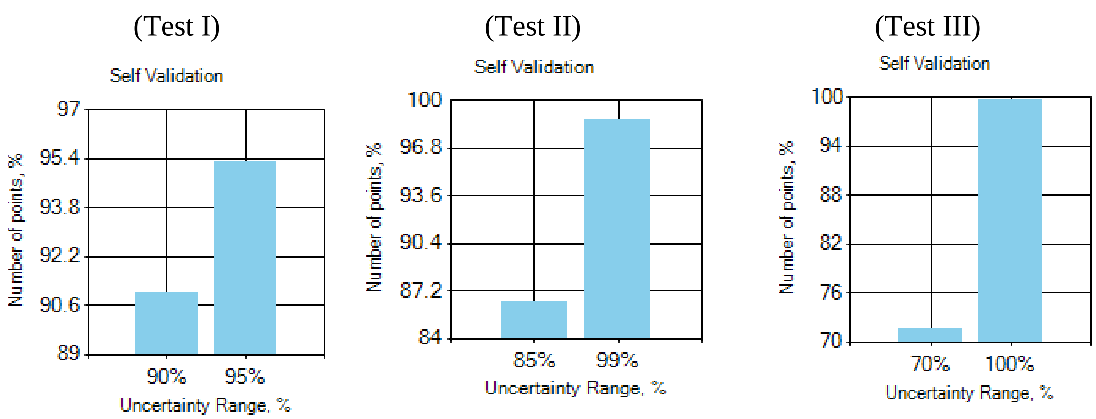

Figure 7.9. Self Validation Results

8.0 Conclusions and Future Work

A methodology capable of evaluating the impact of wind generation and load uncertainties, as well as unexpected generation outages on the balancing resources requirements has been developed. As a result, the uncertainty ranges for the required generation performance envelope can be evaluated for a look-ahead period. The generation performance envelope includes the required balancing capacity, ramping capability and ramp duration capability.

The proposed methodology includes the following elements:

- Evaluation of the capacity and ramping requirements using a specially developed probabilistic algorithm based on the histogram analysis, and incorporating all sources of uncertainties of both continuous (wind and load forecast errors) and discrete (forced generator outages and start-up failures) nature.
- Evaluation of the look-ahead generation performance requirements envelope using a “flying brick” technique for the worst case scenario within a user specified confidence level.
- A self-validation algorithm to assess the accuracy of the predicted uncertainty ranges

A MATLAB prototype of a probabilistic tool based on the proposed methodology has been developed. Preliminary simulation studies using the MATLAB prototype and actual CAISO data have been performed. Study results have shown that the methodology of the generation requirements evaluation for uncertainty management is quite accurate and efficient.

The operating practices at CAISO and BPA have also been studied. The concept of integrating the probabilistic tool with CAISO and AREVA EMS environments has been developed taking into account their current operating practices. To demonstrate the validity of the developed uncertainty evaluation methodology and the impact of uncertainties on grid operation, the initial design of probabilistic tool integration with AREVA’s EMS has been developed through collaboration with AREVA’s specialists.

As part of the efforts in evaluating the impact of uncertainties on grid operation, a unit commitment model based on the genetic algorithm optimization technique has been developed and tested on multi-machine cases.

Besides the integration with the AREVA EMS, the probabilistic tool will be integrated with the CAISO EMS and market systems collaboration with CAISO’s team, with additional financial support from California Energy Commission.

Among the tasks that could be performed in the next phase of the project, a development of the proactive integration approach for the probabilistic tool into an EMS environment will be a focus. It can contribute to the development of a novel probabilistic grid operation philosophy. Future work also includes refinement of the uncertainty assessment tool by integrate more sources of uncertainties and developing alternative methods for uncertainty assessment, integration of the uncertainty assessment tool with market systems to demonstrate the economic impact of uncertainties, integration of the uncertainty assessment tool with wind forecasting services, and pilot demonstration of the uncertainty assessment tool with EMS platforms towards the goal of operator acceptance of the tool in the control room.

9.0 References

[1] J. Zack, "An Analysis of the Errors and Uncertainty in Wind Power Production Forecasts", *Proc. WINDPOWER 2006*, Pittsburgh, June 4-7, 2006. [Online.] Available: http://www.awstruewind.com/files/AWEA_Windpower_2006_ForecastingErrors.pdf

[2] J. Lerner, M. Grundmeyer and M. Garvert, "The Role of Wind Forecasting in the Successful Integration and Management of an Intermittent Energy Source". [Online.] Available: http://www.3tier.com/en/about/publications/role-wind-forecasting-successful-integration-and-management-intermittent-energy-source/

[3] G. Kariniotakis, "ANEMOS, Leading European Union Research on Wind Power Forecasting," Presentations at the International Wind Forecast Techniques and Methodologies workshop, July 24 -25, 2008. [Online.] Available: http://www.bpa.gov/corporate/business/innovation/docs/2008/BPA_California%20ISO%20ANEMOS%20Presentation.pdf

[4] "Wind power prediction Previento," Energy & Meteo Systems. [Online.] Available: http://energymeteo.de/de/media/e_m_Broschuere.pdf

[5] P. Pinson, G. Kariniotakis, H. Aa. Nielsen, T. S. Nielsen, and H. Madsen, "Properties of Quantile and Interval Forecasts of Wind Generation and their Evaluation," *Proc. European Wind Energy Conference & Exhibition*, Greece, 2006.

[6] A. Luig, S. Bofinger and H. G. Beyer, "Analysis of Confidence Intervals for the Prediction of the Regional Wind Power Output," *Proc. 2001 European Wind Energy Conference*, Denmark, June 2001. [Online.] Available: http://home.arcor.de/armin-luig/Projekte/Paper_EWEC_2001.pdf

[7] "WECC Standard BAL-STD-002-0 – Operating Reserves." [Online.] Available: http://www.nerc.com/files/BAL-STD-002-0.pdf

[8] "WSCC Operating Reserve White Paper." [Online.] Available: http://www.wecc.biz/documents/library/PWG/wsc6oprs.pdf

[9] "Integration of Renewable Resources Report," CAISO, November 2007. [Online.] Available: http://www.caiso.com/1ca5/1ca5a7a026270.pdf

[10] Y. V. Makarov, C. Loutan, J. Ma, and P. De Mello, "Operational Impacts of Wind Generation on California Power Systems," *IEEE Trans. on Power Syst.*, vol. 24, pp.1039–1050, May, 2009.

[11] "Statistical toolbox," MATLAB User's Manual.

[12] R. Doherty and M. O'Malley, "A new approach to quantify reserve demand in systems with significant installed wind capacity," *IEEE Trans. on Power Syst.*, vol. 20, May, 2005, pp. 587–595.

[13] R. Billinton and R. Allan, *Reliability Evaluation of Power System*, Plenum Press, N.Y.,1996.

[14] R. Billinton and J. Ge, "A Comparison of Four-state Generating Unit Reliability Models for Peaking Units," *IEEE Trans. on Power Syst.*, vol. 19, May, 2004, pp.763–768.

[15] A. D. Patton, "Duty Cycle Effects on Generating Unit Availability," *IEEE Trans. on Industry Applications*, vol. 29, Sept.-Oct., 1993, pp. 1018–1021.

[16] D. Morrow and L. Gan, "Comparison of Methods for Building a Capacity Model in Generation Capacity Adequacy Studies," *Proc. IEEE WESCANEX'93, Communications, Computers and Power in the Modern Environment* , 1993, pp. 143–149.

[17] "Generating Availability Data System Report," North American Electric Reliability Corporation. [Online.] Available: http://www.nerc.com/files/gar2007.zip

[18] G. M. Curley, "Power Plant Performance Indices in New Market Environment," IEEE Standard 762 Working Group Activities and GADS Database," *Proc. IEEE Power Engineering Society General Meeting*, p. 5, 2006.

[19] "Market Redesign and Technology Update Tutorial for Market Participants," CAISO, 2006. [Online.] Available: http://www.caiso.com/docs/2005/09/22/2005092212224714566.pdf

[20] J. Pease, "Challenges with the Integration of Large Scale Wind by a Regional Utility," BPA, June 2006. [Online.] Available: http://www.bpa.gov/Power/PGC/wind/Challenges_of_large_scale_wind_integration_paper.pdf

[21] "Optimization of the Federal Columbia River Power System," Presentation. BPA, 2006. [Online.] Available: http://www.nwpp.org/ntac/pdf/NTAC%202006-02-09%20Att%207%20BPA_NTAC%202006%20Final.pdf

[22] "Near Real-Time Optimizer," Synexus Global Inc. [Online.] Available: http://www.acresinnovations.com/winter2004/vista.html

[23] Y. Fu and M. Shahidehpour. "Fast SCUC for Large-Scale Power Systems," *IEEE Trans. on Power Syst.*, vol. 22, pp. 2144-2151, Nov. 2007.

[24] "TestLink ver. 1.8," User Manual, Testlink Community, 2009. [Online.] Available: http://www.teamst.org/_tldoc/1.8/user_manual.pdf

Appendix A

Prototype Data Specification

Appendix A

Prototype Data Specification

This appendix describes the data specification for the first phase of prototype integration into the California ISO EMS system.

Table A.1. Load – Day-Ahead Forecast

Field Name	SQL Server data type	Allow Nulls	Comment
Time Stamp	Date/Time	No	Primary key
Hour_01_MW	real	Yes	First hour ending megawatts forecast
Hour_02_MW	real	Yes	
Hour_03_MW	real	Yes	
Hour_04_MW	real	Yes	
Hour_05_MW	real	Yes	
Hour_06_MW	real	Yes	
Hour_07_MW	real	Yes	
Hour_08_MW	real	Yes	
Hour_09_MW	real	Yes	
Hour_10_MW	real	Yes	
Hour_11_MW	real	Yes	
Hour_12_MW	real	Yes	
Hour_13_MW	real	Yes	
Hour_14_MW	real	Yes	
Hour_15_MW	real	Yes	
Hour_16_MW	real	Yes	
Hour_17_MW	real	Yes	
Hour_18_MW	real	Yes	
Hour_19_MW	real	Yes	
Hour_20_MW	real	Yes	
Hour_21_MW	real	Yes	
Hour_22_MW	real	Yes	
Hour_23_MW	real	Yes	
Hour_24_MW	real	Yes	

Table A.2. Load – Hour-Ahead Forecast

Field Name	SQL Server data type	Allow Nulls	Comments
Time Stamp	Date/Time	No	Primary key
Interval_01_MW	real	Yes	First interval MW forecast
Interval_02_MW	real	Yes	Next interval MW forecast
Interval_03_MW	real	Yes	
……	……	……	
Interval_10 _MW	real	Yes	

Table A.3. Load – Real-Time Forecast

Field Name	SQL Server data type	Allow Nulls	Comments
Time Stamp	Date/Time	No	Primary key
Interval_01_MW	real	Yes	First 5 min. ending MW forecast
Interval_02_MW	real	Yes	Next 5 min. ending MW forecast
Interval_03_MW	real	Yes	Next 5 min. ending MW forecast
……………………			
Interval_13 _MW	real	Yes	Last 5 min. ending MW forecast

Table A.4. Load – Actual

Field Name	SQL Server data type	Allow Nulls	Comments
Time Stamp	Date/Time	No	Primary Key
MW_ActualLoad	real	Yes	Interval ending mw actual load

Table A.5. Wind Generation – Day-Ahead Forecast

Field Name	SQL Server data type	Allow Nulls	Comments
Time Stamp	Date/Time	No	Primary Key
Interval_01_MW	real	Yes	First Interval ending MW forecast
Interval_02_MW	real	Yes	
Interval_03_MW	real	Yes	
Interval_04_MW	real	Yes	
Interval_05_MW	real	Yes	
Interval_06_MW	real	Yes	
Interval_07_MW	real	Yes	
Interval_08_MW	real	Yes	
Interval_09_MW	real	Yes	
Interval_10_MW	real	Yes	

Table A.5 (contd)

Field Name	SQL Server data type	Allow Nulls	Comments
Interval_11_MW	real	Yes	
Interval_12_MW	real	Yes	
Interval_13_MW	real	Yes	
Interval_14_MW	real	Yes	
Interval_15_MW	real	Yes	
Interval_16_MW	real	Yes	
Interval_17_MW	real	Yes	
Interval_18_MW	real	Yes	
Interval_19_MW	real	Yes	
Interval_20_MW	real	Yes	
Interval_21_MW	real	Yes	
Interval_22_MW	real	Yes	
Interval_23_MW	real	Yes	
Interval_24_MW	real	Yes	

Table A.6. Wind Generation – Hour-Ahead Forecast

Time Stamp	Date/Time	No	Primary Key
Interval_01_MW	real	Yes	First Interval ending MW forecast
Interval_02_MW	real	Yes	
…….	…..		
Interval_XX _MW	real		

Table A.7. Wind Generation – Real-Time Forecast

Time Stamp	Date/Time	No	Primary Key
Interval_01_MW	real	Yes	First Interval ending MW forecast
Interval_02_MW	real	Yes	
…….	…….		
Interval_XX _MW	real	No	

Table A.8. Wind Generation – Actual

Time Stamp	Date/Time	No	Primary Key
ActualGeneration	real	Yes	Interval ending MW actual generation

Table A.9. Interchange – Day-Ahead Schedule

Time Stamp	Date/Time	No	Primary Key
Tie ID	nvarchar(16)	No	Primary Key
Hour_01_MW	real	Yes	First hour ending MW scheduled
Hour_02_MW	real	Yes	
Hour_03_MW	real	Yes	
Hour_04_MW	real	Yes	
Hour_05_MW	real	Yes	
Hour_06_MW	real	Yes	
Hour_07_MW	real	Yes	
Hour_08_MW	real	Yes	
Hour_09_MW	real	Yes	
Hour_10_MW	real	Yes	
Hour_11_MW	real	Yes	
Hour_12_MW	real	Yes	
Hour_13_MW	real	Yes	
Hour_14_MW	real	Yes	
Hour_15_MW	real	Yes	
Hour_16_MW	real	Yes	
Hour_17_MW	real	Yes	
Hour_18_MW	real	Yes	
Hour_19_MW	real	Yes	
Hour_20_MW	real	Yes	
Hour_21_MW	real	Yes	
Hour_22_MW	real	Yes	
Hour_23_MW	real	Yes	
Hour_24_MW	real	Yes	

Table A.10. Interchange – Hour-Ahead Schedule

Time Stamp	Date/Time	No	Primary Key
Interval_01_MW	real	Yes	First interval ending MW scheduled
Interval_02_MW	real	Yes	
Interval_03_MW	real	Yes	
…….			
Interval_XX_MW	real	Yes	

Table A.11. Interchange – Actual

Time Stamp	Date/Time	No	Primary Key
ActualNetFlow_MW	real	Yes	

Table A.12. Generation – Day-Ahead Schedule

Time Stamp	Date/Time	No	Primary Key
Hour_01_MW	real	Yes	First hour ending MW scheduled
Hour_02_MW	real	Yes	
Hour_03_MW	real	Yes	
Hour_04_MW	real	Yes	
Hour_05_MW	real	Yes	
Hour_06_MW	real	Yes	
Hour_07_MW	real	Yes	
Hour_08_MW	real	Yes	
Hour_09_MW	real	Yes	
Hour_10_MW	real	Yes	
Hour_11_MW	real	Yes	
Hour_12_MW	real	Yes	
Hour_13_MW	real	Yes	
Hour_14_MW	real	Yes	
Hour_15_MW	real	Yes	
Hour_16_MW	real	Yes	
Hour_17_MW	real	Yes	
Hour_18_MW	real	Yes	
Hour_19_MW	real	Yes	
Hour_20_MW	real	Yes	
Hour_21_MW	real	Yes	
Hour_22_MW	real	Yes	
Hour_23_MW	real	Yes	
Hour_24_MW	real	Yes	

Table A.13. Generation – Short-Term Unit Commitment (STUC) Schedule

Time Stamp	Date/Time	No	Primary Key
Interval_01_MW	real	Yes	First interval ending MW scheduled
Interval_02_MW	real		
……..			
Interval_20_MW	real		

Table A.14. Generation –Real-Time Economic Dispatch (RTED)

Time Stamp	Date/Time	No	Primary Key
Interval_01_MW	real	Yes	First interval ending megawatts scheduled
Interval_02_MW	real	Yes	
…………………..			
Interval_13_MW	real	Yes	

Table A.15. Generation – Actual

Time Stamp	Date/Time	No	Primary Key
PGen	real	Yes	
QGen	real	Yes	

Appendix B

Contingency Reserve Activation Model

Appendix B

Contingency Reserve Activation Model

Contribution of a Stochastic Contingency Reserve Activation Forecast to a Deterministic Controllable Generation Requirement

James MacPherson, Hamody Hindi, Richard D. Christie
University of Washington

Abstract –Unprecedented increases in wind power installation require new attention to maintain power system control performance and reliability. One way of improving control performance is through better use of forecasts of stochastic quantities such as wind generation. The Pacific Northwest National Laboratory (PNNL) has proposed using stochastic forecasts of wind, load, capacity outage, and contingency reserve activation to determine the controllable generation requirement (CGR) for the deterministic unit commitment found in existing energy management systems. This report details how to forecast contingency reserve activation using a probability density function (PDF) built from real time observations so that it adapts to system changes over time. This report then shows how to statistically combine the contingency reserve activation forecast with the load-minus-wind forecast provided by PNNL. The combined forecast is used to calculate the controllable generation requirement that is input to the unit commitment algorithm. Forecasting the controllable generation requirement in this way is expected to improve system control performance in the face of wind power variation at an optimal cost. The algorithms proposed in this report were coded in MATLAB, and a software environment with simulated energy management system input data was developed to verify proper operation of the algorithms. Simulations verified that the algorithm outputs are consistent with expected performance.

Table of Contents

Introduction

The limited controllability and inherently high prediction error of wind power generation, coupled with a rapid growth in wind power installation, has fostered increasing interest in incorporating the stochasticity of wind into the unit commitment (UC) used in power system operations. The obvious approach is to reformulate the UC as a stochastic optimization problem. This approach may exhibit improved optimality [1],[2], but is more computationally expensive than a deterministic UC formulation [3].

As an alternative, the Pacific Northwest National Laboratory (PNNL) has proposed using an existing deterministic UC with a controllable generation requirement (CGR) derived from stochastic forecasts of wind, load, capacity outage, and contingency reserve activation [4]. A single CGR value based on these time-varying, stochastic forecasts will be determined for each time interval of the UC. This method allows the current UC algorithm in an energy management system (EMS) – already paid-for and debugged – to remain unchanged while accounting for stochastic variation in wind power generation. The expected result of this method is an EMS that can better manage operations with high wind power penetration. Control performance is expected to improve during large changes in wind generation. The stochasticities of load, capacity outage, and contingency reserve (CR) activation are also included in the CGR computation to further improve control performance.

This method will be applied to the California ISO (CAISO) and Bonneville Power Administration (BPA) systems. The methodology described in this report maintains a theoretically general formulation except as noted when dealing with system-specific procedures.

The UC algorithm requires CGR inputs at 5-minute intervals over a 3 hour time horizon. One minute intervals may eventually be used, and the horizon time may vary. The UC algorithm is repeated every fifteen minutes with updated system information [4]. For each interval, forecasts of wind generation, system load, capacity outage, and CR activation are made. Each forecast is a random variable represented by a probability density function (PDF) derived from an *a posteriori* histogram. The PDFs take into account the forecast errors of each parameter.

PDFs in this report are expressed in discrete form. Discrete PDFs are easier to deal with computationally and can easily be derived from continuous PDFs or histograms. All variables and measures of real power such as wind power, load, and controllable generation assume units of megawatts (MW) unless otherwise noted.

The wind and load forecasts are statistically combined into one *load-minus-wind* forecast, $P_{L\text{-}W}$. The load-minus-wind forecast also includes the forecast errors of scheduled net interchange. This work was done at the Pacific Northwest National Laboratory (PNNL) and is not detailed in this report. The rest of this report continues under the assumption that the PDF of $P_{L\text{-}W}$ is known.

The load-minus-wind forecast is statistically combined with the CR activation forecast to obtain the PDF of the CGR forecast. This function is performed in the Combined Uncertainty Evaluation block of Figure 1, developed at the University of Washington.

The forecast of CR activation is a prediction of what the future CR activation behavior will be. CR activation forecasting is similar in concept (a PDF of a future value) but different in detail from load and wind forecasting. The CR activation forecasts are determined by the Contingency Reserve Activation Model (CRAM) designed at the University of Washington (UW). As seen in

Figure 1, the CRAM receives Contingency Reserve Response Deficiency PDFs and a Capacity Outage PDF Table (COPT) as input. The COPT comes from a Forced Outage Model developed at PNNL that uses historical outage statistics to compute the COPT. The Contingency Reserve Response Deficiency PDFs come from the Update Contingency Reserve Response Deficiency PDF Function developed at the University of Washington. This in turn receives 10 and 15 Minute Contingency Reserve Response Deficiency PDFs from the Contingency Reserve Response Deficiency Sample Evaluation Function, also developed at Washington, which creates these PDFs by monitoring actual Contingency Reserve Response in real time data from the Energy Management System (EMS).

The focus of this report is to propose a theoretical formulation for forecasting CR activation and computing CGR values. The various algorithms that embody the theory were coded in MATLAB and are presented in the following section. A simulation environment called the TestBench was also coded in MATLAB. TestBench provides simulated real time EMS data to verify proper operation of the algorithms. The TestBench simulation and simulation results are discussed in detail near the end of this report. The report concludes with a general discussion of the simulation performance and results, as well as a discussion of the requirements for ultimately incorporating the algorithms in the energy management system of CAISO and BPA.

Overview of Deliverable Program Files

The primary MATLAB m-files developed to realize the theoretical formulation presented in this report are:

1. combined_uncertainty_evaluation.m
2. contingency_reserve_activation_model.m
3. crrd_sample_evaluation.m
4. update_crrd_pdf.m

There are numerous secondary m-files called as subroutines by the primary m-files to perform specific functions. These secondary m-files are detailed in Appendix A.

Of the primary m-files, the first is the Combined Uncertainty Evaluation block of Figure 1. It takes as input the forecasts of CR activation and load-minus-wind and outputs the 95% CGR for every UC time interval. This block must be run every time a new UC is needed (*e.g.* every 15 minutes). The theory behind this function is detailed in parts A and B of the following section, entitled *Determining the Controllable Generation Requirement.*

The second function is the Contingency Reserve Activation Model (CRAM) block in Figure 1. It takes as input a COPT and PDFs of contingency reserve response deficiency (CRR deficiency), and outputs a time-dependent forecast of CR activation for every UC time interval. This block must also be run every time a new UC is needed, and before the Combined Uncertainty Evaluation block. The theory behind this function is detailed in part C of the following section, entitled *Determining the Controllable Generation Requirement.*

Contingency Reserve Response (CRR) Deficiency PDFs are updated each time an actual contingency occurs in the EMS, by the third and fourth functions. The third function, crrd_sample_evaluation.m, is the Contingency Reserve Response Deficiency Sample Evaluation Function block of Figure 1. It is called fifteen minutes after any contingency occurs (where a contingency is defined in this report as a loss of generation). For every contingency, the CRR Deficiency Sample Evaluation Function computes one sample value of the CRR deficiency that exists 10 minutes after the contingency, and one sample value of the CRR deficiency that exists 15 minutes after the contingency. These samples are added to rolling buffers containing the sets of the most recent 10 and 15 minute CRR deficiency samples. The theory behind this function is described in the section entitled *Contingency Reserve Response Deficiency Sample Evaluation.* Although it runs 15 minutes after a contingency is detected, the function requires EMS data from both before and during the contingency event.

The fourth function, update_crrd_pdf.m, is the Update Contingency Reserve Response Deficiency PDFs block of Figure 1. This function is called each time new CRR deficiency samples are computed by crrd_sample_evaluation.m. The inputs to this function are the CRR deficiency rolling buffers, and the outputs are PDFs of CRR deficiency at 10 and 15 minutes after a contingency. This algorithm uses mean and variance confidence intervals to calculate the optimal number of deficiency samples needed to compute the PDFs. The PDFs of CRR deficiency are used by the CRAM to compute CRR activation forecasts. The theory behind this function is described in the section entitled *Updating the Contingency Reserve Response Deficiency Probability Density Functions.*

For testing purposes, a Matlab main function called TestBench was written. TestBench calls the other modules as appropriate, and provides simulated EMS data to update_crrd_pdf.m. The second-by-second acquisition of data from the EMS is simulated in TestBench by reading artificial data from a file. In testing, data representing typical outputs from PNNL block, either provided or assumed, is obtained from files. Figure 1 shows a global view of how these four primary m-files interact with modules developed by PNNL, the energy management system, and other external sources of data.

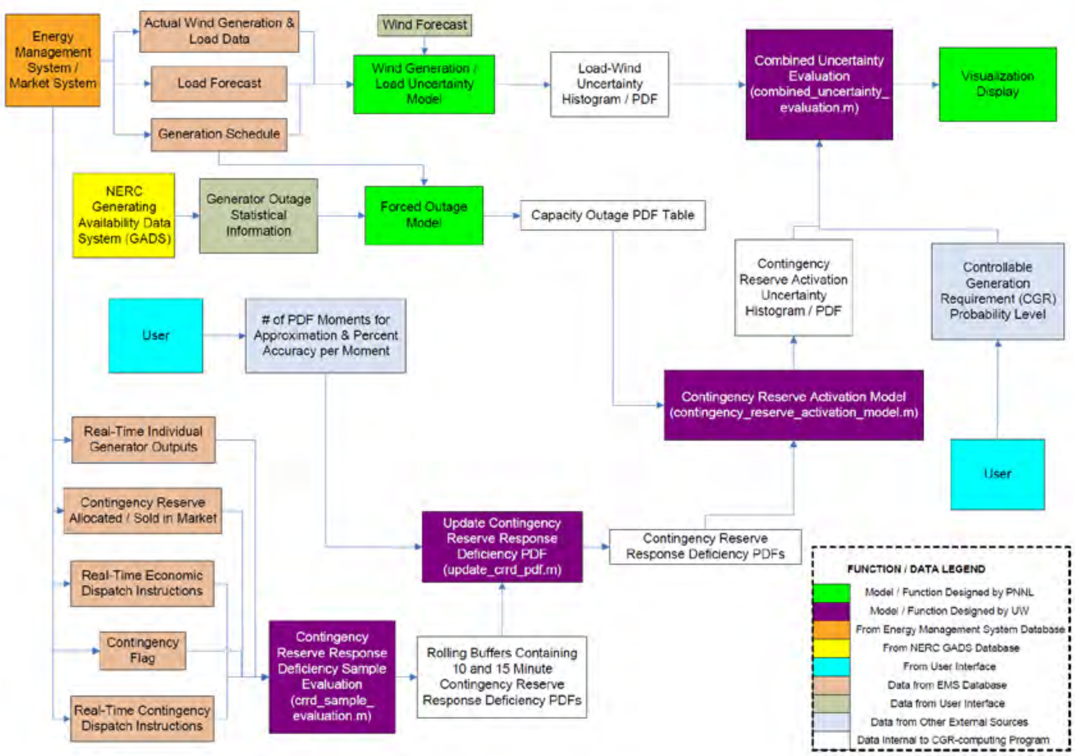

Figure 1. Global View of Organization of CGR Computation Program

Appendix A contains flowcharts depicting the organization and data flow of the algorithms described in this report.

Determining the Controllable Generation Requirement

A. Background

Let $P_{L\text{-}W}$ be the forecast of load minus wind, in MW. Let P_{CR} be the forecast of contingency reserve activation deficiency, in MW, that is, the shortfall in contingency reserve delivered when contingency reserve is activated. P_{CR} includes the effects of capacity outage. Let P_{CGR} be the forecast of Controllable Generation Requirement (CGR), the sum of the outputs of on line controllable generation needed to meet the load minus wind plus contingency reserve activation deficiency. All three are random variables.

Then P_{CGR} is the statistical sum of the random variables $P_{L\text{-}W}$ and P_{CR}, as detailed in section B of this chapter. In general, a positive value of load-minus-wind forecast error at any point in time must be compensated by an increase in controllable generation to maintain a balance of supply and demand, hence the term Controllable Generation Requirement (CGR). The specific relationship between CR activation and CGR is more involved and is explained in section C of this chapter.

For any time interval the CGR value sent to the UC is the value of committed generation that has a certain probability (a 95% probability will be used in this report) of being sufficient to meet the actual CGR for that interval. Equation (1) defines this value as CGR_{95}. Given the PDF of P_{CGR}, CGR_{95} is the value of P_{CGR} such that the area under the PDF of P_{CGR} within the interval $[0, CGR_{95}]$ is 0.95, as shown in the arbitrary PDF of Figure 2.

$$p\left[P_{CGR} \leq CGR_{95}\right] = 0.95 \tag{1}$$

Note that in this document capital P indicates a real power value that is a random variable, while lower case p indicates a probability value.

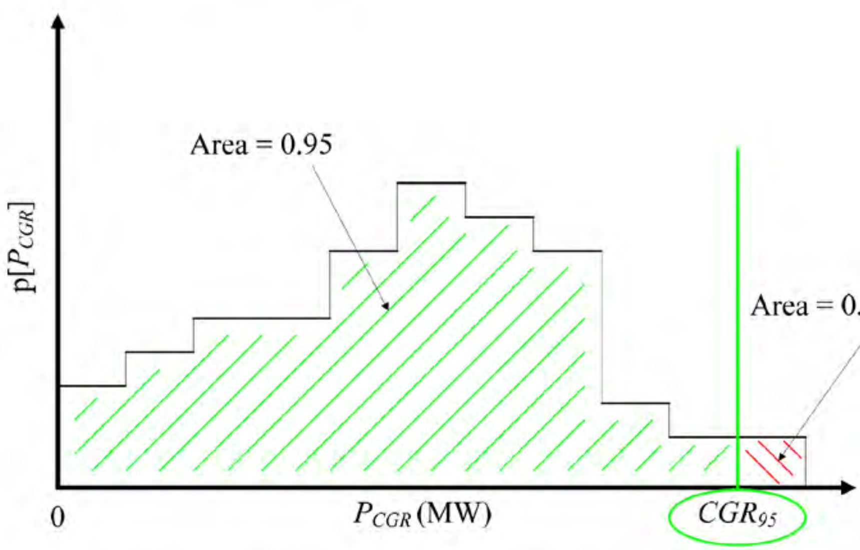

Figure 2. CGR_{95} of an Arbitrary Discrete PDF

Since the PDFs of P_{L-W} and P_{CR} are time-dependent, CGR_{95} and P_{CGR} are also time-dependent. To show this time dependence CGR_{95}, P_{CGR}, P_{CR} and P_{L-W} are rewritten as $CGR_{95,t}$, $P_{CGR,t}$, $P_{CR,t}$, and $P_{L-W,t}$, respectively, to specify forecasts for time interval t of the UC. Since time in the UC is discretized into five minute intervals, $t \in \{0, 5, 10, 15, 20, \ldots 180\}$.

Then $P_{CR,t}$ is the random variable of CR activation deficiency which contributes to the CGR at time t due to a contingency occurring at any previous UC time interval, $0 < t_o \leq t$.

Although in practice t_o can assume any value on a continuous timescale, the effects of the contingency will fall into discrete intervals of t. For example, if t_o occurs in the time interval $-2.5 < t < 2.5$ minutes, its effect ten minutes later will be in the interval $7.5 < t < 12.5$ minutes. Therefore t_o can also be discretized to a five minute timescale where $t_o \in \{5, 10, 15, 20, \ldots 175\}$. The case where $t_o \leq 0$ is not included because any contingency occurring at or before $t = 0$ will be known and will be seen as unusable generation capacity by the UC when scheduling to meet CGR, and so is already taken into account when scheduling generation.

To determine the complete forecast of $P_{CR,t}$ the probability that a contingency occurs in any particular time interval must be taken into account. Let λ be a Bernoulli random variable (value 0 or 1) that represents the probability that a contingency occurs in a 5-minute time interval t_o. This probability will initially be derived from the PDFs of the Capacity Outage Probability Table, *i.e.* it will be taken as the complement of the probability of no capacity outage outage (zero MW out) occurring in the time interval. Once multiple contingencies have been sampled, a system-specific value for the probability of λ can be computed from the mean time between outages.

$P_{\lambda CR,t}$ represents the forecast that includes both CR activation performance, $P_{CR,t}$, and the probability, λ, that a contingency requiring CR activation occurs. Then

$$P_{\lambda CR,t} = \lambda \otimes P_{CR,t} \tag{2}$$

where $\otimes$ indicates product convolution. For detail on how product convolution is performed refer to Appendix B.

B. Combined Uncertainty Evaluation

A contingency may occur in any interval after the start of the UC at $t = 0$ and before the time of the forecast, t. The PDF of $P_{\lambda CR,t}$ is a conditional PDF that depends on all possible values of t_o such that $5 \leq t_o < t$. The total CR contribution is then convolved with $P_{L-W,t}$ to produce $P_{CGR,t}$, *i.e.*

$$P_{CGR,t} = P_{L-W,t} \oplus P_{\lambda CR,t} \tag{3}$$

where $\oplus$ direct indicates summation convolution. Direct summation convolution is also detailed in Appendix B.

C. Contingency Reserve Activation Model

For any UC time interval, t, the PDF of $P_{CR,t}$ can be found from considering NERC's Disturbance Control Performance requirements [5] and WECC's Contingency Reserves Standard [6]. There are three time-specific requirements that a balancing authority must meet following a contingency. A contingency requiring CR activation is defined as a loss of generation causing a disturbance greater than or equal to 80% of the most severe single contingency [5]. This does not include the loss of transmission. If a contingency occurs at time t_o, the balancing authority must act to:

1. fully deploy contingency reserve within 10 minutes (t_o + 10) [6],
2. recover area control error (ACE) according to the Disturbance Recovery Criterion within the 15 minute Disturbance Recovery Period (t_o + 15) [5], and
3. fully restore contingency reserve within the 90 minute Contingency Reserve Restoration Period [5]. This 90 minute restoration period begins at t_o + 15 when the Disturbance Recovery Period ends and therefore ends at t_o + 105.

These three requirements are depicted in Figure 3.

Figure 3. Diagram of NERC and WECC Requirements

Given that a contingency has occurred, one random variable can be associated with actual performance of CR activation when trying to meet each of the first two requirements. Performance is defined as a deficiency in contingency reserve response (CRR), which has units of MW. The CRR deficiency can be either zero or positive. A positive CRR deficiency indicates not meeting the requirement within the specified time, in which case the CGR must be increased to compensate. If the requirement is met at or before the specified time, the CRR deficiency set to zero and the CGR is unaffected.

Let P_{o,t_o} be the random variable for the amount of lost generation (in MW) due to capacity outaged in time interval t_o. Let P_{CRRD10} be the random variable for CRR deficiency 10 minutes after t_o. Let P_{CRRD15} be the random variable for CRR deficiency 15 minutes after t_o.

The PDFs of P_{o,t_o} for all possible values of t_o (*i.e.* $0 < t_o \leq 300$ minutes) comprise the Capacity Outage Probability Table (COPT) sent to the Contingency Reserve Activation Model from the Forced Outage Model supplied by PNNL. Note that the PDFs in the COPT are derived from steady state Markov models of generator status. Thus they do not actually represent the time-dependent probability of losing a specific capacity within a certain time interval, but rather the steady state probability of a specific capacity being out regardless of a prior known state. This theoretical difference is not expected to result in any significant practical difference due to the inherently very low probability of any capacity outage occurring. This issue is discussed further in Appendix D.

At the instant that any contingency occurs, *i.e.* $t - t_o = 0$, the CGR is unaffected, because the lost generation is supplied by other balancing authorities through inadvertent interchange [7]. This inadvertent interchange is permitted temporarily to give contingency reserve time to deploy contingency reserve and restore ACE.

The ideal contingency reserve response is a linear increase in generator output over the 10 minute deployment interval. Thus for $t_o \leq t < t_o + 10$, P_{o,t_o} is nominally supplied by a combination of inadvertent interchange and contingency reserve response. A deficiency could be identified at each time interval less than 10 minutes, such as $t = t_o + 5$. At this time good practice would expect half of the CR to be deployed, but there is no formal performance requirement for this time interval. There is a requirement at $t - t_o = 10$, and the UC will commit units needed to meet $CGR_{95,t}$ for $t - t_o = 10$. This should satisfy any CRR deficiency at $t = t_o + 5$. For these two reasons the CRR deficiency for $t_o \leq t < t_o + 10$ is ignored (or, taken to be zero).

When $t = t_o + 10$, CR is nominally fully deployed and nominally replaces all of the generation lost in the contingency. In this nominal case, ACE is fully restored and the 10 Minute CRR Deficiency value P_{CRRD10} is zero. If CR is not fully deployed by this time (due to any sort of problem in CR activation, such as a generator not moving as ordered, or not ordered to move when it should have been, or failing to start, if non-spinning reserve, etc.), the 10 Minute CRR Deficiency Value P_{CRRD10} is positive.

If ACE is restored by $t = t_o + 15$, CR nominally supplies all of the lost generation, and the 15 Minute CRR Deficiency Value P_{CRRD15} is zero. If ACE is not fully recovered by this time, P_{CRRD15} is positive (and may be different from P_{CRRD10}).

It is assumed that any positive CRR deficiency at $t = t_o + 15$ is due to some lasting malfunction and that this CRR deficiency will persist until the end of the Contingency Reserve Restoration Period. P_{CRRD15} is therefore used as the persistent CRR deficiency. (P_{CRRD10} could be used to be more conservative, i.e. produce a higher CGR_{95} value.) Thus the contribution to CR activation for $t_o + 15 \leq t < t_o + 105$ is P_{CRRD15}.

After $t = t_o + 105$, CR is required to be fully restored, and can no longer supply any of P_{o,t_o}. The CGR must now supply all of P_{o,t_o} for $t \geq t_o + 105$.

When computing $P_{\lambda CR,t}$, the total PDF of CR activation at time t, the possibility of a contingency occurring in any previous UC time interval must be taken into account. $P_{\lambda CR,t}$ is zero for $t < 10$ minutes because enough time has not elapsed for WECC's 10 minute CR deployment requirement to be binding. At $t = 10$,

$$P_{\lambda CR,10} = \lambda \otimes P_{CRRD10} = P_{\lambda CRRD10} \tag{4}$$

At $t = 15$, $P_{\lambda CR,15}$ must represent the possibility of a contingency occurring in the first or second time interval. This is accomplished by applying the conditional summation convolution operation (detailed in Appendix C) to sum the two dependent random variables P_{CRRD10} and P_{CRRD15}. These two random variables are dependent because the sum of the two CRR deficiencies cannot exceed the total amount of contingency reserve that was allocated prior to the start of the UC.

The conditional summation convolution operation is identical to the direct summation convolution operation detailed in Appendix B except for that it enforces an upper limit of possible CRR deficiency. The conditional summation convolution operation is represented by the symbol $\widehat{\oplus}$.

Using conditional summation convolution, $P_{\lambda CR,15}$ is

$$P_{\lambda CR,15} = P_{\lambda CRRD10} \hat{\oplus} (\lambda \otimes P_{CRRD15}) = P_{\lambda CRRD10} \hat{\oplus} P_{\lambda CRRD15,15} \tag{5}$$

Likewise, $P_{\lambda CR,20}$ is

$$P_{\lambda CR,20} = P_{\lambda CRRD10} \hat{\oplus} (\lambda \otimes P_{CRRD15}) \hat{\oplus} (\lambda \otimes P_{CRRD15}) = P_{\lambda CRRD10} \hat{\oplus} P_{\lambda CRRD15,20} \tag{6}$$

Note that if the UC time interval is changed from 5 minutes to 1 minute, the conditional summation convolution operation must also be applied using P_{CRRD10} to compute $P_{\lambda CRRD10,11}$, $P_{\lambda CRRD10,12}$, $P_{\lambda CRRD10,13}$, and $P_{\lambda CRRD10,14}$. This is discussed in Appendix C.

The use of the conditional summation convolution operation is repeated until $t = 105$ minutes at which point $P_{o,t-105}$ must be summed with $P_{\lambda CR,100}$, *i.e.*

$$P_{\lambda CR,105} = P_{\lambda CR,100} \oplus P_{o,t-105} = P_{\lambda CRRD10} \hat{\oplus} P_{\lambda CRRD15,100} \oplus P_{o,t-105} \tag{7}$$

Unlike when summing successive CRR deficiency PDFs, a direct summation convolution operation is used to add $P_{o,t-105}$ because capacity outage is independent of CRR deficiency.

A summary of the effects of CRR deficiency and capacity outage on $P_{\lambda CR,t}$ at various values of t is shown in Table 1.

Table 1.

Time Interval (min)	$P_{\lambda CR,t}$
$0 \le t < 10$	0
$10 \le t < 15$	$P_{\lambda CRRD10}$
$15 \le t < 105$	$P_{\lambda CRRD10} \hat{\oplus} P_{\lambda CRRD15,t}$
$105 \le t \le 300$	$P_{\lambda CRRD10} \hat{\oplus} P_{\lambda CRRD15,100} \oplus P_{o,t-105}$

As a graphical example, Figure 4 shows the full contribution of $P_{\lambda CR,t}$ to the CGR when $t = 20$ minutes.

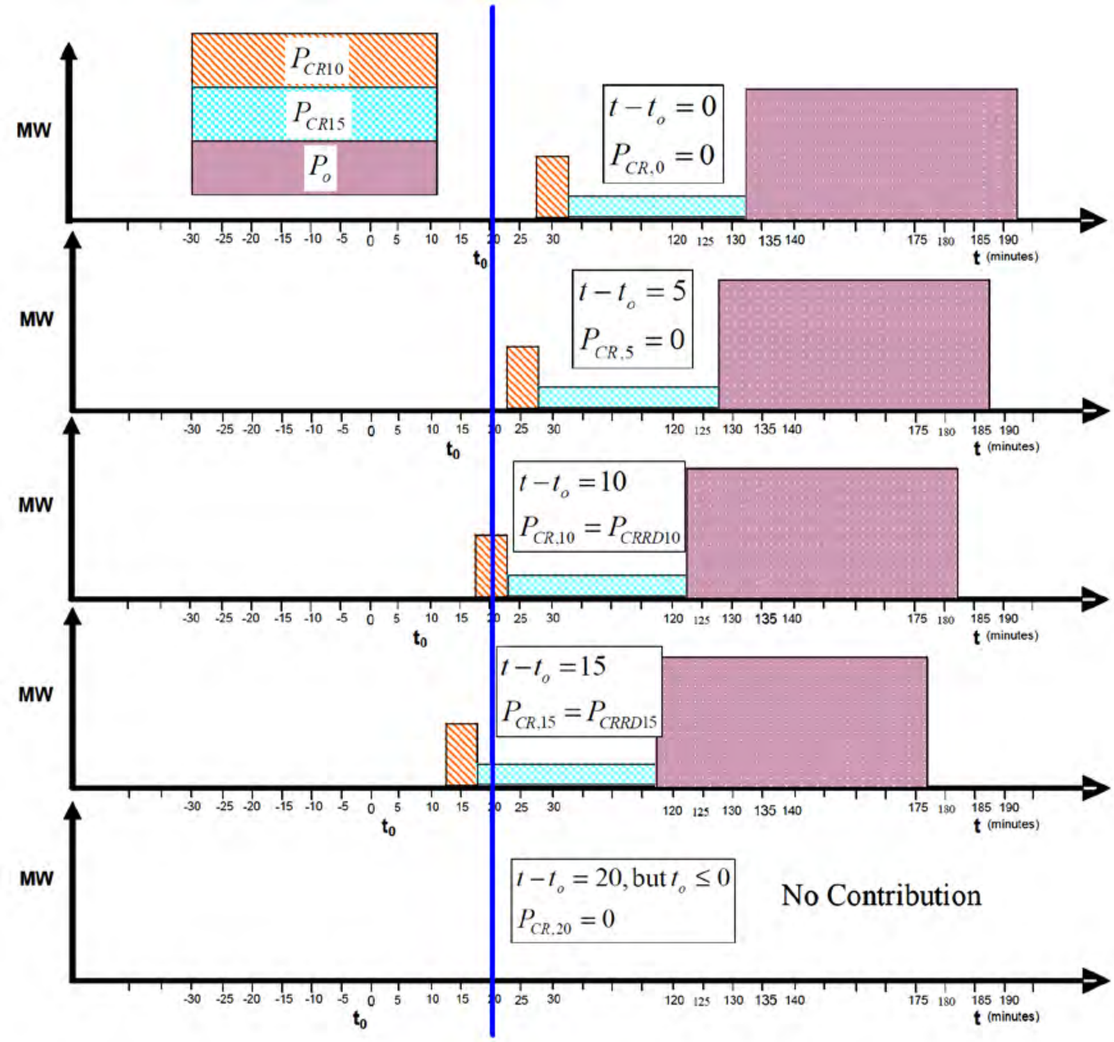

$$
\begin{aligned}
P_{\lambda CR,20} &= (\lambda \otimes P_{CRRD15}) \hat{\oplus} (\lambda \otimes P_{CRRD10}) \hat{\oplus} (\lambda \otimes P_{CR,5}) \hat{\oplus} (\lambda \otimes P_{CR,0}) \\
&= (\lambda \otimes P_{CRRD15}) \hat{\oplus} (\lambda \otimes P_{CRRD10})
\end{aligned}
$$

Figure 4. Summing $P_{\lambda CR,t}$ Over t_o When $t = 20$ Minutes

D. Calculating the Controllable Generation Requirement

Recall that $CGR_{95,t}$ is the value of $P_{CGR,t}$ that is higher than 95% of all other possible values of $P_{CGR,t}$. In other words, $CGR_{95,t}$ is the value of $P_{CGR,t}$ such that the area under the PDF of $P_{CGR,t}$ within the interval $[0, CGR_{95,t}]$ is 0.95, as shown in Figure 2. Therefore, the algorithm that calculates $CGR_{95,t}$ from the discrete PDF of $P_{CGR,t}$ must sum the probabilities of all values of $P_{CGR,t}$ beginning reasonably close to $-\infty$ and stopping when the sum equals 0.95. Expressed mathematically, $CGR_{95,t}$ is

$$\begin{aligned} CGR_{95,t} &= p_{CGR,t,m} \left| \sum_{i=0}^{m} p_{P_{CGR,t}}(p_{CGR,t,i}) = 0.95 \right. \\ &= p_{CGR,t,m} \left| \sum_{i=m}^{P_{\max}} p_{P_{CGR,t}}(p_{CGR,t,i}) = 0.05 \right. \end{aligned} \tag{8}$$

The second line in equation (8), *i.e.* calculating an area of 0.05, is used in practice for computational efficiency. The PDF of $P_{CGR,t}$ can be interpolated to arrive at a value of $CGR_{95,t}$ that is more precise than the bin resolution of $P_{CGR,t}$ would otherwise allow.

Contingency Reserve Response Deficiency Sample Evaluation

A. Background

Estimation of Contingency Reserve Response Deficiency, specifically the PDFs for P_{CRRD10} and P_{CRRD15}, is ultimately based on observed performance of actual CR activation. Initial estimates can be obtained from historical data. Then PDF accuracy will continually improve as new performance data is recorded in real time. These PDFs must be determined for the California ISO (CAISO) and the Bonneville Power Administration (BPA) systems. The sampling algorithms for the CAISO and BPA are based on system-specific CR procurement and dispatch (activation) procedures and are therefore different. Section B and Section C describe how samples of P_{CRRD10} and P_{CRRD15} are obtained from generators in the CAISO and BPA, respectively.

B. Sampling Contingency Reserve Response Deficiency in the California ISO

During normal operation in the CAISO the Real-Time Economic Dispatch (RTED) runs every five minutes to re-dispatch units to balance supply and demand [8]. Running in parallel with the RTED is Automatic Generation Control (AGC) which – in an effort to maintain ACE close to zero – sends new generation setpoints every four seconds to those generators that have sold regulation up and/or regulation down reserves. Imbalance Energy is dispatched through the RTED to cover a persistent supply-demand imbalance, thereby replenishing regulation reserves.

The CAISO procures its ancillary services (*e.g.* regulation up, regulation down, spinning and non-spinning reserves) by awarding bids to specific generators through Scheduling Coordinators for providing such services. Therefore it is known before a contingency occurs which generators have sold spinning reserves only, non-spinning reserves only, or both spinning and regulating reserves to the CAISO. Non-spinning reserves can also be purchased from interruptible loads.

When a contingency occurs, there is a sudden loss of generation that is temporarily supplied by inadvertent interchange. The Real-Time Contingency Dispatch (RTCD) is invoked in place of the RTED to dispatch Contingency Only Operating Reserves (COOR) to offset the inadvertent interchange and restore ACE. The set of generators and the quantity of MW dispatched to mitigate the contingency can therefore be determined from the dispatch instructions of the RTCD.

Contingency Only Operating Reserves are defined by the CAISO as spinning and non-spinning reserves that may be dispatched only in the event of a contingency to meet WECC and NERC reliability standards. These COOR may come from resources internal to CAISO's balancing authority area, or from Dynamic System Resources that come from outside CAISO's balancing authority area [9]. Both internal and Dynamic System Resources are monitored for performance [10], so records of their outputs during the 15 minutes following a contingency are known.

It is not currently known if AGC "dispatch" signals following a contingency are known.

Both spinning and non-spinning reserves are required by the CAISO Contingency Reserve Standard to reach a new generation setpoint within 10 minutes after the dispatch instructions are sent [6].

Samples of $P_{CRRD10,i}$ and $P_{CRRD15,i}$ for the i^{th} generator (or interruptible load) during a contingency at t_o, and λ for the system can be computed if the following data is collected:

1. t_o
2. $CR_{sold,i}$, COOR sold to generator i before or during the RTCD
3. $CR_{CD,i}$, Dispatch instructions from RTCD at t_o
4. $CR_{ED,i}$, most recent Dispatch instructions from RTED before t_o
5. $G_i(t_o^-)$, Generator output at t_o^- (or $D_i(t_o^-)$, Interruptible Load demand at t_o^-)
6. $G_i(t)$, Generator output during the time interval $t_o < t \leq t_o + 15$ (or $D_i(t)$, Interruptible Load demand during the time interval $t_o < t \leq t_o + 15$)

To set up the calculation of $P_{CRRD10,i}$ and $P_{CRRD15,i}$ from the above data, consider a case where the RTCD is run and dispatches nonzero quantities of both COOR and Imbalance Energy from generator i. A single dispatch, $CR_{CD,i}$, will be sent that contains components for both COOR and Imbalance Energy dispatches. Since only $CR_{CD,i}$ is known, the values of individual COOR and Imbalance Energy dispatches are not known. However, the amount of COOR dispatched can be estimated based on comparing $CR_{CD,i}$ to $CR_{sold,i}$, the COOR sold to generator i in the market. It is assumed that the actual amount of COOR dispatch equals $CR_{CD,i}$ if $CR_{sold,i}$ is greater than $CR_{CD,i}$, and equals $CR_{sold,i}$ otherwise, as in equation (11).

The samples of $P_{CRRD10,i}$ and $P_{CRRD15,i}$ are computed as

$$P_{CRRD10,i} = \Delta G_{sched,i} - \left\{ \max\left[G_i(t)\right] : t_o \leq t \leq t_o + 10 \right\} - G_i\left(t_o^-\right) \tag{9}$$

and

$$P_{CRRD15,i} = \Delta G_{sched,i} - \left\{ \max\left[G_i(t)\right] : t_o \leq t \leq t_o + 15 \right\} - G_i\left(t_o^-\right) \tag{10}$$

where

$$\Delta G_{sched,i} = \max\left[0, \min\left(\left[CR_{CD,i} - CR_{ED,i}\right], CR_{sold,i}\right)\right] \tag{11}$$

and $\Delta G_{sched,i}$ is the expected change in generator output for full CR deployment. If either $P_{CRRD10,i}$ or $P_{CRRD15,i}$ is negative, it will be set to zero because no CRR deficiency exists.

The time between two successive contingencies will be one sample of λ.

If for any contingency M generators are dispatched during the RTCD, their individual CRR deficiencies must be summed to arrive at a total value of P_{CRRD10} and P_{CRRD15} for the entire system. Thus, for a single contingency sample, P_{CRRD10} and P_{CRRD15} are computed as

$$P_{CRRD10} = \sum_{i=1}^{M} P_{CRRD10,i} \tag{12}$$

and

$$P_{CRRD15} = \sum_{i=1}^{M} P_{CRRD15,i} \tag{13}$$

After N contingencies have been acquired, histograms of P_{CRRD10}, P_{CRRD15}, and λ data can be determined directly. The PDFs of P_{CRRD10}, P_{CRRD15}, and λ can be found by dividing each value in its histogram by N. Section IV addresses the optimal size of N.

It is important to note that any effect of regulation during a contingency is ignored in this sampling process. Some, but not all, generators will have sold both regulation and spinning reserves. The generators that have sold both will be known, and how much of each reserve type sold will be known. It is known that AGC will automatically "dispatch" regulation reserves to mitigate the ACE deviation during a contingency, but precisely how regulation is dispatched by AGC is not presently known. Therefore the effect of regulation on contingency response is ignored.

It can be expected that the interaction between regulation and COOR can cause $P_{CRRD10,i}$ or $P_{CRRD15,i}$ to appear higher in certain cases and lower in others. Consider a generator that has sold Regulation Up, Regulation Down, and COOR. If COOR performs nominally (reaches $CR_{CD,i}$ by t_o + 10 minutes), and Regulation Up adds to the contingency response, $P_{CRRD10,i}$ will appear lower due to regulation. If, on the other hand, COOR performs better than nominal, *e.g.* reaches $CR_{CD,i}$ by $t_o + 5$ minutes, and between $t_o + 5$ and $t_o + 10$ Regulation Down causes the generator's output to go below $CR_{CD,i}$, $P_{CRRD10,i}$ will appear higher due to regulation.

C. Sampling Contingency Reserve Response Deficiency in the Bonneville Power Administration

In general, the procedure for sampling CR response deficiencies of individual generators for BPA is the same as for the CAISO. The performance of BPA's contingency reserves is subject to the same NERC and WECC standards, and a similar interaction exists between regulating reserves (controlled by AGC) and contingency reserves.

BPA, however, does not have a market structure as does the CAISO, and so ancillary service procurement is different. As part of the Northwest Power Pool (NWPP) Reserve Sharing Group (RSG), BPA is required to carry enough CR to meet or exceed their Contingency Reserve Obligation (CRO). This CRO is equal to the sum of 7% of all thermal generation and 5% of all hydro generation [11].

Since 89% of BPA's generation is hydro [12], BPA has full control of almost all generation within its control area. Following a contingency, BPA's EMS will instruct certain generators to provide CR. It is assumed that these dispatch instructions – as well as generator outputs following the contingency – are available in BPA's EMS and can be used as in equation (9) and equation (10) to compute samples of P_{CRRD10} and P_{CRRD15} for each generator instructed to provide CR.

If BPA's CRO is not sufficient to mitigate the contingency, BPA may request the use of other NWPP participants' CROs to meet NERC and WECC reliability standards [11],[13]. In this case BPA's request for additional CR is sent to a NWPP Reserve Sharing Program which determines which RSG balancing authorities will supply the additional CR. The Reserve Sharing Program sends electronic signals to each balancing authority's AGC to increase generation [11].

If CR activation performance of generators outside BPA's control area are to be included in the PDFs of P_{CRRD10} and P_{CRRD15}, access to historical data within the NWPP's Reserve Sharing Program – in addition to historical data in BPA's EMS – will be required.

Updating the Contingency Reserve Response Deficiency Probability Density Functions

A. Background

The PDFs of P_{CRRD10} and P_{CRRD15} are forecasts of the true behavior of CR activation. The accuracy of these estimated PDFs clearly depends on the number of samples, N. The weak law of large numbers implies that the estimated PDFs become more accurate as N increases, so ideally N should be as large as possible [14]. However, the power system changes with time, so N should also be small enough for the estimated PDFs to adapt quickly to these changes. To satisfy this tradeoff, N can be set so the estimated PDFs meet some user-specified accuracy criteria. A smaller sample set has the advantages of containing only the most current information and allowing the PDF to adjust more quickly to changes in CR activation performance. Generator outages occur infrequently (*e.g.* 4 per year in the Bonneville Power Administration [15]), so the time horizon of the sample set may be on the order of a half dozen years. It is possible that the performance of CR activation will undergo changes within this time horizon, so older samples can be rolled out to keep the sample sets up to date (refer to Section VI for more detail).

The measures of PDF accuracy adopted are confidence intervals on the sample means and sample variances of the PDFs of P_{CRRD10} and P_{CRRD15}. Confidence intervals are calculated each time a new sample is recorded. Each confidence interval requires two predefined accuracy metrics. The first metric is the confidence interval width, which limits how much the sample quantity (i.e. sample mean or sample variance) can differ from its true value. The second metric is confidence, which specifies the probability that the true value of the quantity exists within the confidence interval. These metrics are defined in detail for the confidence intervals of the sample mean and sample variance in Section B and Section C, respectively, before using them to calculate N in Section D.

The confidence interval procedures outlined in Sections B and C presuppose a normally distributed random variable, but the distributions of P_{CRRD10} and P_{CRRD15} may be different from Gaussian (normal). To manage this potential incompatibility, the samples of each random variable, P_{CRRD10} and P_{CRRD15}, will be randomly separated into subsets of, for example, ten samples per subset, and the mean of each subset will be calculated. The distribution of the subset means should be approximately Gaussian regardless of the shape of the original random variable [14]. The mean and variance confidence interval procedures are therefore applied to the subset means of P_{CRRD10} and P_{CRRD15} instead of their raw sample sets. This method will require more samples of P_{CRRD10} and P_{CRRD15}, but will prevent statistical inaccuracies in the event that P_{CRRD10} and P_{CRRD15} are not normally distributed.

B. Confidence Interval for the Sample Mean

Let X be a random variable with a normal distribution. X has a true mean μ and true variance σ^2. In the scope of this report, X would be a random variable representing the subset mean of P_{CRRD10} or P_{CRRD15}. Let $\overline{X}_n$ be the sample mean of N samples of X. The Confidence Interval of the sample mean (CI_μ) is defined as an interval symmetric about the sample mean that has a probability of (1- α_μ) that μ exists within the interval. The second accuracy metric, confidence, is defined by choosing α_μ, the probability that μ does not exist within the interval. CI_μ represents how accurately $\overline{X}_n$ estimates the true mean, E[X] = μ. The CI for the sample mean when μ and σ^2 are unknown is based on Student's t-distribution with N -*1* degrees of freedom [14], and is defined as

$$\left[\bar{X}_N - \frac{t_{\alpha_\mu/2,N-1}\hat{\sigma}_N}{\sqrt{N}}, \bar{X}_N + \frac{t_{\alpha_\mu/2,N-1}\hat{\sigma}_N}{\sqrt{N}}\right] \tag{14}$$

The first metric, confidence interval width, β_μ is defined as

$$\beta_\mu = \frac{t_{\alpha_\mu/2,N-1}\hat{\sigma}_N}{\sqrt{N}} \tag{15}$$

Therefore β_μ is half the width of the CI that surrounds the sample mean, $\bar{X}_N$. The variable, $\hat{\sigma}_N$, is the standard deviation of the sample set. The variable, $t_{\alpha\mu/2,N-1}$, is the critical value of the t-distribution that represents the probability that μ lies within the CI. This t-value can be determined from a table if α_μ, and N, the number of samples, are known. The probability α_μ is most often written as $(1-\alpha_\mu)$x100% CI which defines the percent confidence that μ exists within the interval $\bar{X}_N \pm \beta_\mu$. It is therefore desired that α_μ is small for a high confidence (95% confidence is common), and that β_μ is also small so the accuracy of $\bar{X}_N$ is high. The probability that μ is within the CI can be written explicitly as:

$$\begin{aligned} 1-\alpha_\mu &= P\left[t_{\alpha_\mu/2,N-1} \le \frac{\bar{X}_N - \mu}{\hat{\sigma}_N/\sqrt{N}} \le t_{\alpha_\mu/2,N-1}\right] \\ &= P\left[\bar{X}_N - \frac{t_{\alpha_\mu/2,N-1}\hat{\sigma}_N}{\sqrt{N}} \le \mu \le \bar{X}_N + \frac{t_{\alpha_\mu/2,N-1}\hat{\sigma}_N}{\sqrt{N}}\right] \end{aligned} \tag{16}$$

C. Confidence Interval for the Sample Variance

For the same random variable, X, determining the CI for the sample variance with N samples is similar to the CI of the sample mean. For sample variance, the confidence interval width and confidence metrics to be defined are β_σ and α_σ, respectively. The main difference from the CI of the sample mean is that for the sample variance a chi-square distribution (with $N-1$ degrees of freedom) is used [14].

Given the unbiased sample variance estimator,

$$\hat{\sigma}_N^2 = \frac{1}{N-1}\sum_{j=1}^{N}\left(X_j - \bar{X}_N\right)^2 \tag{17}$$

it can be shown that the random variable, $\frac{(N-1)\hat{\sigma}_N^2}{\sigma^2}$, has a χ^2 distribution with $N-1$ degrees of freedom, *i.e.*

$$\chi^2 = \frac{(N-1)\hat{\sigma}_N^2}{\sigma^2} = \frac{1}{\sigma^2}\sum_{j=1}^{N}\left(X_j - \bar{X}_N\right)^2 \tag{18}$$

The following defines an interval that contains σ_X^2 with a probability of $(1-\alpha_\sigma)$:

$$1-\alpha_\sigma = P\left[\chi^2_{1-\alpha_\sigma/2,N-1} \le \frac{(N-1)\hat{\sigma}_N^2}{\sigma^2} \le \chi^2_{\alpha_\sigma/2,N-1}\right]$$
$$= P\left[\frac{(N-1)\hat{\sigma}_N^2}{\chi^2_{\alpha_\sigma/2,N-1}} \le \sigma^2 \le \frac{(N-1)\hat{\sigma}_N^2}{\chi^2_{1-\alpha_\sigma/2,N-1}}\right] \tag{19}$$

The (1- α_σ)x100% confidence interval for the variance, σ^2 is

$$\left[\frac{(N-1)\hat{\sigma}_N^2}{\chi^2_{\alpha_\sigma/2,N-1}}, \frac{(N-1)\hat{\sigma}_N^2}{\chi^2_{1-\alpha_\sigma/2,N-1}}\right] \tag{20}$$

and

$$\beta_\sigma = \frac{(N-1)\hat{\sigma}_N^2}{\chi^2_{1-\alpha_\sigma/2,N-1}} - \frac{(N-1)\hat{\sigma}_N^2}{\chi^2_{\alpha_\sigma/2,N-1}} \tag{21}$$

is the full width of the confidence interval.

D. Determining the Optimal Sample Size

The following describes how to determine the optimal sample size of X. For a given sample mean, $\overline{X}_N$, there exists a minimum number of samples, N_μ^{min}, for which the confidence interval width, β_μ, and confidence, α_μ, and are satisfied. Likewise, for the sample standard deviation, $\hat{\sigma}_n$, there exists a minimum number of samples, N_σ^{min}, for which the two accuracy metrics β_σ and α_σ are satisfied. Equation (15) is rearranged to become equation (22) to determine N_μ^{min}, and equation (21) is rearranged to become equation (23) to determine N_σ^{min}. Given values of all accuracy metrics, α_μ, α_σ, β_μ, and β_σ, an initial value for $\hat{\sigma}_N$ is needed. This initial value can be extracted from historical data or estimated using engineering judgment. Because $t_{\alpha\mu/2,N-1}$, $\chi^2_{1-\alpha_\sigma/2,N-1}$, and $\chi^2_{\alpha_\sigma/2,N-1}$ depend on N, equations (22) and (23) must be solved iteratively.

$$N_\mu^{\min} = \left(\frac{t_{\alpha_\mu/2,N_\mu^{\min}-1}\,\hat{\sigma}_{N_\mu^{\min}}}{\beta_\mu}\right)^2 \tag{22}$$

$$N_\sigma^{\min} = \frac{\beta_\sigma}{\hat{\sigma}^2_{N_\sigma^{\min}}\left[\frac{1}{\chi^2_{1-\alpha_\sigma/2,N_\sigma^{\min}-1}} - \frac{1}{\chi^2_{\alpha_\sigma/2,N_\sigma^{\min}-1}}\right]} + 1 \tag{23}$$

Ideally, N_{min} samples are used to create a PDF, where N_{min} is the minimum sample size required to satisfy all four accuracy metrics and is

$$N_{\min} = \max\left(N_\mu^{\min}, N_\sigma^{\min}\right) \tag{24}$$

Experience with power systems suggests N_{min} would typically be close to 25. Figure 5 summarizes the procedure for determining N_{min}.

The estimate for $\hat{\sigma}_n$ can be determined easily from an existing sample set of *X*, if available. If a sufficiently large number of samples are not available, $\hat{\sigma}_N$ can be estimated by *e.g.* surveying experts.

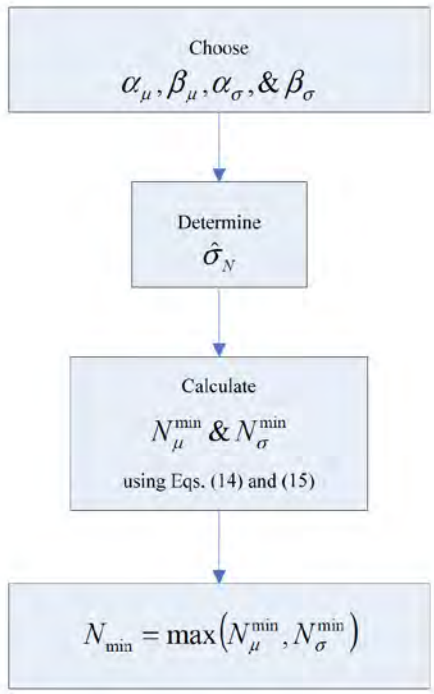

Figure 5. Determining the Optimal Sample Size

Since the confidence interval theory assumes the distribution being estimated is Gaussian in nature, an additional technique called the *method of batch means* may be required if in practice the distribution being estimated is not inherently Gaussian [14]. Instead of using the raw sample set, the method of batch means divides the raw sample set into batches or subsets. Each batch may contain, for example, 10 raw samples. The mean of each batch is computed, and the sample set *X* used in the confidence interval formulation is the set of batch means. As the number of raw samples increases, the central limit theorem asserts that the sample set of batch means will approach a Gaussian distribution, even if the raw distribution being sampled is not. Using the method of batch means would increase the accuracy of an estimated distribution, but may be difficult to apply to contingency reserve response deficiency samples because the method requires more samples (*e.g.* an order of magnitude increase in the number of samples).

Updating the Probability Density Functions of Contingency Reserve Activation With a Rolling Buffer

The samples used to create PDFs of either P_{CRRD10} or P_{CRRD15} are stored in a rolling buffer. The buffer will actively roll out (*i.e.* discard) the oldest sample when a new sample comes in and the oldest sample is not needed for PDF accuracy. Thus the PDF updates for changes in the power system.

Before any samples are acquired the buffers must be initialized with the PDFs of P_{CRRD10} and P_{CRRD15} reflecting nominal CR activation performance, *i.e.* no CRR deficiency,

$$\mathrm{p}[P_{CRRD10} = 0] = 1 \tag{25}$$

$$\mathrm{p}[P_{CRRD15} = 0] = 1 \tag{26}$$

Let n be the total number of samples acquired by the Contingency Reserve Activation Model at any given time. Let n_{buff} be the number of samples in a buffer at any given time. Let N_{max} be the maximum number of samples that a buffer can hold, where N_{max} would be on the order of a couple dozen. Note that

$$n_{buff} = \begin{cases} n, & \text{if } n < N_{\max} \\ N_{\max} & \text{if } n \geq N_{\max} \end{cases} \tag{27}$$

Let N be the number of samples used to create a PDF at any given time where

$$N \leq n_{buff} \tag{28}$$

The value of N is such that the metrics of confidence, α_μ and α_σ, and confidence interval width, β_μ and β_σ, are satisfied. Each time a new sample is acquired, N may need adjusting. Figure 6 shows how N is adjusted where $N_{old} = N$ before the new sample, $N_{new} = N$ after the new sample, and M is a temporary variable used for N while adjusting. If with the new sample N can be reduced and still satisfy the confidence interval metrics, it is reduced. If N cannot satisfy the confidence interval metrics at its previous value or lower, N is increased until the confidence interval metrics are satisfied or until all the samples in the buffer are being used.

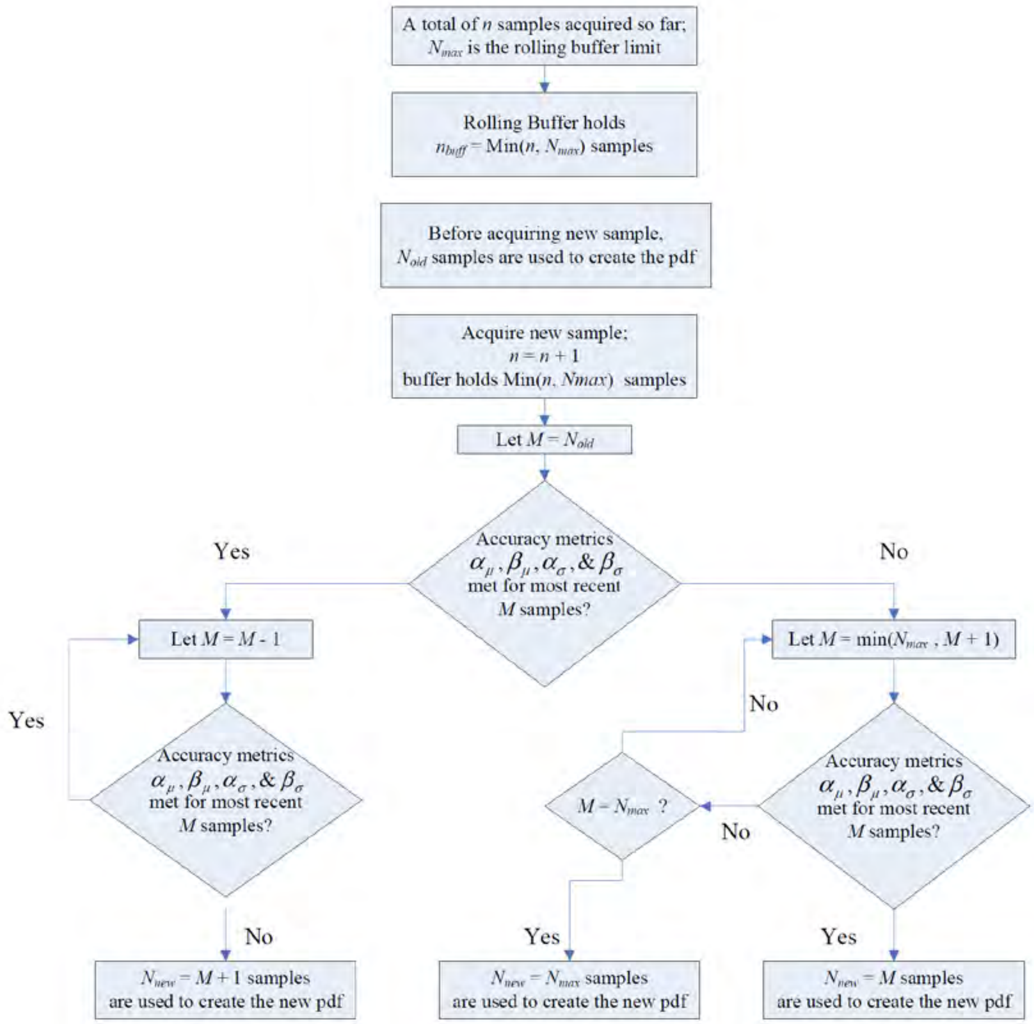

Figure 6. Updating a Sample Set

TestBench Simulation

A. Overview

The TestBench is the highest level MATLAB m-file in the set of m-files developed for this project. The TestBench was created to simulate a processor operating in real-time in parallel with an Energy Management System (EMS). The simulation assumes a data communication link with the EMS database exists so information in the EMS database can be accessed in the TestBench and then passed to subroutines when appropriate. Two versions of artificial EMS data were created prior to running simulations. These sets of EMS data were stored in Matlab binary .mat files. The details of the data in the first version .mat files can be seen in Table 2. The second version .mat files have identical file names except that the string "v2" is appended to each file name.

The timestep in TestBench was discretized to one second. The time period of one full simulation was 69 hours or 62100 seconds.

Artificial data for five individual generators was created, and TestBench was setup to simulate up to five generators by defining the variable $N_{gen} \in \{1, 2, 3, 4, 5\}$. All five generators were assumed to provide both energy and contingency reserve, and therefore each generator had a Real-Time Economic Dispatch Instruction (RTEDI) during normal operation, and a Real-Time Contingency Dispatch Instruction (RTCDI) following a contingency.

Generator output power measurements were assumed to refresh every four seconds, thus TestBench "acquired" N_{gen} new generator outputs every four seconds. Generator output values were stored in a rolling buffer of N_{gen} columns and enough rows to hold 15 minutes of four second data (225 rows). Seventy-two hours (64800 4-second values) of generator data was created in total.

TestBench assumed a Unit Commitment (UC) would be run every 15 minutes, and therefore the TestBench was setup to call *combined_uncertainty_evaluation.m* every 15 minutes to compute the CGR_{95} values for each time interval in the UC time horizon. The primary m-file *compute_cr_activation.m* was called prior to calling *combined_uncertainty_evaluation.m* to provide input to *combined_uncertainty_evaluation.m*.

Running in parallel with the Combined Uncertainty Evaluation Function was an IF-statement that polled the Contingency Flag (acquired from the EMS database) every four seconds to determine when contingencies occurred. Fifteen minutes after a contingency did occur, TestBench called *crrd_sample_evaluation.m*, the Contingency Reserve Response Deficiency (CRRD) Sample Evaluation Function, to compute 10 and 15 minute CRRD samples. Once new CRRD samples were computed, *update_crrd_pdf.m* was called to update P_{CRRD10} and P_{CRRD15}.

In order to verify proper operation of the estimation of P_{CRRD10} and P_{CRRD15} using confidence intervals, an unrealistically high number of contingencies were generated in the artificial EMS data. A total of 68 contingencies were simulated, one at the top of each hour. Separate buffers were used to store 10 and 15 minute CRRD samples. These buffers were sized to hold all 68 contingency samples, but a smaller CRRD buffer size could be chosen to realize a rolling buffer.

B. Input and Output Data Formats

A list of inputs needed to run the TestBench is shown in Table 2. A list of TestBench outputs is shown in Table 3.

Table 2. Inputs to TestBench

Description	File Name	Variable Name	Data Type	Dimensions
Generator output power 4-sec values	allgenvalues.mat	allgenvalues	double	64801 x 5
Contingency Flag 4-sec values	allflag_cont.mat	allflag_cont	double	62100 x 5
Real-Time Economic Dispatch Instructions	allRTEDI.mat	allRTEDI	double	71 x 5
Real-Time Contingency Dispatch Instructions	allRTCDI.mat	allRTCDI	double	71 x 5
Contingency Reserve Allocated / Sold to each generator	allCRSold.mat	allCRSold	double	71 x 5
Capacity Outage Probability Table Probability Values	genstat.mat	probability	double	1652 x 300
Capacity Outage Probability Table Bin Values	genstat.mat	capacity	double	1652 x 1

Table 3. Outputs of TestBench

Description	File Name	Variable Name	Data Type	Dimensions
Estimated PDF of CRRD10, Probabilities	pdf_CRRD10.mat	P_CRRD10	double	variable
Estimated PDF of CRRD10, Bin Values	pdf_CRRD10.mat	bins_CRRD10	double	variable
Estimated PDF of CRRD15, Probabilities	pdf_CRRD15.mat	P_CRRD15	double	variable
Estimated PDF of CRRD15, Bin Values	pdf_CRRD15.mat	bins_CRRD15	double	variable
CGR95 Values	cgr95values.mat	CGR95	double	301 x 2
Time Intervals Corresponding to CGR95 Values	cgr95values.mat	intvl_values	double	301 x 1

The matrix CGR95 has two columns of information. The first column of CGR95 contains the MW values of controllable generation requirement for each UC time interval. The second column contains the actual probability value corresponding to the MW value (which should be close to 0.95 but could be slightly greater). Inputs and outputs of the primary m-files are detailed in the flowcharts in Appendix A.

C. *Simulation Procedure*

In addition to the .mat files listed in Table 2, two additional .mat files containing 10 and 15 minute CRR deficiency values for each of the five generators were created. These .mat files (see Table 4 for file details) were used along with *allRTEDI.mat* and *allRTCDI.mat* to generate *allgenvalues.mat*. The CRR deficiency values stored in the files in Table 4 were chosen by hand pseudo-randomly, but they were chosen such that the 15 minute deficiency was always less than or equal to the 10 minute deficiency. The CRR deficiencies – and the corresponding input CRR deficiency PDFs – may lack realism, but were sufficient for verifying the accuracy of the CRR deficiency sampling subroutine as the input PDFs need not be realistic, only known beforehand.

Table 4. Predefined Contingency Reserve Response Deficiency Values

Description	File Name	Variable Name	Data Type	Dimensions
10 minute Contingency Reserve Response Deficiencies	allCRRD10.mat	allCRRD10	double	70 x 5
15 minute Contingency Reserve Response Deficiencies	allCRRD15.mat	allCRRD15	double	71 x 5

The files in Table 4 contain "small" deficiency values. "Large" deficiency values were also created (*i.e. allCRRD10v2.mat* and *allCRRD15v2.mat*), from which a separate file of generator output values was generated (*i.e. allgenvaluesv2.mat*). Having two distinct sets of TestBench inputs allowed for a measure of consistency by analyzing the two sets of TestBench outputs.

At the end of the TestBench, the PDFs generated from the first 68 samples in *allCRRD10.mat* and *allCRRD15.mat* were plotted against the estimated PDFs P_{CRRD10} and P_{CRRD15} to visually verify correct operation of the CRRD sampling algorithm.

Table 5. Arbitrary $P_{L\text{-}W}$

$p_{L\text{-}W}(MW)$	$p_{P_{L-W}}(p_{L-W})$
0	0.4
10	0.2
20	0.1
30	0.2
40	0.05
50	0.05

Table 5 shows the arbitrary PDF of load minus wind forecast error ($P_{L\text{-}W}$) used as a placeholder for CGR_{95} computation.

Simulation Results

A. Effect of Confidence Interval Width on Estimated Contingency Reserve Deficiency PDFs

The results presented here are meant to show that trends seen in the outputs of the TestBench for small and large contingency reserve response deficiency (CRRD) values are consistent with what is expected.

Figures 7 and 8 show how estimated PDFs of P_{CRRD10} and P_{CRRD15} (of five simulated generators) compare to the corresponding input (*i.e.* predefined) PDFs of 10 and 15 minute deficiencies. Figure 7 shows the case of small deficiencies, and Figure 8 shows the case of large deficiencies. The comparisons are shown for three different confidence interval (CI) width metrics. The three CI width metrics shown are:

1. a wide width of 0.1
2. a moderate width of 0.05
3. a narrow width of 0.01

As expected, the loose CI width of 0.1 shows that the fewest number of deficiency samples are required to satisfy the CI metrics. The number of samples required to satisfy the CI metrics is higher for the moderate CI width of 0.05, and for the 0.01 width all contingency samples are required. The three CI widths were experimentally determined to show this trend. The method of batched means was not used in these simulations.

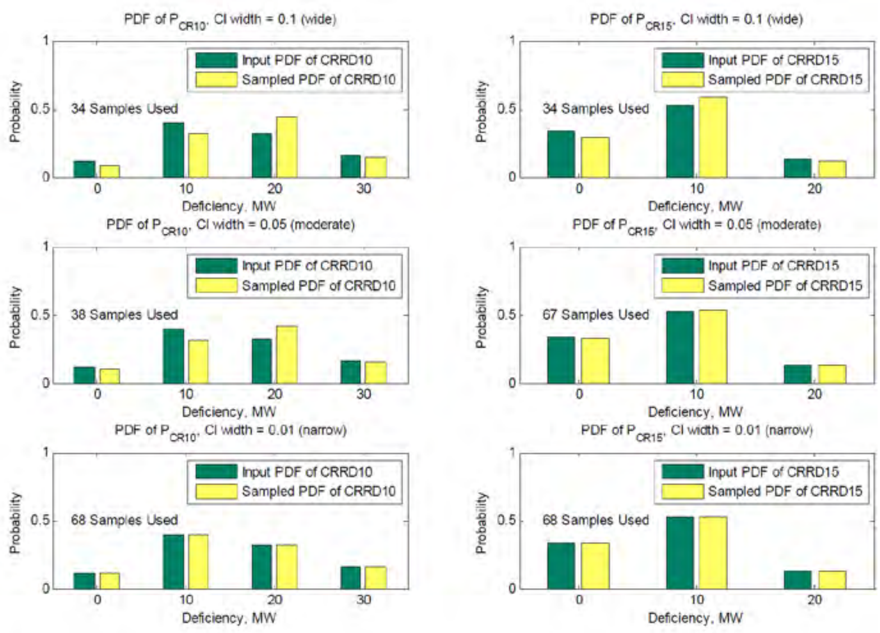

Figure 7. Comparison of Input and Sampled CRRD PDFs, Small Deficiencies

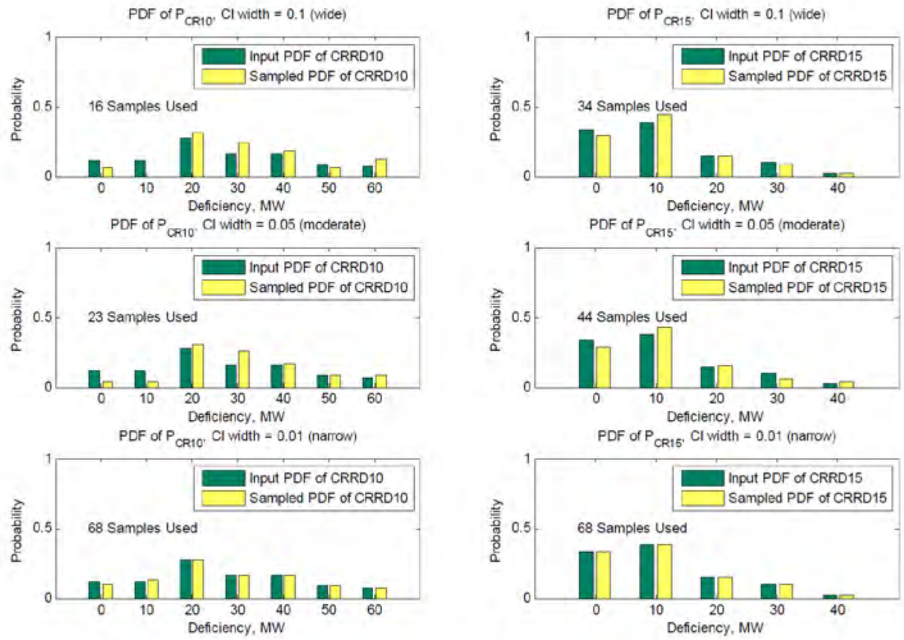

Figure 8. Comparison of Input and Sampled CRRD PDFs, Large Deficiencies

B. Effect of Contingency Reserve Deficiency Size on Controllable Generation Requirement

Two distinct trends depicting how CRR deficiency affects CGR_{95} over the unit commitment time horizon can be seen in the graphs in Figure 9. The first trend is the near-linear increase in CGR_{95} over the time interval $10 \leq t < 105$ minutes. This increase is due to the repetitive summing of CRR deficiency random variables (*i.e.* convolving P_{CRRD15} again and again) as time progresses within this time interval, accounting for the increased likelihood that a contingency will occur as time progresses. As shown in Figures 7 and 8, the predefined input PDFs of CRR deficiencies have significant nonzero probabilities. Applying the conditional summation convolution operation results in a PDF with even higher nonzero probabilities, which in turn results in a higher CGR_{95} value.

The second trend is the increase in slope of the first trend as the number of simulated contingency-reserve-providing generators is swept from one to five. Since all simulated generators were (randomly) given many nonzero 10 and 15 minute deficiency values, the expectation is that the probability of greater system deficiencies occurring would increase as N_{gen} is increased. As expected, Figure 9 shows that CGR_{95} increases if either the number of generators or the size of input deficiencies is increased.

Over the interval $105 \leq t \leq 300$ minutes CGR_{95} does not increase because during this time interval the PDF of capacity outage ($P_{o,t}$) is summed with the cumulative PDF of P_{CGR}. Since $P_{o,t}$ (from the Capacity Outage Probability Table) is a steady state random variable, it does not change over time. For more discussion of this issue see Appendix D.

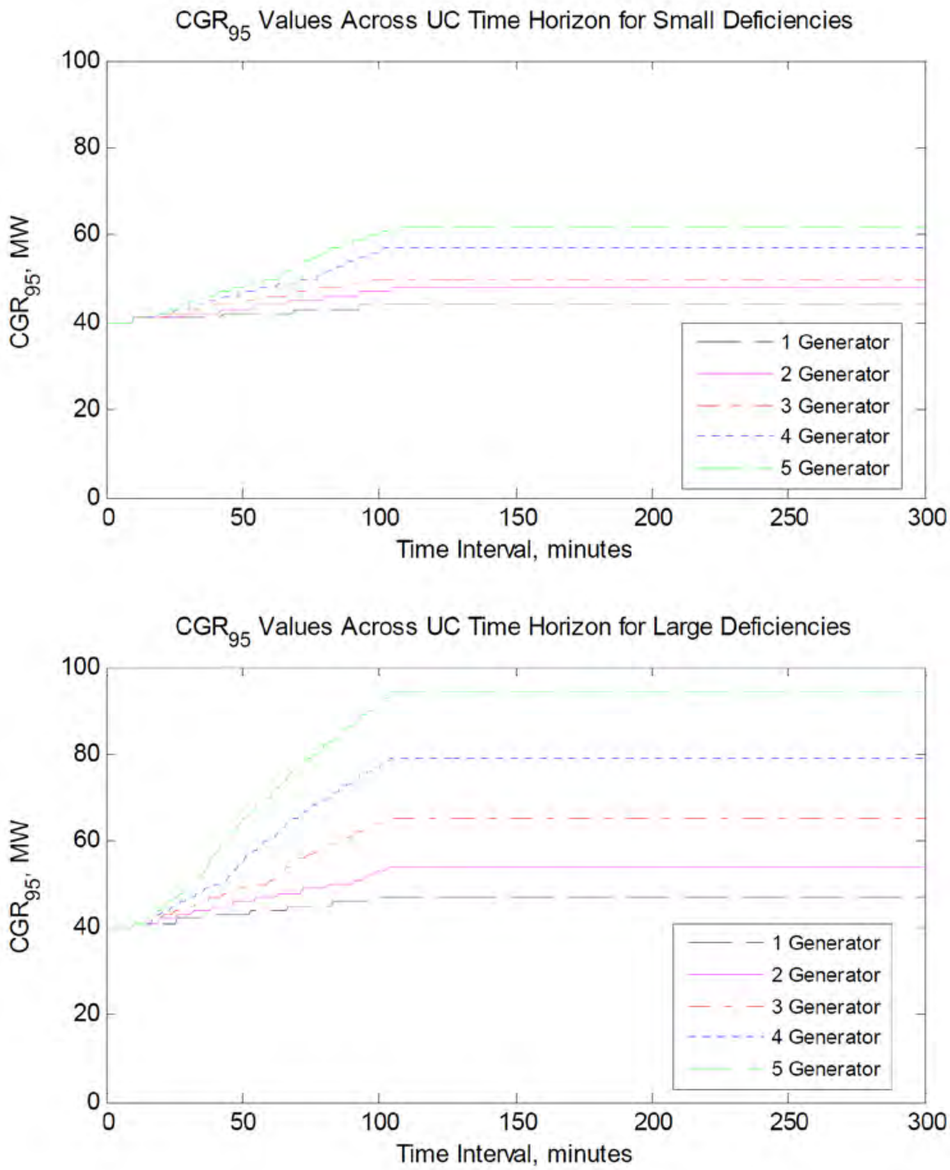

Figure 9. Comparison of CGR_{95} Values for Various N_{gen}

Conclusion

This report details the theory and implementation of a method for forecasting stochastic contingency reserve (CR) activation, as well as a method for combining the CR activation forecast with a forecast that includes the stochastic effects of wind, load, contingency size, and scheduled net interchange. A method based on convolution is proposed for statistically combining all forecasts in order to calculate a controllable generation requirement for a deterministic unit commitment algorithm. The methodology for forecasting CR activation is based on the expected behavior of CR activation in a control area that must adhere to NERC and WECC control performance standards. CR activation forecasts rely heavily on two probability density functions (PDFs) which are built from sample measurements of CR response deficiencies. Samples of CR response deficiency are measured by monitoring individual generator outputs in real-time when contingencies occur, and the resulting PDFs represent the fundamental stochastic variation of CR activation. Using a rolling buffer, the accuracy of the CR activation forecast can be sustained as new CR response deficiency samples will reflect power system changes. If historical data is used to initialize the rolling buffer, a higher CR activation forecast accuracy will be immediately available.

The algorithms for building PDFs of CR response deficiencies, forecasting CR activation, and computing CGR_{95} were verified to operate as expected via the TestBench simulations. The simulations verified that CGR_{95} increases faster if CR response deficiencies are greater. The increase in deficiency size was simulated in two ways, *i.e.* by either increasing the number of simulated generators that could contribute to the overall system CR response deficiency, or by increasing the predefined deficiencies associated with individual generators.

The success of the proposed algorithm for sampling of CR response deficiency is contingent on an ability to acquire real-time power system data from the energy management system database.

References

[1] A. Tuohy, P. Meibom, E. Denny, and M. O'Malley, "Unit commitment for systems with significant wind penetration," *IEEE Trans. Power Syst.*, vol. 24, no. 2, pp. 592-601, May 2009.

[2] F. Bouffard, and F.D. Galiana, "Stochastic security for operations planning with significant wind power generation," *IEEE Trans. Power Syst.*, vol. 23, no. 2, pp. 306-316, May 2008.

[3] P.A. Ruiz, C.R. Philbrick, E. Zak, K.W. Cheung, and P.W. Sauer, "Uncertainty management in the unic commitment problem," *IEEE Trans. Power Syst.*, vol. 24, no. 2, pp. 642-651, May 2009.

[4] Y. Makarov, "Overall Scope of Wind EMS Integration," Pacific Northwest National Laboratory, PowerPoint presentation, April 21, 2009.

[5] *NERC Standard BAL-0020-0 – Disturbance Control Performance*, Feb 2005. [Online] Available: http://www.nerc.com/files/BAL-002-0.pdf. [Accessed June 19, 2009].

[6] *WECC Standard BAL-002-WECC-1 - Contingency Reserves*, Oct 2008. [Online]. Available: http://www.nerc.com/files/BAL-002-WECC-1.pdf. [Accessed: May 6, 2009].

[7] *NERC Standard BAL-006-1 – Inadvertent Interchange*, May 9, 2007. [Online] Available: http://www.nerc.com/files/BAL-006-1.pdf. [Accessed July 29, 2009].

[8] California ISO. "Real-Time Market," *CAISO Tariff*. June 22, 2009. pp. 631. [Online]. [Available: http://www.caiso.com/23d5/23d5ccbb9800.pdf], [Accessed: August 18, 2009].

[9] California ISO. "Ancillary Service Procurement – Real-Time," Operating Procedure M-403A, April 1, 2009. [Online]. [Available: http://www.caiso.com/2381/238172f914620.pdf]. [Accessed: August 13, 2009].

[10] California ISO. "Appendix X: Dynamic Scheduling Protocol," *CAISO Tariff*, June 22, 2009. pp. 1772-1777. [Online]. [Available: http://www.caiso.com/23d5/23d5cfa1255a0.pdf]. [Accessed: August 18, 2009].

[11] *Northwest Power Pool Reliability Through Cooperation Reserve Sharing Program*, June 2008. [Online]. Available: http://www.wspp.org/filestorage/nw_power_pool_reserves_issue_060508.pdf. [Accessed: May 6, 2009].

[12] Bonneville Power Administration, "BPA Fast Facts," May 2009. [Online]. Available: http://www.bpa.gov/corporate/about_BPA/Facts/FactDocs/BPA_Facts_2008.pdf. [Accessed: June 4, 2009].

[13] *NWPP Reserve Sharing Group Practices and Procedures Frequently Asked Questions*, April 2004. [Online]. Available: http://www.nwpp.org/pdf/PRRS%20FAQ%20-%202004%200610.pdf. [Accessed: May 6, 2009].

[14] A. Leon-Garcia. *Probability, Statistics, and Random Processes for Electrical Engineering*, 3rd Ed, Upper Saddle River: Pearson Prentice Hall, 2008, pp. 367, 432-435.

[15] B.L. Silverstein, and D.M. Porter, "Contingency Ranking for Bulk System Reliability Criteria," *Trans. on Power Syst.*, vol. 7, no. 3, pp. 956-964, Aug 1992.

[16] J.W. Barnes, *Statistical Analysis for Engineers and Scientists: A Computer Based Approach*, McGraw Hill, 1994, pp. 109.

[17] C.M. Grinstead, J.L. Snell, *Introduction to Probability, 2nd ed.*, American Mathematical Society, 1997, pp. 285. [Online]. [Available: http://www.dartmouth.edu/~chance/teaching_aids/books_articles/probability_book/amsbook.mac.pdf]. [Accessed: July 2, 2009].

[18] P. Etingov, "Generators Forced Outage Model," Pacific Northwest National Laboratory, June 18, 2009.

[19] R. Billinton, and R.N. Allan, *Reliability Evaluation of Engineering Systems*, 2nd ed., Plenum Press, New York, 1992.

[20] R. Billinton, and R.N. Allan, *Reliability Evaluation of Power Systems*, 2nd ed., Plenum Press, New York, 1996.

Appendix A: Flowcharts of Program Organization & Data Flow

The function hierarchy of the program developed and described in this report is as follows. The highest level function is Mainfunction_TestBench.m (a.k.a. "TestBench," shown in enlarged, bold font). This function was developed to test the operation of the primary and secondary m-files that realize the theoretical algorithms described in the body of this report. The TestBench was designed to roughly mimic the highest level function in the processor that would run in parallel with the EMS and compute CGR_{95} values for the unit commitment algorithm in the EMS. The TestBench was designed to run as a real-time simulation for a user-specified amount of time (2.5 days was used for testing), and was designed to call the primary m-files at times in accordance with expected real world operation.

The primary MATLAB m-files are shown in bold, and each secondary m-file is indented beneath the primary m-file that calls it.

- **Mainfunction_TestBench.m**
  - **combined_uncertainty_evaluation.m**
    - direct_summation_conv.m
  - **contingency_reserve_activation_model.m**
    - product_conv.m
    - conditional_summation_conv.m
    - direct_summation_conv.m
  - **crrd_sample_evaluation.m**
  - **update_crrd_pdf.m**
    - get_pdf_from_sampleset.m
    - tinv (function built in to MATLAB's Statistics Toolbox)
    - chi2inv (function built in to MATLAB's Statistics Toolbox)

The flowcharts that follow show the logical organization of the TestBench and the primary m-files.

TestBench / Main Function and EMS Interface

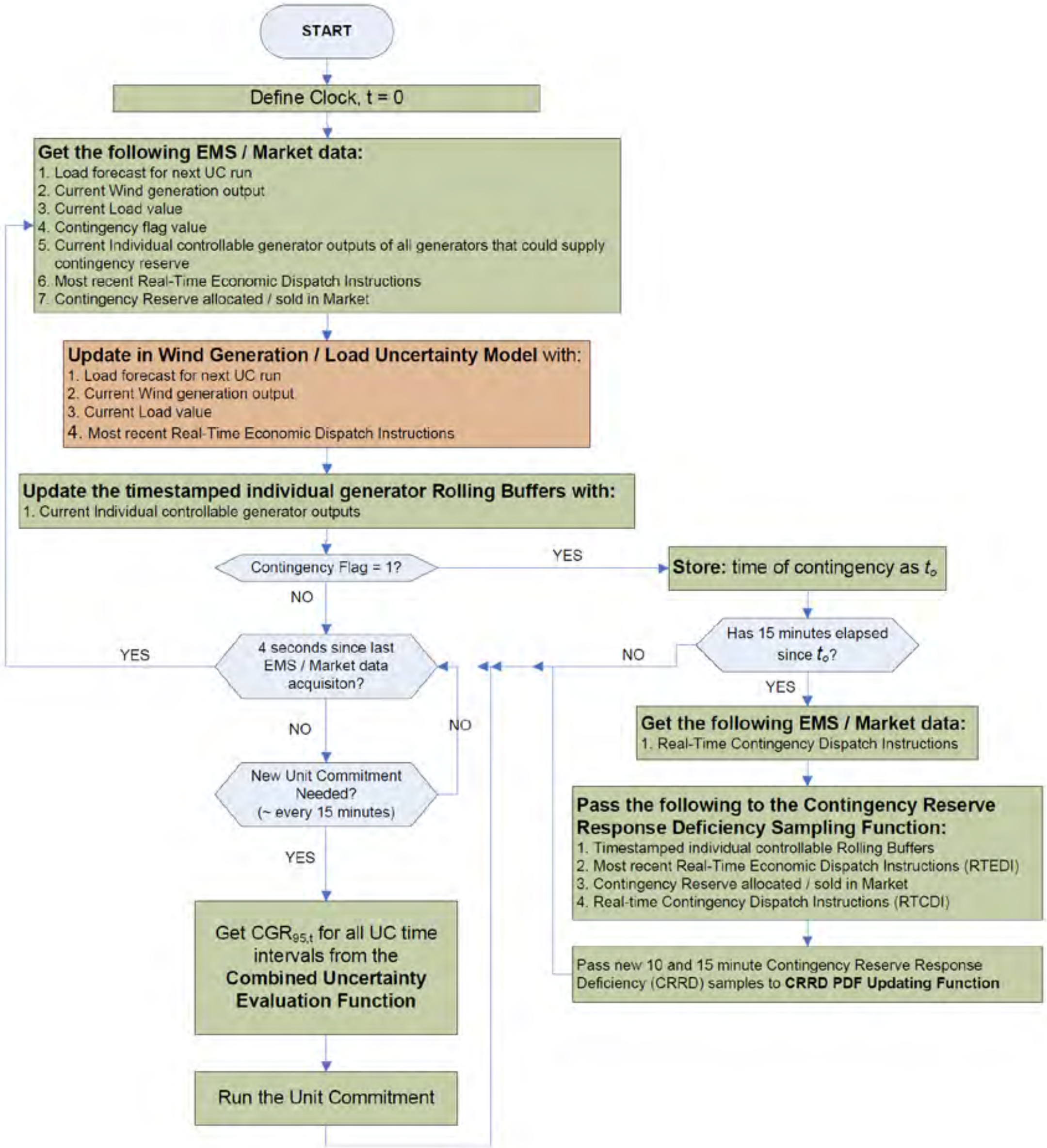

Combined Uncertainty Evaluation Function

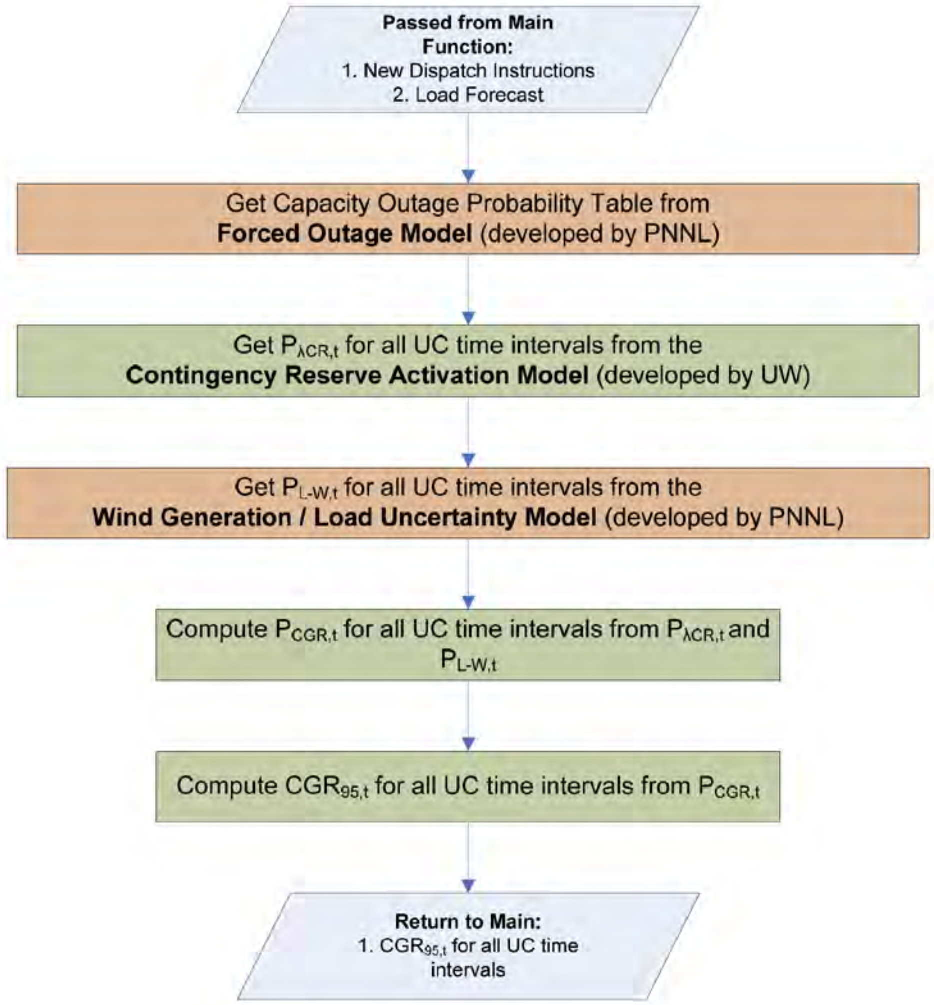

Contingency Reserve Activation Model

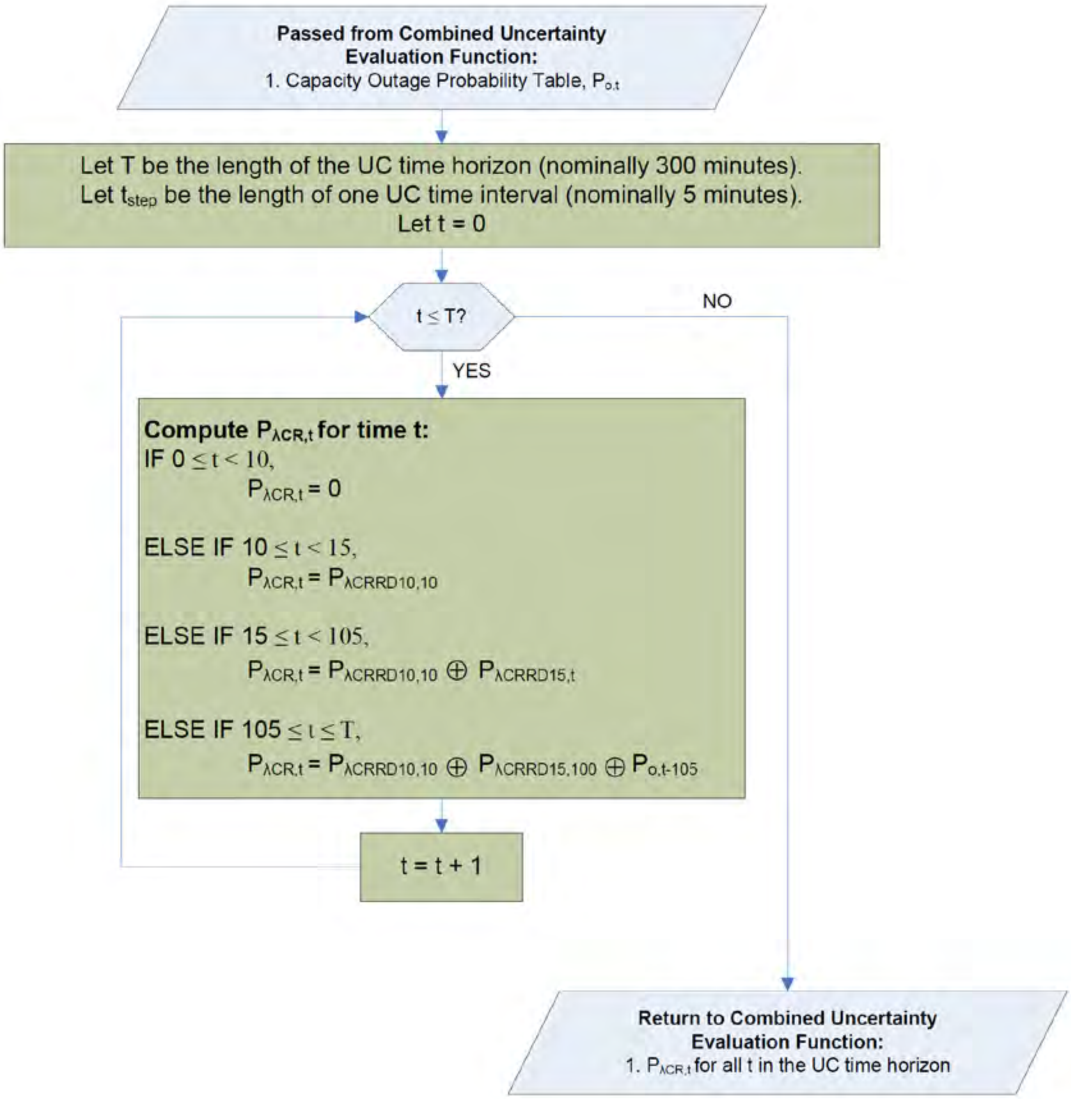

Contingency Reserve Response Deficiency Sample Evaluation Function

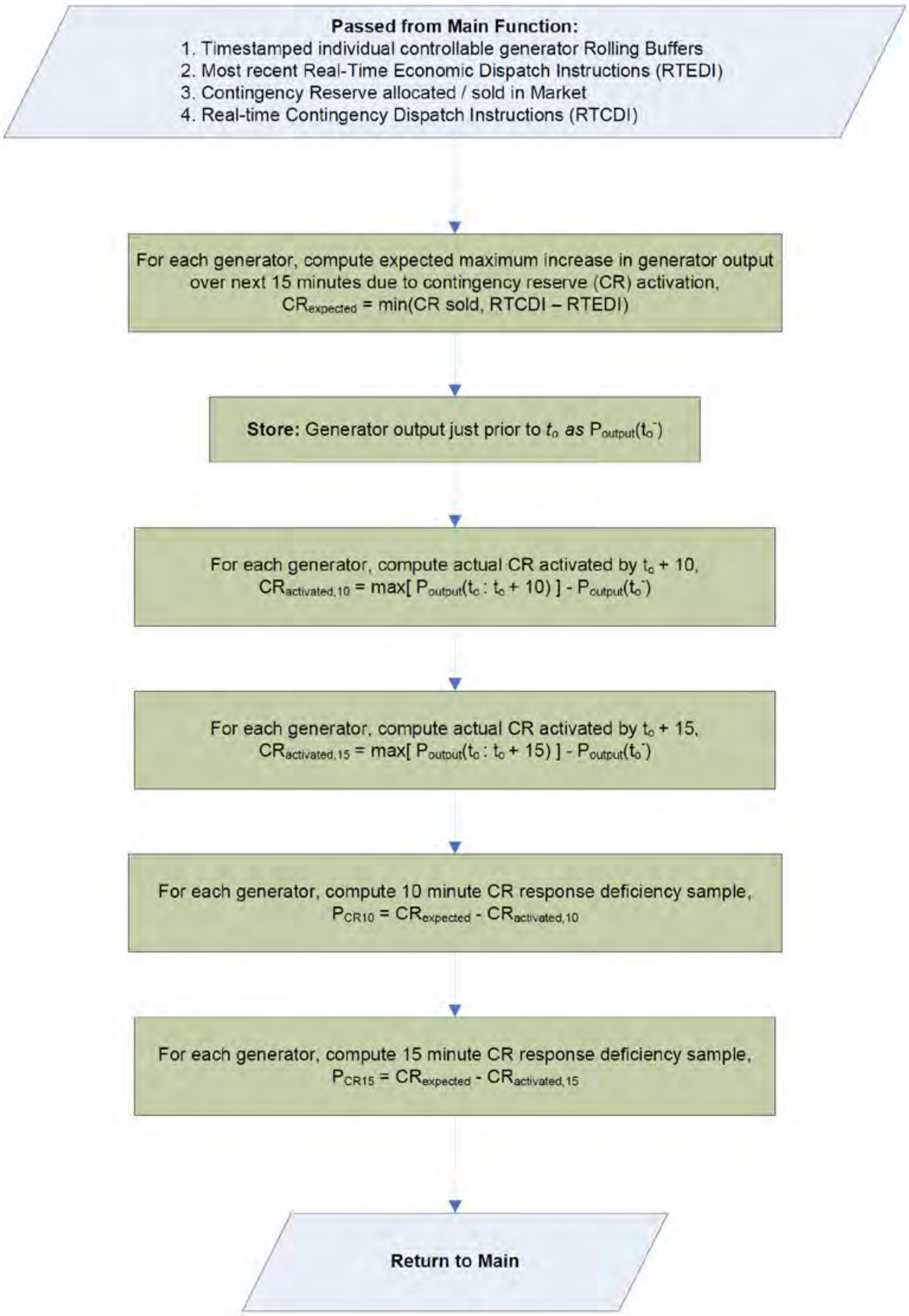

Update CRRD PDF Function

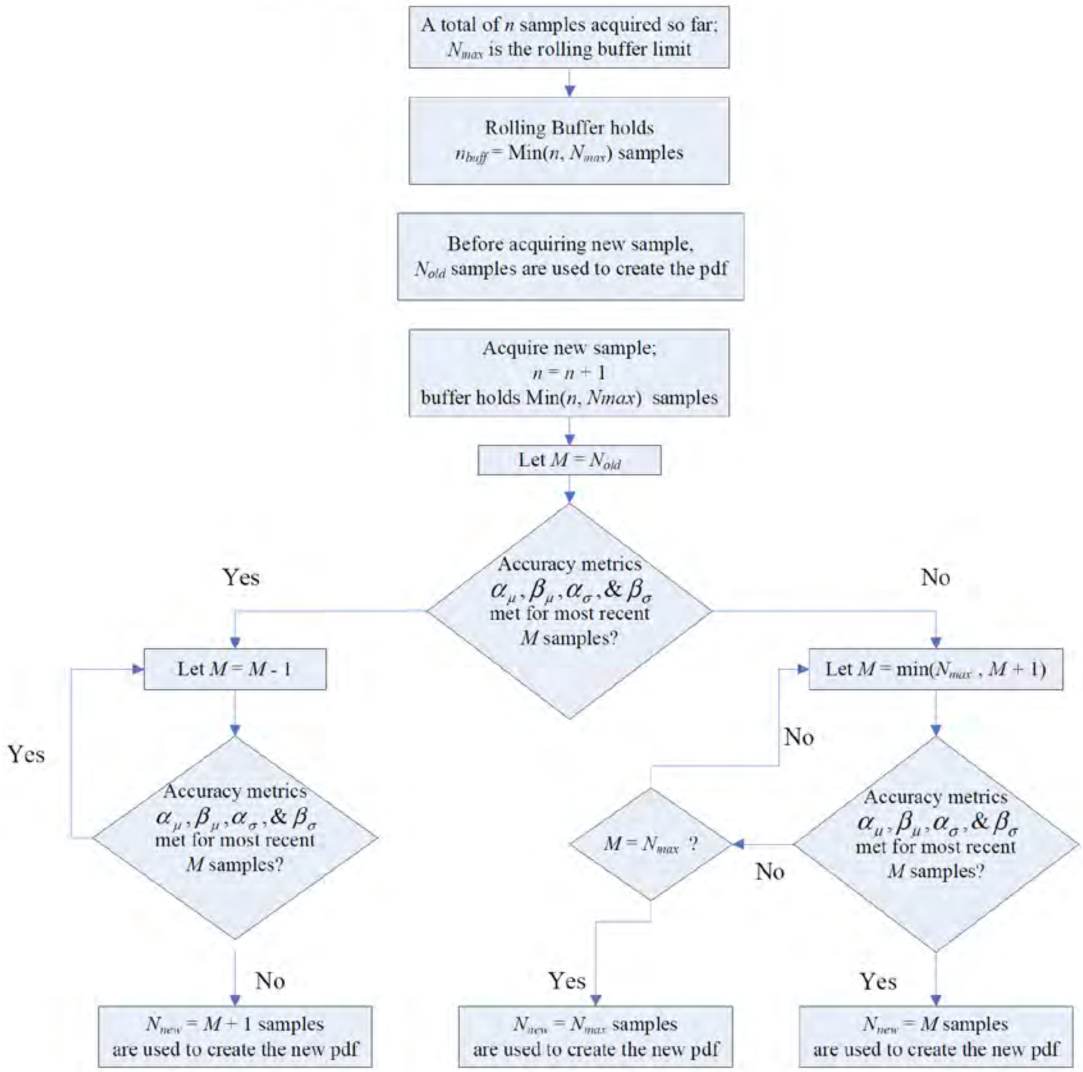

10-46

Appendix B: Combining Two Independent Random Variables

A. Background

Once the PDF of P_{CR} for a specific time interval is obtained it must be statistically combined with the PDF of λ, the Bernoulli random variable representing the probability of a contingency occurring in that time interval, to obtain $P_{\lambda CR}$, the conditional probability of CR activation. $P_{\lambda CR}$ is, in effect, P_{CR} weighted by the probability that a contingency has occurred. The operation used to combine P_{CR} and λ to produce $P_{\lambda CR}$ is *product convolution* [16], and is expressed as

$$P_{\lambda CR} = \lambda \otimes P_{CR} \tag{B.1}$$

$P_{\lambda CR}$ is then combined with P_{L-W} via *direct summation convolution* [16], expressed as

$$P_{CGR} = P_{L-W} \oplus P_{\lambda CR} \tag{B.2}$$

to generate the PDF of the total controlled generation requirement, P_{CGR}. It is assumed a PNNL process will supply the probability distribution for load-minus-wind as the discrete PDF of P_{L-W} for each time interval of the UC time horizon.

The mechanics of convolution are straightforward when the random variables are discrete [16],[17]. The PDFs of continuous random variables can be discretized to any desired resolution. The discrete bin sizes for all PDFs will be equalized to a single, common resolution, with the only exception being λ which has a value set of {0, 1}.

Section B and *Section C* provide examples of direct summation and product convolution of discrete random variables, respectively. The use of these two convolution algorithms is appropriate when the input random variables are independent. Appendix C describes an algorithm that uses conditional probability to convolve two dependent random variables.

B. Example 1: Direct Summation Convolution

Consider the generic random variables *X*, *Y*, and *Z* with PDFs $p_X(x_j)$, $p_Y(y_k)$, and $p_Z(z_i)$, respectively. Tables B-1 and B-2 define $p_X(x_j)$ and $p_Y(y_k)$, respectively.

Table B-1.

y_k	$p_Y(y_k)$
1	0.1
3	0.2
5	0.5
7	0.2

Table B-2.

x_j	$p_X(x_j)$
-2	0.3
0	0.2
2	0.5

The direct summation convolution of *X* and *Y* to produce *Z* is

$$Z = X \oplus Y \tag{B.3}$$

This operation involves first summing the values of each element of *X* and *Y* to produce one or more outcomes of *Z*,

$$z_i = x_j + y_k \tag{B.4}$$

where the probability of z_i is the product of the probabilities of x_j and y_k, i.e.

$$p_Z(z_i) = p_X(x_j) \cdot p_Y(y_k) \tag{B.5}$$

For any set of combinations of x_j and y_k that produce the same sum, the probabilities of the combinations are summed to produce the final probability of the outcome, z_i. This is expressed mathematically as

$$p_Z(z_i) = \sum_{j,k|z_j+y_k=z_i} p_X(x_j) \cdot p_Y(y_k). \tag{B.6}$$

Figure B-1(a) shows in tabular form (A.6) being applied using the PDFs in Tables B-1 and B-2. Figure B-1(b) shows graphically $p_Z(z_i)$ resulting from the direct summation convolution of $p_X(x_j)$ and $p_Y(y_k)$.

x_j	y_k	z_i	Probability
-2	1	-1	(0.3)(0.1) = 0.03
-2	3	1	(0.3)(0.2) = 0.06
-2	5	3	(0.3)(0.5) = 0.15
-2	7	5	(0.3)(0.2) = 0.06
0	1	1	(0.2)(0.1) = 0.02
0	3	3	(0.2)(0.2) = 0.04
0	5	5	(0.2)(0.5) = 0.1
0	7	7	(0.2)(0.2) = 0.04
2	1	3	(0.5)(0.1) = 0.05
2	3	5	(0.5)(0.2) = 0.1
2	5	7	(0.5)(0.5) = 0.25
2	7	9	(0.5)(0.2) = 0.1

$$\sum_{j,k|z_j+y_k=z_i}$$

z_i	$p_Z(z_i)$
-1	0.03
1	0.08
3	0.24
5	0.26
7	0.29
9	0.1

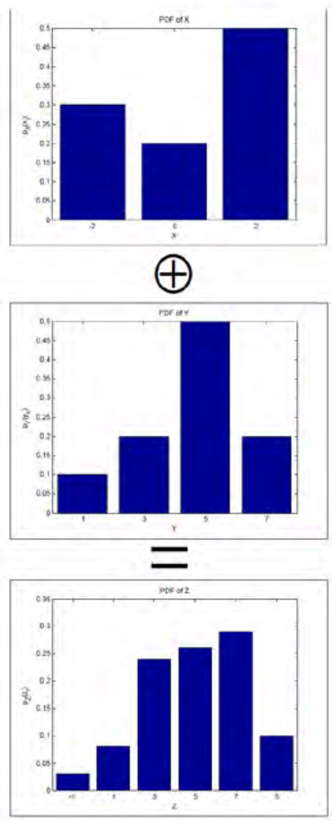

(a) **(b)**

Figure B-1. Direct Summation Convolution Example

C. Example 2: Product Convolution

Consider the generic random variables X, Y, and Z with PDFs $p_X(x_j)$, $p_Y(y_k)$, and $p_Z(z_i)$, respectively. Tables B-3 and B-4 define $p_X(x_j)$ and $p_Y(y_k)$, respectively, and $p_Z(z_i)$ is to be found. To be consistent with the use of product convolution in the special case of (A.1) (also equation (2)), X is a Bernoulli random variable for this example.

Table B-3.

x_j	$p_X(x_j)$
0	0.8
1	0.2

Table B-4.

y_k	$p_Y(y_k)$
1	0.1
3	0.2
5	0.5
7	0.2

The process for the product convolution of Y and X to produce Z is very similar to that of direct summation convolution. The product convolution is expressed as

$$Z = Y \otimes X \tag{B.7}$$

In this case, the values of each element of X and Y are multiplied instead of summed, *i.e.*

$$z_i = x_j \cdot y_k \tag{B.8}$$

As before, (A.5) is used to find $p_Z(z_i)$ for a specific combination of x_j and y_k. A slight adjustment to (A.6) is needed to find the final value of $p_Z(z_i)$ for product convolution, *i.e.*

$$p_Z(z_i) = \sum_{j,k|z_j \cdot y_k = z_i} p_X(x_j) \cdot p_Y(y_k) \tag{B.9}$$

Figure B-2(a) shows in tabular form (A.9) being applied using the PDFs in Tables B-3 and B-4. Figure B-2(b) shows graphically $p_Z(z_i)$ resulting from the product convolution of $p_X(x_j)$ and $p_Y(y_k)$.

x_j	y_k	z_i	Probability
0	1	0	(0.8)(0.1) = 0.08
0	3	0	(0.8)(0.2) = 0.16
0	5	0	(0.8)(0.5) = 0.4
0	7	0	(0.8)(0.2) = 0.16
1	1	1	(0.2)(0.1) = 0.02
1	3	3	(0.2)(0.2) = 0.04
1	5	5	(0.2)(0.5) = 0.1
1	7	7	(0.2)(0.2) = 0.04

$$\downarrow$$

$$\sum_{j,k \mid z_j \cdot y_k = z_i}$$

$$\downarrow$$

z_i	$p_Z(z_i)$
0	0.8
1	0.02
3	0.04
5	0.1
7	0.04

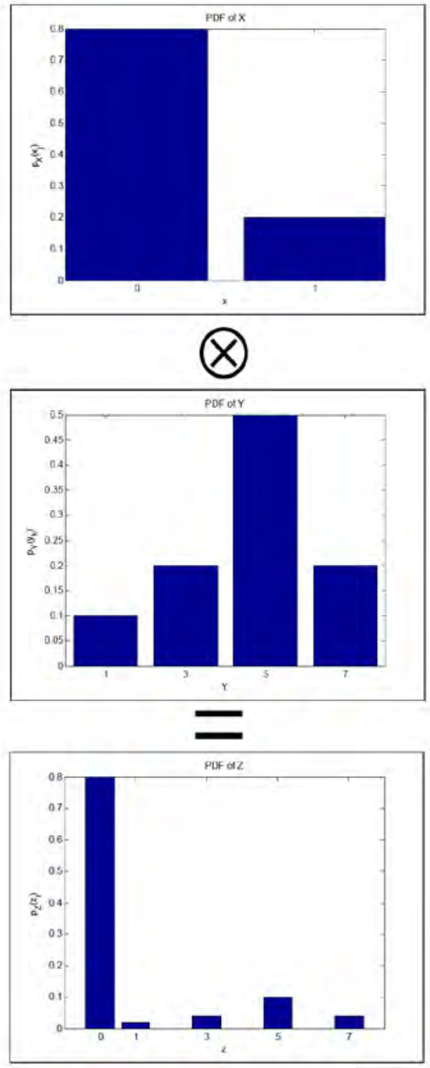

(a) **(b)**

Figure B-2. Product Convolution Example

D. Example 3: Determine P_{CGR} From λ, P_{CR}, and $P_{L\text{-}W}$

P_{CGR} is found by first performing a product convolution on λ and P_{CR} to arrive at $P_{\lambda CR}$, and then performing a direct summation convolution on $P_{\lambda CR}$ and $P_{L\text{-}W}$ to arrive at P_{CGR}, *i.e.*

$$P_{CGR} = (\lambda \otimes P_{CR}) \oplus P_{L-W} \tag{B.10}$$

As a hypothetical example, let the PDFs of λ, P_{CR}, and $P_{L\text{-}W}$ be as shown in Tables B-5, B-6 and B-7, respectively.

Table B-5.

p_{λ}	$p_{P_{\lambda}}(p_{\lambda})$
0	0.8
1	0.2

Table B-6.

p_{CR} (MW)	$p_{P_{CR}}(p_{CR})$
0	0.05
100	0.2
200	0.5
300	0.2
400	0.05

Table B-7.

$p_{L\text{-}W}$ (MW)	$p_{P_{L\text{-}W}}(p_{L-W})$
0	0.15
100	0.35
200	0.25
300	0.15
400	0.05
500	0.05

To apply (B.1) to the PDFs in Tables B-5 and B-6, let $X = \lambda$, $Y = P_{CR}$, and $Z = P_{\lambda CR}$, and then perform the product convolution outlined in Example 2. Figure B-3 shows the result of this product convolution.

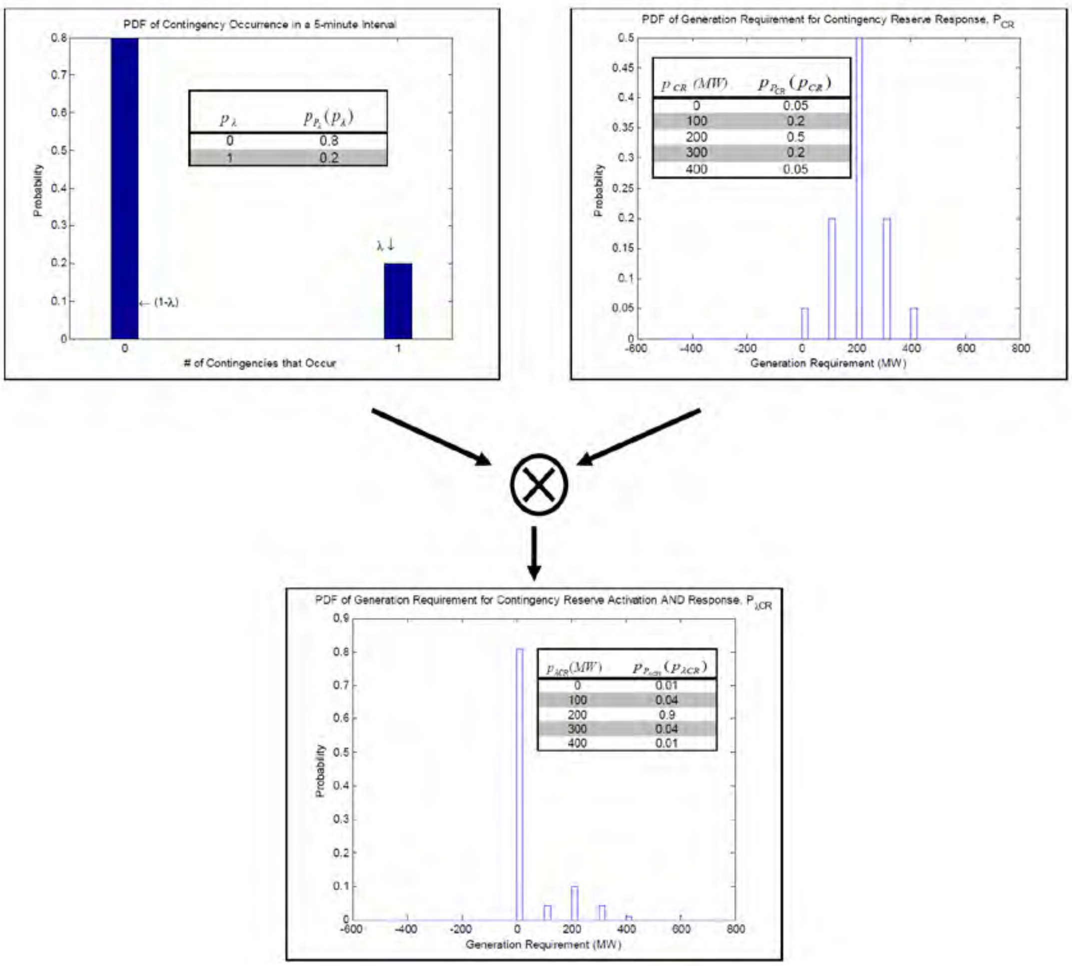

Figure B-3. Example of $P_{\lambda CR} = \lambda \otimes P_{CR}$

In Figure B-3 the value of p[λ=*1*] is unrealistically high so that the probabilities of nonzero values of $P_{\lambda CR}$ remain visible. Although these PDFs are arbitrary, they do demonstrate the expectation that the contribution to CGR by CR activation is significantly lowered by λ.

Table B-8.

$p_{\lambda CR}(MW)$	$p_{P_{\lambda CR}}(p_{\lambda CR})$
0	0.01
100	0.04
200	0.9
300	0.04
400	0.01

To apply (A.2) to the PDFs in Tables B-7 and B-8, let $X = P_{L\text{-}W}$, $Y = P_{\lambda CR}$, and $Z = P_{CGR}$, and then perform the direct summation convolution outlined in Example 1. Figure B-4 shows the result of this direct summation convolution. Because the PDFs shown in Figure B-4 are arbitrary, this example is not included for any reason other than to show how convolution will be used in the process of determining CGR_{95}.

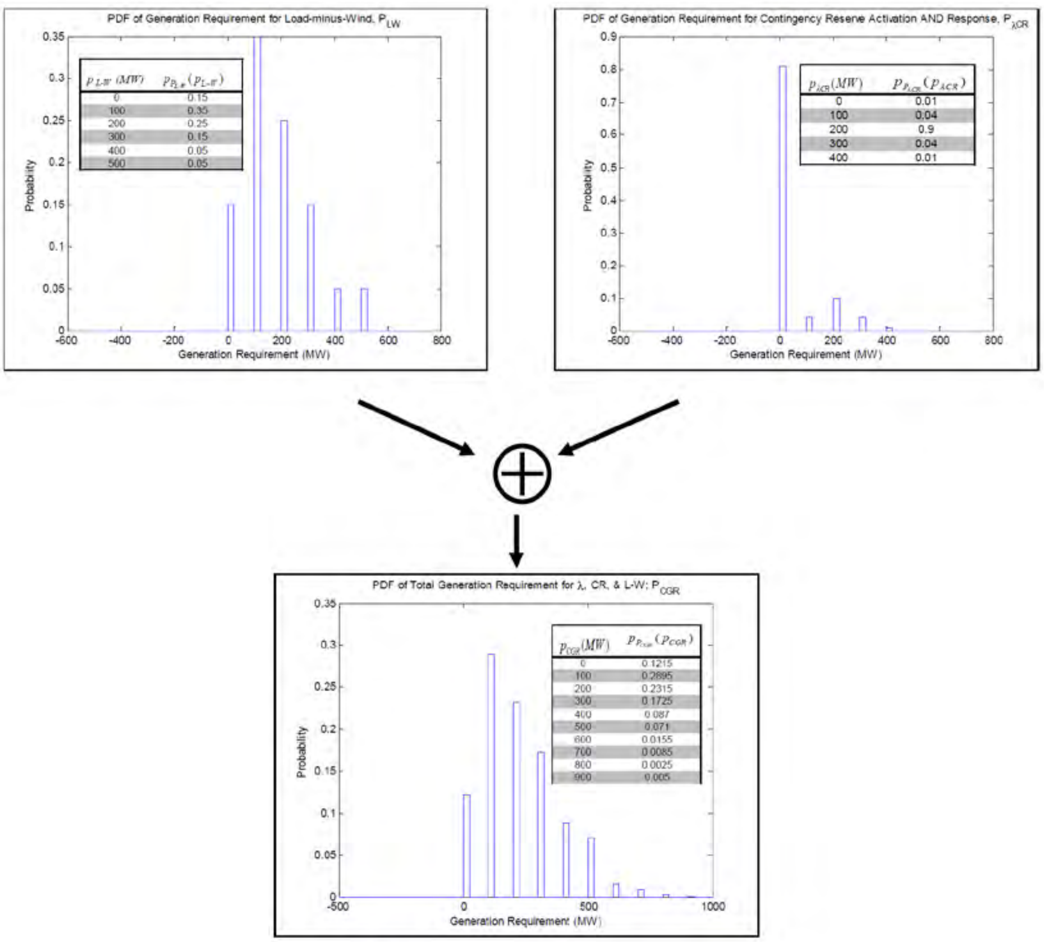

Figure B-4. Example of $P_{CGR} = P_{L-W} \oplus P_{\lambda CR}$

Appendix C: Combining Two Dependent Random Variables

A. Background

This section describes the need to use a summation convolution algorithm based on conditional probability instead of direct summation convolution (described in Appendix B) to sum the contingency reserve response deficiencies due to contingencies occurring in successive time intervals. This conditional probability method performs the same summation convolution operation but allows the dependence between the two input random variables to be included in the formulation. This method will be used in practice to when computing successive PDFs of 10 and 15 minute CRR deficiencies. The following explanation and example will use a unit commitment time interval of one minute to exemplify the most general formulation, and it will focus on computing the 10 minute contingency reserve response (CRR) deficiency, $P_{\lambda CRRD10}$, at time interval $t = 11$ given that $P_{\lambda CRRD10}$ is known at $t = 10$.

The importance of this conditional summation convolution operation is that the dependence of $P_{\lambda CRRD10,t}$ at, for example, $t = 11$ on $P_{\lambda CRRD10,t}$ at $t = 10$ (the previous interval) can be explicitly included when statistically transitioning from the CRR deficiency of one time interval to the next. $P_{\lambda CRRD10,10}$ corresponds to the 10 minute CRR deficiency from a contingency occurring in the first time interval, $P_{\lambda CRRD10,11}$ corresponds to the 10 minute CRR deficiency from a contingency occurring in the second time interval, $P_{\lambda CRRD10,12}$ corresponds to the 10 minute CRR deficiency from a contingency occurring in the third time interval, and so on.

The dependence between $P_{\lambda CRRD10,t}$ at successive time intervals is due to the known amount of contingency reserve at the start of the unit commitment (UC). This quantity sets the upper limit of CRR deficiency that can be forecasted for any time interval in the UC. It is this upper limit on CRR deficiency that enforces a dependence on the CRR deficiency forecasted for successive time intervals.

The transition from $P_{\lambda CRRD10,10}$ to $P_{\lambda CRRD10,11}$ could be similarly computed using direct summation convolution with a possibility of error. In fact, the PDF of $P_{\lambda CRRD10,11}$ resulting from conditional summation convolution with no upper limit (thereby removing the dependence) would be exactly the same as if it were computed using direct summation convolution.

The time-dependent transition from $P_{\lambda CRRD10,10}$ to $P_{\lambda CRRD10,11}$ is needed to compute $P_{\lambda CR,11}$, *i.e.*

at $t = 10$,

$$\mathrm{P}_{\lambda \mathrm{CR},10} = \mathrm{P}_{\lambda \mathrm{CRRD}10,10} = \mathrm{P}_{\lambda \mathrm{CRRD}10}. \qquad \text{(C.1)}$$

and at $t = 11$,

$$P_{\lambda CR,11} = P_{\lambda CRRD10,11} = P_{\lambda CR,10} \,\bar{\oplus}\, P_{\lambda CRRD10,10} \qquad \text{(C.2)}$$

where $\bar{\oplus}$ signifies a conditional summation convolution operation. Direct summation convolution and conditional summation convolution are similar, but only the conditional probability method enforces the constraint that the forecasted CRR deficiency at any UC time interval cannot exceed the total allocated contingency reserve.

The remainder of Appendix C details how the conditional summation convolution operation is used to transition from $P_{\lambda CR,10}$ to $P_{\lambda CR,11}$. *Section B* outlines the general theory behind conditional probability, and *Section C* shows the theory being applied to a numerical example.

B. General Conditional Probability Theory [14]

The general equation to compute the conditional probability of event B occurring given event A is

$$\mathrm{P}(B|A) = \frac{\mathrm{P}(B \cap A)}{\mathrm{P}(A)} \tag{C.3}$$

Applying Bayes' Theorem, equation (C.3) equates to

$$\mathrm{P}(B|A) = \frac{\mathrm{P}(A|B)\mathrm{P}(B)}{\mathrm{P}(A)} \tag{C.4}$$

and for the specific partitions, B_i and A_j, in the event space, equation (C.4) is written as

$$\mathrm{P}(B_i|A_j) = \frac{\mathrm{P}(A_j|B_i)\mathrm{P}(B_i)}{\sum_h \mathrm{P}(A_j|B_h)\mathrm{P}(B_h)} \tag{C.5}$$

C. Example: Determine $P_{\lambda CRRD10,t+1}$ Given $P_{\lambda CRRD10,t}$

Let $P^*_{\lambda CRRD10,11}$ be the random variable representing the probability of CRR deficiency *in* time interval $t = 11$, and let $P_{\lambda CRRD10,11}$ be the random variable of the cumulative CRR deficiency from any possible previous UC interval. $P^*_{\lambda CRRD10,11}$ is computed directly from $P_{\lambda CRRD10,10}$, and is then used to compute $P_{\lambda CRRD10,11}$.

Equation (C.5) is used to determine the conditional probability of a specific outcome of $P^*_{\lambda CRRD10,11}$ (equivalent to B_i) occurring given a specific outcome of $P_{\lambda CRRD10,10}$ (equivalent to A_j) having occurred. Equation (C.6) shows the application of (C.5) to the time-dependent CRR deficiency, where i and h denote specific outcomes of $P^*_{\lambda CRRD10,11}$, and j denotes a specific outcome of $P_{\lambda CRRD10,10}$ in MW.

$$\mathrm{P}\left[P^*_{\lambda CRRD10,11} = i \middle| P_{\lambda CRRD10,10} = j\right] = \frac{\mathrm{P}\left[P_{\lambda CRRD10,10} = j \middle| P^*_{\lambda CRRD10,11} = i\right]\mathrm{P}\left[P^*_{\lambda CRRD10,11} = i\right]}{\sum_h \mathrm{P}\left[P_{\lambda CRRD10,10} = j \middle| P^*_{\lambda CRRD10,11} = h\right]\mathrm{P}\left[P^*_{\lambda CRRD10,11} = h\right]} \tag{C.6}$$

Bayes' Theorem conveniently defines the probability P($P^*_{\lambda CRRD10,11} = i \mid P_{\lambda CRRD10,10} = j$) (which is unknown) in terms of the reverse, *i.e.* P[$P_{\lambda CRRD10,10} = j \mid P^*_{\lambda CRRD10,11} = i$], and the independent probability P[$P^*_{\lambda CRRD10,11} = i$], both of which can be found easily. P[$P^*_{\lambda CRRD10,11} = i$] is given by $P_{\lambda CRRD10}$, and P[$P_{\lambda CRRD10,10} = j \mid P^*_{\lambda CRRD10,11} = i$] equals P[$P_{\lambda CRRD10,10} = j$] (given by $P_{\lambda CRRD10}$) unless the sum of j and i is greater than the total allocated contingency reserve, in which case P[$P_{\lambda CRRD10,10} = j \mid P^*_{\lambda CRRD10,11} = i$] equals zero. The sum over h in the denominator of equation (C.6) acts to normalize over all other outcomes of $P_{\lambda CRRD10,10}$.

Equation (C.7) is used to find the total probability of an outcome, i, of $P^*_{\lambda CRRD10,11}$.

$$\mathrm{P}\left[P^*_{\lambda CRRD10,11}=i\right]=\sum_j \mathrm{P}\left[P^*_{\lambda CRRD10,11}=i \middle| P_{\lambda CRRD10,10}=j\right]\mathrm{P}\left[P_{\lambda CRRD10,10}=j\right] \quad \text{(C.7)}$$

To illustrate the computation with an example, let the PDF of $P_{\lambda CRRD10}$ be defined by Table C-1, and let the total allocated contingency reserve be 40 MW.

Table C-1.

h, i, or j	$\mathrm{P}[P_{\lambda CRRD10} = h, i, or\ j]$
0	0.7
10	0.2
20	0.05
30	0.03
40	0.02

The use of equation (C.6) for the first outcome of $P^*_{\lambda CRRD10,11}$ ($i = 0$) given $P_{\lambda CRRD10,10} = 0$ would look like

$$\begin{aligned}
&\mathrm{P}\left[P^*_{\lambda CRRD10,11}=0 \middle| P_{\lambda CRRD10,10}=0\right]= \\
&=\frac{\mathrm{P}\left[P_{\lambda CRRD10,10}=0 \middle| P^*_{\lambda CRRD10,11}=0\right]\mathrm{P}\left[P^*_{\lambda CRRD10,11}=0\right]}{\mathrm{P}\left[P_{\lambda CRRD10,10}=0 \middle| P^*_{\lambda CRRD10,11}=0\right]\mathrm{P}\left[P^*_{\lambda CRRD10,11}=0\right]+...+\mathrm{P}\left[P_{\lambda CRRD10,10}=0 \middle| P^*_{\lambda CRRD10,11}=40\right]\mathrm{P}\left[P^*_{\lambda CRRD10,11}=40\right]} \quad \text{(C.8)} \\
&=\frac{(0.7)(0.7)}{(0.7)(0.7)+...+(0.7)(0.02)}=0.7
\end{aligned}$$

A result of 0.7 is to be expected. In fact, the PDF of $P^*_{\lambda CRRD10,11}$ given $P_{\lambda CRRD10,10} = 0$ would be equal to that of $P_{\lambda CRRD10}$ since no CRR deficiency has yet occurred.

To show how conditional summation convolution takes into account the constraint of maximum online capacity, consider the last outcome of $P^*_{\lambda CRRD10,11}$ ($i = 30$) given $P_{\lambda CRRD10,10} = 10$MW:

$$\begin{aligned}
&\mathrm{P}\left[P^*_{\lambda CRRD10,11}=30 \middle| P_{\lambda CRRD10,10}=10\right]= \\
&=\frac{\mathrm{P}\left[P_{\lambda CRRD10,10}=10 \middle| P^*_{\lambda CRRD10,11}=30\right]\mathrm{P}\left[P^*_{\lambda CRRD10,11}=30\right]}{\mathrm{P}\left[P_{\lambda CRRD10,10}=10 \middle| P^*_{\lambda CRRD10,11}=0\right]\mathrm{P}\left[P^*_{\lambda CRRD10,11}=0\right]+...+\mathrm{P}\left[P_{\lambda CRRD10,10}=10 \middle| P^*_{\lambda CRRD10,11}=40\right]\mathrm{P}\left[P^*_{\lambda CRRD10,11}=40\right]} \quad \text{(C.9)} \\
&=\frac{(0.2)(0.03)}{(0.2)(0.7)+...+(0)(0.02)}=0.0306
\end{aligned}$$

The above equation shows that $\mathrm{P}[P_{\lambda CRRD10,10} = 10 \mid P^*_{\lambda CRRD10,11} = 40] = 0$. This is to say that if in fact $P^*_{\lambda CRRD10,11} = 40$MW, then $P_{\lambda CRRD10,10}$ could not have been 10MW. Cases like this where $i + j > 40$MW happen less often than the case where $i + j \leq 40$MW. For the latter case, $P_{\lambda CRRD10,10}$ is independent of $P^*_{\lambda CRRD10,11}$.

The following uses equation (C.7) to compute the complete probability of $P^*_{\lambda CRRD10,11}$ = 30MW.

$$\begin{aligned}
\mathrm{P}\left[P^*_{\lambda CRRD10,11}=30\right] &= \sum_j \mathrm{P}\left[P^*_{\lambda CRRD10,11}=30 \middle| P_{\lambda CRRD10,10}=j\right]\mathrm{P}\left[P_{\lambda CRRD10,10}=j\right] \\
&= \mathrm{P}\left[P^*_{\lambda CRRD10,11}=30 \middle| P_{\lambda CRRD10,10}=0\right]\mathrm{P}\left[P_{\lambda CRRD10,10}=0\right]+ \\
&= \mathrm{P}\left[P^*_{\lambda CRRD10,11}=30 \middle| P_{\lambda CRRD10,10}=10\right]\mathrm{P}\left[P_{\lambda CRRD10,10}=10\right]+ \\
&= \mathrm{P}\left[P^*_{\lambda CRRD10,11}=30 \middle| P_{\lambda CRRD10,10}=20\right]\mathrm{P}\left[P_{\lambda CRRD10,10}=20\right]+ \\
&= \mathrm{P}\left[P^*_{\lambda CRRD10,11}=30 \middle| P_{\lambda CRRD10,10}=30\right]\mathrm{P}\left[P_{\lambda CRRD10,10}=30\right]+ \\
&= \mathrm{P}\left[P^*_{\lambda CRRD10,11}=30 \middle| P_{\lambda CRRD10,10}=40\right]\mathrm{P}\left[P_{\lambda CRRD10,10}=40\right] \\
&= (0.03)(0.7)+(0.0306)(0.2)+(0)(0.05)+(0)(0.03)+(0)(0.02) \\
&= 0.02712
\end{aligned} \tag{C.10}$$

As expected, the probability of a 30MW CRR deficiency at $t = 11$ is less than that of $t = 10$ because it reflects the impossibility of those transitions from $P_{\lambda CRRD10,10} = j$ to $P^*_{\lambda CRRD10,11} = i$ that would result in a cumulative CRR deficiency greater than the total allocated contingency reserve. PDFs of $P_{\lambda CRRD10,10}$ and $P^*_{\lambda CRRD10,11}$ are shown in Figure C-1.

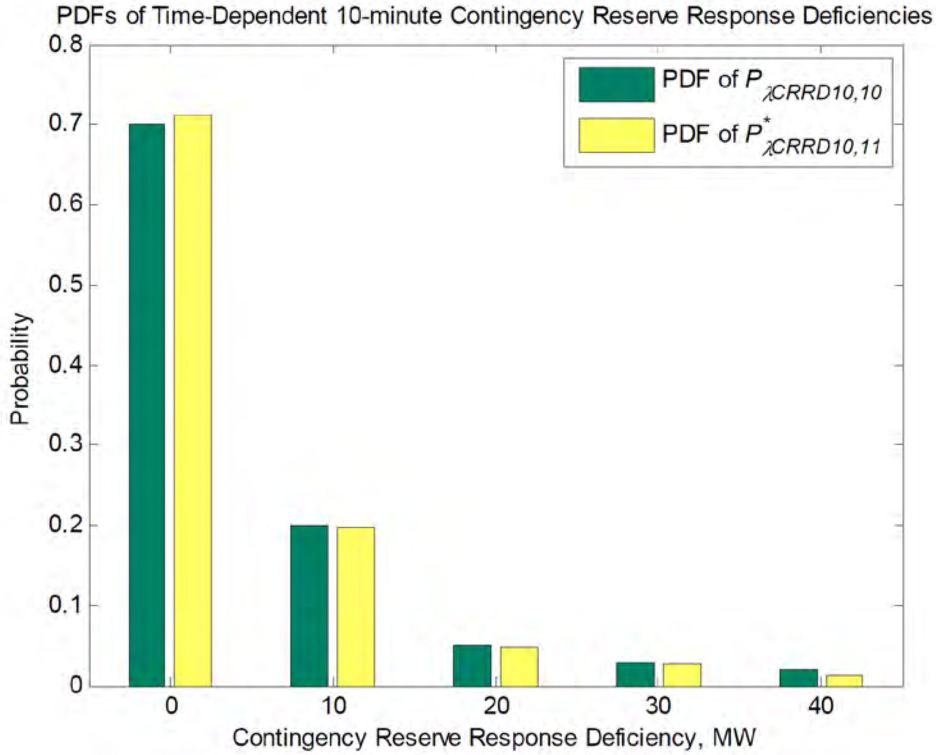

Figure C-1: Comparison of $P_{\lambda CRRD10,10}$ and $P^*_{\lambda CRRD10,11}$

$P_{\lambda CRDR10,11}$ represents the cumulative CRR deficiency realized *by* the start of time interval t = 11. $P_{\lambda CRRD10,11}$ therefore contains the cumulative influence of a contingency happening at any prior time interval, and is what is ultimately used by the CRAM to compute $P_{\lambda CRRD,11}$. Equation (C.11) is used to compute $P_{\lambda CRRD10,11}$ from $P^*_{\lambda CRRD10,11}$.

$$P\left[P_{\lambda CRRD10,11}=k\right]=\sum_{i,j|i+j=k}P\left[P_{\lambda CRRD10,10}=j\right]\cdot P\left[P^*_{\lambda CRRD10,11}=i\right] \qquad \text{(C.11)}$$

The resulting PDF of $P_{\lambda CRRD10,11}$ is depicted in Figure C-2. As expected, an increase in the probabilities of nonzero CRR deficiencies can be seen from the transition from $P_{\lambda CRRD10,10}$ to $P_{\lambda CRRD10,11}$.

Because $P_{\lambda CRRD10,11}$ contains all of the conditional information from possible outcomes of $P_{\lambda CRRD10,10}$, when continuing to $P_{o,t+2}$, this methodology can be repeated exactly to find P[$P_{\lambda CRRD10,12} = i \mid P_{\lambda CRRD10,11} = k$]. Including P[$P_{\lambda CRRD10,12} = i \mid P_{\lambda CRRD10,10} = k$] in the calculation of $P_{\lambda CRRD10,11}$ is unnecessary and redundant.

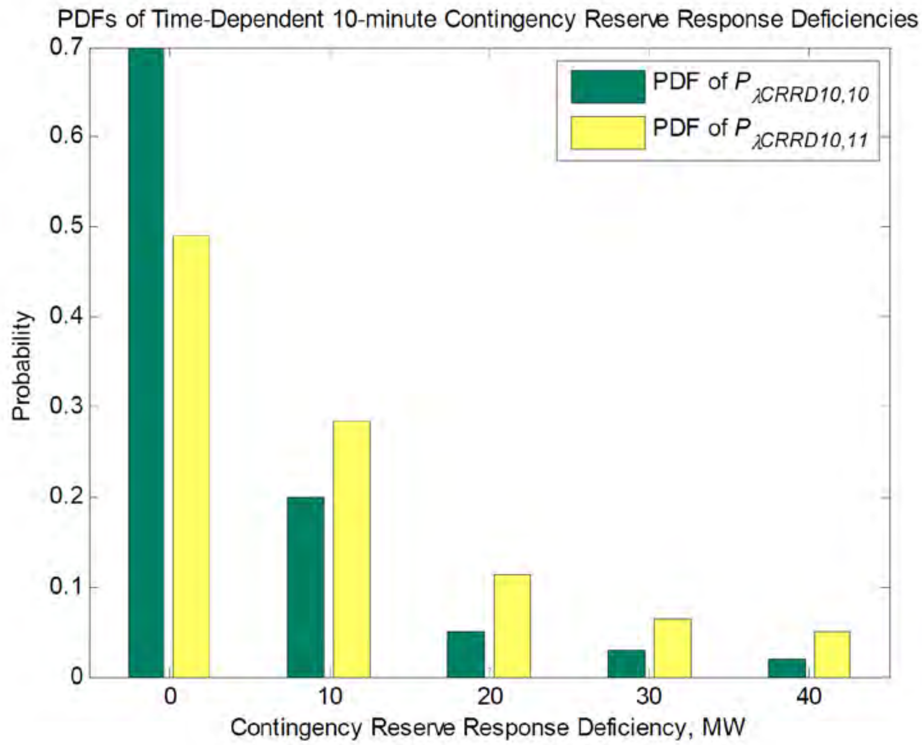

Figure C-2: Comparison of $P_{\lambda CRRD10,10}$ and $P_{\lambda CRRD10,11}$

Appendix D: Comparing the Capacity Outage Probability Table Generated from Time-Dependent and Steady State Markov Models

The theoretical formulation of the Contingency Reserve Activation Model (CRAM) requires a Capacity Outage Probability Table (COPT) containing probability density functions (PDFs) representing the probability that some specific generating capacity will be forced out within the next unit commitment (UC) time interval.

When analyzing the input requirements of the Contingency Reserve Activation Model, we noticed a potential source of error in the Capacity Outage Probability Table that would overestimate the contribution of contingency reserve activation to the controllable generation requirement. The purpose of this document is to detail the potential error and comment qualitatively on its expected effects.

The purpose of the Contingency Reserve Activation Model (CRAM) is to forecast the contribution of stochastic contingency reserve activation to the controllable generation requirement (CGR). This contribution is formulated as a discrete probability density function (PDF) and is computed from the PDFs of contingency reserve response deficiency and generation capacity forced out by a given unit commitment (UC) time interval.

The PDF of forced outage by time interval t after the start of the UC is supplied to the CRAM by the Forced Outage Model as a Capacity Outage Probability Table (COPT) [18]. The COPT has 300 PDFs of forced outage, one PDF for every minute in the five hour UC time horizon. A PDF in the COPT represents the probability that a certain amount of generation capacity will be unavailable at some time, t, after the start of the UC run. As we understand it, the COPT is derived from a steady state Markov model [18]. The steady state Markov model assumes no information is known about the initial state of the system (this is the Markov property).

If our understanding is correct, we think the COPT PDFs formulated in [18] will overestimate the CGR since in practice the exact state of the units is known at the start of the UC. When a Markov model starts from a known state it converges to the steady state with time constants determined by the failure and repair rates of the model, as described below.

Let U be the state of a single generating unit, where $U = 0$ if the unit is forced out, and $U = 1$ if the unit is operating. Let λ and μ be the failure rate and repair rate of the unit, respectively. For the simple two-state Markov model the steady state probability that the unit is forced out is

$$\mathrm{P}[U=0]=\frac{\lambda}{\lambda+\mu} \tag{D.1}$$

and the steady state probability that the unit is operating is

$$\mathrm{P}[U=1]=\frac{\mu}{\lambda+\mu} \tag{D.2}$$

Equations (D.1) and (D.2) are derived in [19], and equation (D.1) is shown in [18] to be used to build the COPT PDFs. The probabilities of the possible states of the unit are time-independent in this model, and we would not expect the PDF of forced outage to change significantly with time. Let us compare this model and its above equations with the stochastic model of contingency reserve response and restoration used to compute the contribution of contingency reserve activation to the CGR.

When an outage occurs, the lost capacity is nominally supplied by contingency reserve during the first 105 minutes, and then must be supplied by an increase in the controllable generation until it is repaired (repair can be neglected over the five hour time horizon of the UC). We expect the probability that a particular capacity is forced out by a particular UC time interval should increase as the time interval increases or as time moves forward in the UC. It follows that we expect the contribution of forced outage to the CGR to increase as time moves forward in the UC.

The COPT would ideally be computed by the Forced Outage Model be based on time-dependent probabilities to capture this trend over time. Given that the unit is operating at $t = 0$, *i.e.* the start of the UC, it can be shown that the time-dependent probabilities of the unit being forced out or operational at any time interval, t, in the UC time horizon are given by Equations (D.3) and (D.4), respectively.

$$\mathrm{P}\left[U(t)=0\right]=\frac{\lambda}{\lambda+\mu}-\frac{\lambda e^{-(\lambda+\mu)t}}{\lambda+\mu} \tag{D.3}$$

$$\mathrm{P}\left[U(t)=1\right]=\frac{\mu}{\lambda+\mu}+\frac{\lambda e^{-(\lambda+\mu)t}}{\lambda+\mu} \tag{D.4}$$

Checking the probabilities at the time extremes, *i.e.* at $t = 0$ and $t = \infty$, using equations (D.3) and (D.4), we see that

$$\mathrm{P}\left[U(0)=0\right]=0 \tag{D.5}$$

$$\mathrm{P}\left[U(0)=1\right]=1 \tag{D.6}$$

$$\mathrm{P}\left[U(\infty)=0\right]=\frac{\lambda}{\lambda+\mu} \tag{D.7}$$

$$\mathrm{P}\left[U(\infty)=1\right]=\frac{\mu}{\lambda+\mu} \tag{D.8}$$

Thus equations (D.3) and (D.4) give the known state of the unit at $t = 0$, and the steady state Markov model results at $t = \infty$. The steady state Markov model equations hold under the condition that $(\lambda + \mu)t$ is large enough to drive the exponential term in Equations (D.3) and (D.4) to zero. Since the values of λ and μ are small (λ may be on the order of 10^{-6} min^{-1} [20]), and the maximum value of t in a five hour UC time horizon is 300 minutes, we might expect the UC time horizon to be too short for the steady state condition to be a close approximation. The consequence of using COPT PDFs based on the steady state Markov model would be to overestimate the expected forced outage and contribution to the CGR over the duration of the UC time horizon.

Simply put, a COPT based on a steady state Markov model would result in a systematic error in those CGR values that include information from the COPT. The expected effect would be to cause the CGR values to be greater than if a time-dependent model were used. This would lead to greater unit commitment costs which may or may not be significant and/or acceptable.

In fact, through analysis of the example COPT supplied to us by Dr. Pavel Etingov, it seems probable that the error is negligible because in the example COPT the probability of zero capacity outaged is consistently 0.998. This being the probability of zero capacity outaged at $t = \infty$ is only

0.2% different from the other extreme, *i.e.* the probability of zero capacity outaged at $t = 0$ should be 1.

In this example case, the 95% probability value for both the time-dependent and steady state models is the same, *i.e.* 0 MW. When using the example COPT in the complete CGR_{95} algorithm with estimated PDFs of contingency reserve response deficiency, the effect of capacity outage on CGR_{95} was to increase it by 0 MW or 1MW, depending on if CGR_{95} was computed for every 1 minute or every 5 minutes of the UC time horizon. This analysis lends itself to the hypothesis that the difference between time-dependent and steady state Markov models is small because of the inherently rare occurrence of generation outages.

In the interest of theoretical rigor, we thought this discussion was worth noting, even though the expected error is perceived to be small. We are prepared to use a COPT derived from either type of Markov model, ignoring the discrepancy and accepting the error if the steady state model is used.

Distribution

No. of
<u>Copies</u>

\# Name
Organization
Address
City, State and ZIP Code

\# Organization
Address
City, State and ZIP Code
Name
Name
Name
Name
Name (#)

\# Name
Organization
Address
City, State and ZIP Code

No. of
<u>Copies</u>

\# **Foreign Distribution**

\# Name
Organization
Address
Address line 2
COUNTRY

\# **Local Distribution**
Pacific Northwest National Laboratory

Name	Mailstop
Name	Mailstop
Name	Mailstop
Name	Mailstop
Name	(PDF)

Pacific Northwest
NATIONAL LABORATORY

U.S. DEPARTMENT OF
ENERGY

Proudly Operated by **Battelle** *Since 1965*

902 Battelle Boulevard
P.O. Box 999
Richland, WA 99352
1-888-375-PNNL (7665)
www.pnl.gov